PROPERTIES OF
THERMOPLASTIC STARCH/POLY(LACTIC ACID) BLENDS

PROPERTIES OF
THERMOPLASTIC STARCH/POLY(LACTIC ACID) BLENDS

By

XUE-CHENG HUANG

A Thesis

Submitted to the School of Graduate Studies

in Partial Fulfillment of the Requirements

for the Degree

Master of Applied Science

McMaster University

MASTER OF APPLIED SCIENCE (2005) McMaster University

(Chemical Engineering) Hamilton, Ontario

TITLE: Properties of thermoplastic starch/poly(lactic acid) blends

AUTHOR: Xue-Cheng Huang

M. Eng. (East China University of Science and Technology)

B. Eng. (Da-Lian University of Technology)

SUPERVISOR: Dr. Andrew Hrymak

NUMBER OF PAGES: xviii, 160

ABSTRACT

High amylose cornstarch, normal cornstarch and waxy cornstarch were plasticized using water and glycerol as plasticizers in a Haake Rheomix 3000 batch mixer. A two-level factorial experiment design was used to investigate the effects of processing conditions and the water/glycerol ratio on the mechanical properties of the thermoplastic starches. The significances of factors (processing temperature, time, roller rolling rate and ratio of water to glycerol) on the mechanical properties were evaluated. The morphology, thermal properties, average molecular weight and molecular weight distribution of the thermoplastic starches were analyzed using scanning electron microscopy (SEM), differential scanning calorimetry (DSC) and high performance size exclusion chromatography (HPSEC). The mechanical properties and rheological properties of the materials were measured using an Instron tensile testing machine and a Rosand capillary rheometer.

The thermoplastic starches were further blended with poly(lactic acid)(PLA) at different composition ratios. The morphology, thermal properties, molecular weight and molecular weight distribution of the thermoplastic starch/PLA blends were analyzed using SEM, DSC, HPSEC. Mechanical and rheological properties of the blends were investigated using the same methods as those used in the investigation of thermoplastic starches.

The effects of amylose content in the starches, composition (starch/plasticizer ratio, water/glycerol ratio, starch/PLA ratio), molding methods and molding temperature on structure and properties of thermoplastic starches and thermoplastic starch/PLA blends were also investigated and compared. A power law model and a cross model were used to fit the experimental rheological data of the thermoplastic starches and the thermoplastic starch/PLA blends. The thermoplastic normal starch with starch/plasticizer ratio of 2/1 (wt/wt%) shows a tensile strength of 2.81 MPa, a modulus of 55.09MPa and an elongation at break of 76.0%. The post-extruded thermoplastic normal starch/PLA blend with the starch/PLA ratio of 50/50 (wt/wt) and the starch/plasticizer ratio of 2/1(wt/wt) exhibits a tensile strength of 15 MPa, a modulus of 926 MPa and an elongation at break of 6 %.

ACKNOWLEDGEMENTS

The author wishes to express his gratitude and appreciation to those who contributed to this study. In particular, he is indebted to:

Dr. Andrew Hrymak, his supervisor, professor of Chemical Engineering, McMaster University, for his interest, guidance and encouragement through the work.

Dr. Qiang Liu, in Food Research Program, Agriculture and Agri-Food Canada, for his enthusiasm, advice and discussions in the research project.

Ms. Elizabeth Takacs, Lab manager of Chemical Engineering, McMaster University, for her assistance in the experiments.

Ms. Elizabeth Donner, in Food Research Program, Agriculture and Agri-Food Canada, for her assistance in the material property characterization.

The financial sponsorship from Food Research Program, Agriculture and Agri-Food Canada for the research program is deeply appreciated.

Table of Contents

Figure Index

Table index

Nomenclature

DMTA	dynamic mechanical thermal analysis
DSC	differential scanning chlorimetry
E	activation energy, J/g
E_D	modulus predicted by Davies model, Pa
E_i	modulus of phase *i* in a blend, Pa
E_L	modulus predicted by series model, Pa
E_U	modulus predicted by parallel model, Pa
ΔH	thermal transition enthalpy, J/g
HAS	high amylose cornstarch
HPSEC	high performance size-exclusion chromatography
m	consistency index in a power law equation, $Pa \cdot s^n$
MFI	melt flow index, g/10mins
MW	molecular weight, g/mol
MWD	molecular weight distribution
n	power law index, no unit
NA	normal cornstarch
PCL	poly(ε - caprolactone)
PEA	polyester amide
PEG	polyethylene glycol
PHA	poly(3-hydroxyalkanoates)

PHBV	Copolymers of hydroxybutyrate and hydroxyvalerate
PLA	poly(lactic acid)
PVA	poly(vinyl acetate)
R	gas constant, 8.314 J/mol-K
SEM	scanning electron microscopy
T_g	glass trasition temperature, °C
T_c	crystallization temperature, °C
T_m	melting temperature, °C
T_p	peak temperature of gelatinization, °C
TPS	thermoplastic starch
WS	waxy cornstarch
wt	weight percent
X	degree of crystallinity
β_i	effect of variable *i*
$\dot{\gamma}$	shear rate, s^{-1}
ε_0	elongation at break of matrix, %
ε_{comp}	elongation at break of the composite, %
ϕ_f	volume fraction of the filler in the composite, vol%
$\phi\, i$	volume fraction of phase *i* in a blend, vol%
η	shear viscosity, Pa·s
η_0	zero shear viscosity, Pa·s

λ	relaxation time, s^{-1}
σ_0	tensile strength of the matrix, Pa
σ_{comp}	tensile strength of the composite, Pa

Chapter 1

Introduction

Currently, the global consumption of synthetic petroleum-based plastics stands at over 120 million tonnes. The disposal of plastic products brings serious environmental pollution since synthetic polymers have poor biodegradability and may have lifetimes of hundreds of years. One solution to this problem is to develop biodegradable plastics that have comparable properties and cost with traditional petroleum-based synthetic polymers, but are biodegradable in a reasonable amount of time. Biodegradable plastics are defined as "degradable plastics in which the degradation results from the action of naturally occurring microorganisms such as bacteria, fungi and algae" (ASTM D 6400-99, ASTM Publications). Among the biodegradable polymeric materials, starch is given more attention because of its low cost and wide availability. Starch is a major component of our food and also has many industrial applications as a thickener, colloidal stabilizer, gelling agent, bulking agent, water retention agent and adhesive. However, the applications of starch as industrial plastics such as packaging materials and films will provide high-value added product possibilities and help to conserve the petroleum resources.

Starch can be made thermoplastic under conditions of controlled temperature, pressure, shear in the presence of limited water and/or given amounts of plasticizers using traditional plastic process equipment. Thermoplastic starch (TPS) can be molded like traditional petroleum-based thermoplastic polymers through extrusion, injection, blow molding and thermoforming (Halley *et al*, 2001; Funk *et al*, 1998; Averous and Boquillon, 2004). TPS has mechanical properties suitable for some particular applications; however, thermoplastic starch also has some weaknesses such as water sensitivity, poor mechanical properties and changes in mechanical properties with time (crystallization due to ageing and plasticization by water absorption). These drawbacks limit its industrial applications. One of the methods to overcome the drawbacks of TPS is to blend TPS with biopolymers, such as:

- poly(ε - caprolactone) (PCL) (Averous *et al*, 2000a; Koenig *et al*, 1995),
- poly(lactic acid) (PLA) (Martin *et al*, 2001a; Ke *et al*, 2003),
- poly(3-hydroxyalkanoates)(PHAs) (Avella and Errico, 2000; Petersen *et al*, 2001),
- polyester amide (Averous *et al*, 2000a).

The addition of TPS into the biopolymers also lowers the production cost of products made from these expensive high performance biopolymers.

PLA is a commercially available and biodegradable thermoplastic aliphatic polyester derived from renewable resources. It is produced by condensation polymerization of D- or L- lactic acid or by ring opening polymerization of the lactide (Lunt, 1998; Drumright *et al*, 2000). Lactic acid monomers are derived from the fermentation of cornstarch and sugar beets. PLA has high strength and high modulus and can be processed using traditional equipment for thermoplastic. The products made from PLA are presently applied in the industrial packaging and the biocompatible/bioabsorbable medical device fields. As a high performance biopolymer, PLA has a drawback of relatively high cost compared to petroleum-based synthetic polymers. Blending of starch with PLA is expected to improve the properties of TPS-based materials and reduce the production cost of PLA-based products.

The transformation of native starch into thermoplastic starches under plasticization conditions in a single or twin-screw extruder or a heated pressure molding machine has been reported by a number of authors (Stepto, 2003; Funke *et al*, 1998; Van Soest *et al*, 1997). Some commercial TPS-based products are also available (Bastioli, 1998). However, few publications have reported on the plasticization of starch in a closed batch mixer and the effects of processing conditions, composition and their interactions on the structure and properties of TPS. The thermal and mechanical properties of starch/PLA composites where starch exists as a filler were reported by Ke *et al* (2003), Jun (2000) and Wang *et al* (2002). Martin and Averous (2001a) reported the thermo-mechanical properties of thermoplastic wheat starch/PLA blends extruded through a single extruder. Cornstarch is the primary source of starch in North America. The amylose/amylopectin ratio in the starch is determined by means of genetics and is affected by environmental conditions during biosynthesis (Singh *et al*, 2003). The properties of thermoplastic starch are influenced by the amylose/amylopectin ratio. For example, the moisture resistance of TPS was reported to increase with increasing amylose content (Ke *et al*, 2003). The amylose molecules are thought to form more effective entanglements than amylopectin molecules, resulting in an increase in tensile strength (Soest and Borger, 1997). However, the structure and properties, especially rheological properties, of the thermoplastic cornstarches containing various amylose contents or blends with PLA have not been extensively reported.

In this thesis, various types of cornstarch with different amylose content were plasticized using water and glycerol as plasticizers. Effects of processing conditions and ratio of water to glycerol on the properties of TPS were investigated according to a full factorial experimental design. The plasticized starch was then blended with PLA, and the structures and properties of TPS and TPS/PLA blends were studied.

The work in this thesis will help to formulate starch-based materials and optimize processing conditions in order to develop biodegradable starch-based products with a balance between mechanical properties, water absorption, biodegradability and cost for applications in packaging materials. The application of starch-based materials in the plastic industry may relieve the impact of petroleum-based plastics waste on the environment and add the values of agricultural products such as starch.

Chapter 2

Literature Review - Biodegradable Starch-based Materials

2.1 Structure and properties of starch

2.1.1 Chemical structure and morphology of native starch

Starch is the major polysaccharide in plants and exists in the form of granules within plant cells. The most common sources of starch are corn, potato, wheat, tapioca and rice. Starch is a mixture of essentially linear amylose (poly-α-1,4-D-glucopyranoside) and highly branched amylopectin (poly-α-1,4-D-glucopyranoside and poly-α-1,6-D-glucopyranoside). The chemical structures of amylose and amylopectin are shown in Figure 2-1. The length of the amylose chain varies with plant source, but in general the average length range from 500 to 2,000 glucose units. The average length of side chains of amylopectin is 20-30 glucose units. Amylopectin contains 4%-5% α-1,6 bonds at the branched points (Lai and Kokini, 1990). The ratio of amylose to amylopectin varies with the botanical source of the starch and is also affected by the climatic conditions and soil type. The amylose content of normal cornstarch varies from 22.4 % to

32.5% (wt%), and high amylose corn starch can run as high as 80 wt% amylose while waxy corn starch has 1.4-2.7 wt% amylose content (Morrison *et al*, 1984).

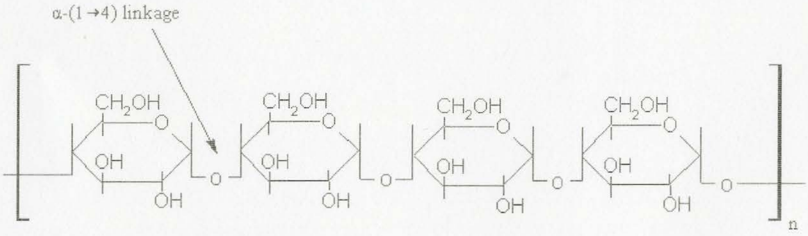

Amylose

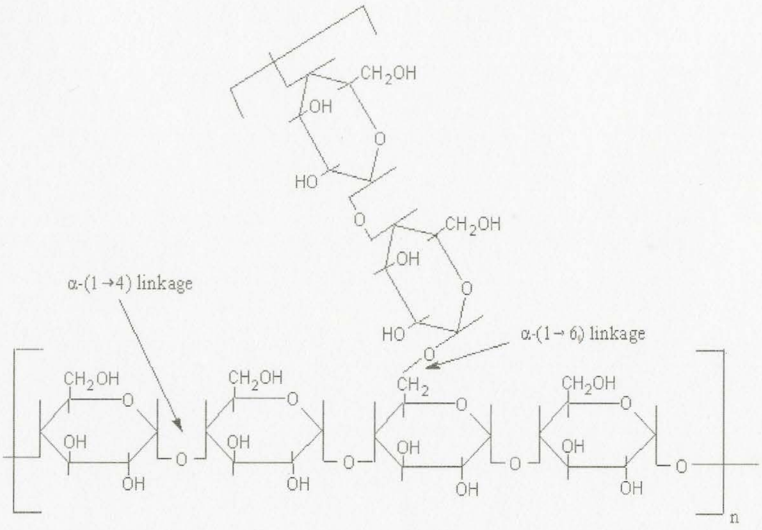

Amylopectin

Figure 2-1. The chemical structure of amylose and amylopectin.

The granular structure of starch, as shown in Figure 2-2, may be loosely defined on four separate levels (Waigh *et al*, 1998): molecules (~Å), lamellae (~9 nm), growth rings (~100's nm) and the whole granular morphology (μm). When viewed by SEM, starch granules from different botanical sources show significant variations in size and shapes, as shown in Figure 2-3. The cornstarch granules are polygonal and round, and have rough surfaces. The average diameter of cornstarch granules ranges from 1 to 20 μm (Singh *et al*, 2003).

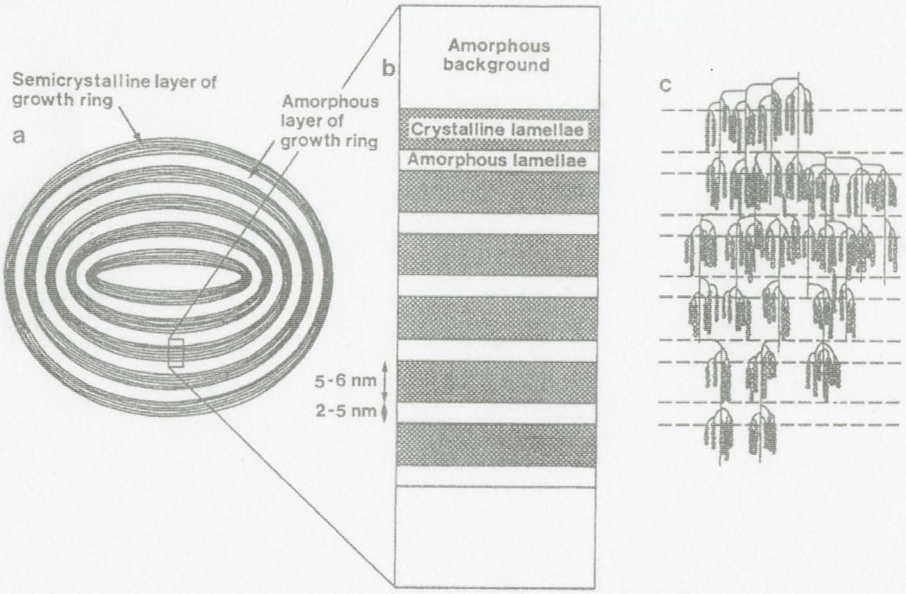

Figure 2-2. The structure of a starch granule (Waigh *et al*, 1998).

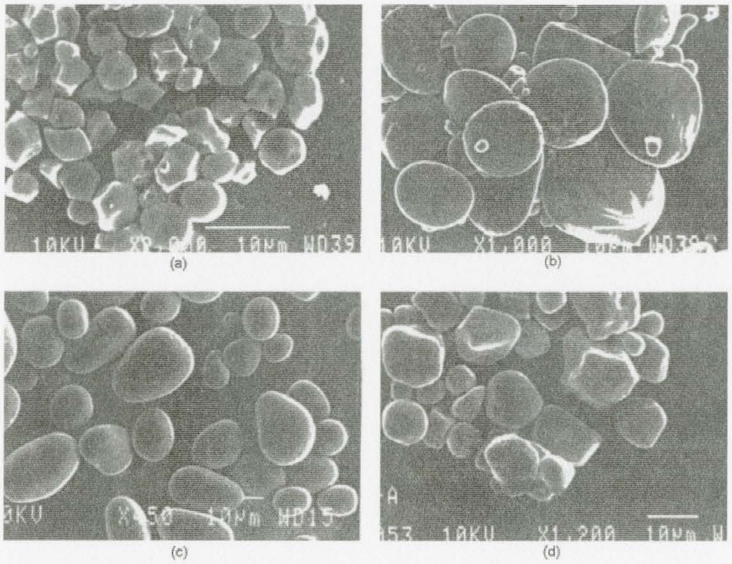

Figure 2-3. Scanning electron micrographs (SEM) of starches from different sources: (a) rice, (b) wheat, (c) potato, and (d) corn (Singh *et al*, 2003).

2.1.2 Crystallinity and thermal properties of the native starch

Starch is semi-crystalline in nature with a crystallinity of 15-45% (Stepto, 2003). The branch chains of amylopectin are partially in the form of double helices and are arranged in crystalline domains. Wherever possible, adjacent single helical amylose molecules and outer branches of amylopectin are associated in a form of hybrid amylose-amylopectin helix that gives radially oriented crystalline bundles. Starches from different sources differ in the packing of the double helices. As a result, A, B, and C type crystalline pattern appear in X-ray diffraction diffractometry. B-type crystalline structure shows the peaks that are both broad and weak and with two main reflections centered at 5.5 and 17 ° 2θ (Hoover, 2001). The A-type crystalline structure is denser than B-type pattern. The C-type crystallites are believed to be a combination of A-type and B-type (Poutanen and Forssell, 1996). The cereal starches exhibit the typical A-type X-ray diffraction pattern while the tuber starch showes the B-type pattern and legumes reveal the mixed state pattern "C" (Hoover, 2001). Small amounts of lipids in the starch are believed to complex with amylose molecules, and those lipid complexes form a specific V-type of crystalline structure (Poutanen and Forssell, 1996). The V-type pattern exhibits main peaks at 12.6 and 19.4 ° 2θ in X-ray diffraction diffractometry (Van Soest, 1997). The major types of X-ray diffraction patterns of starch are shown in Figure 2-4 (Zobel, 1988a).

Differential scanning calorimetry (DSC) has been used to investigate the thermal properties of starch. Poutanen and Forssell (1996) reported that the glass transition temperature, T_g, of dry amorphous starch is experimentally inaccessible because starch thermally degrades before it approaches its T_g which was estimated to be in the range of

230-250°C, depending on the estimation methods used. The degradation temperature of high amylose cornstarch was reported to be around 260°C (Avella and Errico, 2002).

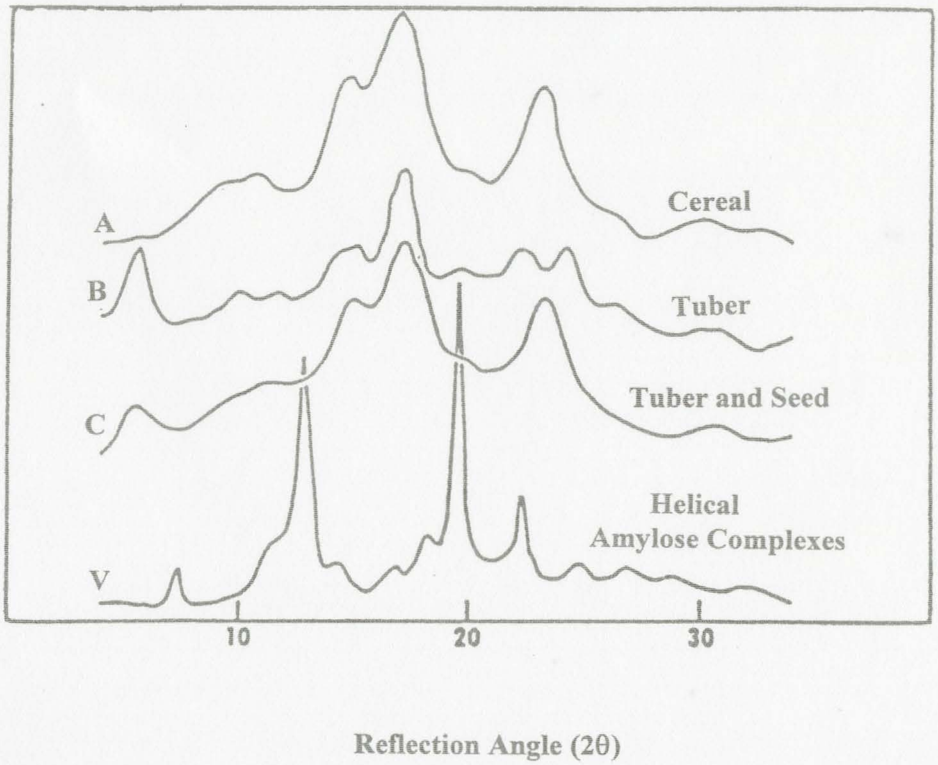

Figure 2-4. X-ray diffractograms of A, B, C and V types of starch crystalline structures (Zobel, 1988a).

2.1.3 Gelatinization and retrogradation of starch

When starch granules are heated in excess water under a non-shear condition, an order-disorder phase transition occurs. This process is called "gelatinization". Starch gelatinization is the disruption of molecular orderliness within the starch granules along with concomitant and irreversible changes in properties such as granular swelling, crystallite melting, loss of birefringence, viscosity development and solubilization. Differential scanning calorimetry (DSC) has been extensively used to investigate the gelatinization of the starch by heating an aqueous suspension of starch granules. Gelatinization transition temperatures are considered as ranges covering the temperatures at which loss of birefringence is first noticed and less than 10% remains. The gelatinization behaviors of the starch are partially controlled by the molecular structure of amylose and amylopectin (chain length, extent of branching, molecular weight, and polydispersity) in the granules, starch composition (amylose to amylopectin ratio and phosphorus content) and granule structure (crystalline to amorphous ratio). The gelatinization temperature, T_p, reflects the extent of crystalline perfection of native starch, starch composition and granule architecture.

The mechanism of starch gelatinization as a function of water content has been studied by many researchers (Nonovan, 1979; Evans and Haisman, 1982; Colonna and Mercier, 1985; Slade and Levine, 1987) based on DSC study. Donovan (1979) suggested that there are two distinct mechanisms by which ordered regions of starch undergo phase transition over a wide range of moisture contents. The low temperature endotherm reflects "stripping" and disorganization of polymer chains from crystallites; processes that are facilitated by the swelling action of water on the amorphous regions. As the water content decreases and becomes insufficient for the above process of complete melting, the partially hydrated crystallites tends to melt at a higher temperature whose values depends on the volume fraction of the diluent (water), as predicted by Flory theory.

As the granules swell, amylose molecules dissolve in the solvent and leach out into solution. After cooling of the gelatinized starch paste, these molecules and branches of amylopectin molecules re-associate and form hydrogen bonds. This process is referred to as "retrogradation". During retrogradation, amylose forms double-helical associations of 40-70 glucose units. Ultimately, under favorable conditions, amylopectin crystallization occurs by association of the outermost short branches and physical phase separation appears. The retrograded starch, which shows a B-type X-ray diffraction pattern, contains both crystalline and amorphous regions (Zobel, 1988b). In DSC thermograms of retrograde starch, the transition temperatures and retrodegradation enthalpies are lower compared to gelatinization transition temperatures and enthalpies of native starches.

2.1.4 Structure and properties of thermoplastic starch

Starch is blended with a limited amount of water, as well as a certain amount of other plasticizers in single or twin-screw extruders, intensive batch mixers or between hot cylinders, resulting in plasticized starch. During plasticization, the plasticizer molecules quickly enter into the interior of starch granules under the action of mechanical energy and thermal energy, resulting in the disruption of the granule structure. In addition to water, typical plasticizers include glycerol, propylene glycol, triethylene glycol, sorbitol, amine and other low-molecular weight polyhydroxy compounds such as polyethylene glycol (PEG), triethyl and tributyl citrate, and urea.

When dry starch is plasticized using other low molecular weigh plasticizers but without water, the process is exothermic (Lorcks, 1998). The resulting thermoplastic starch is homogenized and no longer recrystallizes. The plasticization process is endothermic when starch with more than 5% water content is blended with plasticizers (Lorcks, 1998). With only water as a plasticizer, starch products are brittle and transformed foams are obtained (Mercier *et al*, 1980). The use of water and other plasticizers such as glycerol is a common practice in plasticizing starch because the properties and enthalpy can be adjusted by changing the ratio of water to other plasticizers.

The effects of various plasticizers on the thermal properties (mainly T_g) of plasticized starch have been investigated. The glass transition temperature of thermoplastic starch (TPS) depends on starch type, plasticizer content and water/plasticizer ratio. Averous and Boquillon (2004) reported that the glass transition of plasticized starch is sometimes difficult to determine by differential scanning calorimetry analysis because the heat capacity change is quite low at the glass transition. In another paper, Averous *et al* (2000b) reported the T_g of thermoplastic wheat starch (containing 25 wt % amylose) from DSC and DMTA (dynamic mechanical thermal analysis). The T_g values from DSC increased from –20.1 to 43.4°C as the glycerol content in the TPS decreased from 35 wt % to 10 wt % and the water content increased from 0 wt % to 16 wt % correspondingly. The T_g values from DMTA were between 1.4°C and 63.2°C for same materials. Forssell *et al* (1996) reported that the T_g of barley starch blends with water and glycerol decreased from –53 °C to –105 °C when water content increased from 12% to 30% (the glycerol content increased from 14% to 39%). Rodriguez-Gonzalez *et al* (2004) studied the thermal properties of TPS using glycerol as a plasticizer (no water). They reported the T_g of the TPS decreased from –45 °C to –56 °C as glycerol content increases from 29% to 40%. Stepto (2003) reported that the T_g of potato starch-water mixtures range from around 85 °C to around 20 °C when the water contents are in the range of 12 wt % to 20 wt%.

Structure

Yu *et al* (1996) reported, on SEM micrographs of TPS, that starch granular structure was disappeared after extrusion, with a few crystalline pieces dispersed in the continuous amorphous phase.

Valle *et al* (1998) reported X-ray diffraction patterns of TPS with different botanical sources (no added water, glycerol content = 32 wt%). For extruded and press-molded wheat starch, the x-ray diffraction pattern demonstrated the existence of a single helical amylose crystalline structure ($2\theta=12.9°$ and 19.8°), similar to one formed by amylose-lipid complexes. Such a structure is initiated by the complexation of amylose with endogenous lipids and is supposed to be formed upon cooling after processing. In DSC thermograms, no melting endotherm was observed, indicating that the single helical amylose crystalline structure was temperature resistant and still existed at the test temperature. Van Soest *et al* (1997) also reported the existence of such a structure for TPS from maize starch. Since the TPS is soft at ambient temperature ($T_g < 20$ °C), its microstructure could be thought to be composed of small crystalline domains (15-30Å), embedded in an amorphous matrix of low glass transition.

Mechanical properties

At ambient temperature, plasticized starch can be made from glassy to rubber-like materials, depending on plasticizer and water contents. Table 2-1 shows the glass transition temperature of TPS with different formulations prepared by Averous *et al* (2001).

Table 2-1. Glass transition temperature (T_g) of TPS with different formulations (Averous *et al*, 2001b)

Samples	Starch Content Dry basis (wt%)	Glycerol Content (wt%)	Water content (wt%)	Glycerol/starch ratio (initial)	Tg (°C)*	Modulus (Mpa)	Impact Test (KJ/M^2)
S74G10W16	74	10	16	0.14	43	9800	0.79
S70G18W12	70	18	12	0.26	8	100	
S67G24W9	67	24	9	0.36	-7		
S65G35	65	35	0	0.54	-20	15	

Sample S74G10W16 contains74%(wt) starch (S), 10%(wt) water(W) and 16%(wt) glycerol(G).

Yu *et al* (1996) reported the mechanical properties of TPS plasticized with alcohol, glycerol or hexylene glycol. The tensile strength of the TPS decreased as the plasticizer content increased, while the elongation at break increased with increasing plasticizer content. By comparing the mechanical properties of TPS with the same plasticizer content but different plasticizers, it was found that the TPS with ethyl alcohol gave the lowest tensile strength but the highest elongation while hexylene glycol showed the highest tensile strength but the lowest elongation.

You *et al* (2003) investigated the mechanical properties of thermoplastic starch with glycerol and urea as plasticizers (raw starch contained 12% water). The tensile strength of the extruded thermoplastic starch samples decreased to 1.8 MPa from 5.7MPa with increasing urea content to 5% from 1% (glycerol content changed from 15-19% responsively). The elongation at break increased to 145% from 40% for the same formulations.

Rheological measurements

Many techniques, including capillary rheometry, on-line rheological measurement using an extruder equipped with a capillary die or a slit die, as well as oscillatory measurement, have been used for characterization of rheological properties of thermoplastic starch. Willett *et al* (1995) used a single screw extruder with a capillary die (Brabender PL 2000) to measure the apparent viscosity of cornstarch melt. The starch was first plasticized and pelletized. Rheological measurements were taken during a second extrusion step using the pellets as feed. You *et al* (2003) used a XLY-II capillary rheometer to conduct the rheological measurements of the extruded cornstarch, after extrusion and pelletization through a twin extruder. *Valle et al* (1998) studied rheological properties of various starches, including wheat, potato and maize starch with different amylose contents. The starches were plasticized in a Clextral BC45 twin-screw extruder, and then pelletized. The rheological measurements of the plasticized starches were performed on a slit die rheometer (Rheopac), attached to the die head of the extruder. Two dynamic rheometers, a Rheometrics RMS 800 (controlled shear rate) and a Bohlin CSM (controlled shear stress), were also used for oscillatory measurements. Lai *et al* (1990) conducted on-line rheological measurements of cornstarches by using a capillary die and a slit die viscometers in conjunction with a single screw extruder.

In all these studies, extruded starches exhibit a shear-thinning behavior, which can be described by a power law expression:

$$\eta = k\,\dot{\gamma}^{\,n-1} \qquad (2\text{-}1)$$

Where k is consistency; n is power-law index, n < 1 for pseudo-plastic materials.

Effects of plasticizers on rheological properties

The effect of moisture content on the dynamic rheological behavior of extruded wheat starch was reported by Valle *et al* (1998). The storage modulus G' and loss modulus G" of plasticized wheat starch increase as the moisture content decrease. At lower dynamic frequencies, the loss modulus G" increases more than the storage modulus G', indicating that the water content preferentially affects the amorphous phase. The increase of the storage modulus with decreasing moisture content may not be due only to the lower water content of the amorphous phase, but also to the presence of a denser crystalline network. The effect of moisture content on the viscosities of maize starches (amylose content of 0 and 70 wt%) shows that the viscosities decrease with increasing moisture content (Valle *et al*, 1996). Willett *et al* (1995) reported the impact of moisture content during the pelletizing step on cornstarch melt. At low temperatures (<130 °C), the starch pelletized with 15 wt% moisture content had the lowest viscosity, starch pelletized with 20 wt% moisture content had the highest, while that pelletized with 30 wt% moisture content had an intermediate viscosity value. At higher temperatures (>160 °C), moisture content during pelletizing had little effect on melt viscosity.

Valle *et al* (1998) investigated the effect of glycerol content on the dynamic rheological properties of plasticized wheat starch. The values of G' and G" decrease as the glycerol content increases. Glycerol acts as a plasticizer by increasing the molecular mobility in the amorphous phase. However, when the glycerol content increases from 27 wt% to 37 wt%, the increase in G' and G" is very limited, showing that the plasticizer does not influence the rheological properties of the plasticized starch as the glycerol content approaches a limiting value (about 30wt% for glycerol). Yu *et al* (1996) studied the effect of polyhydric alcohol (glycol, glycerol, hexylene) on the rheological properties of the extruded cornstarch. All samples behaved as a pseudoplastic liquid, although the polyhydric alcohols and the amounts added were different. For the same plasticizer content, TPS plasticized with hexylene had the lowest viscosity, while TPS with ethyl alcohol had the highest viscosity.

Effect of macromolecular structure and amylose/amylopectin ratio in starch

Valle and Buleon (1998) compared the values of the storage and loss modulus from plasticized potato and wheat starches. The plasticized potato starch has considerably larger values of G' and G'', up to five times that of the plasticized wheat starch. The potato-based TPS also shows a lower $\tan\delta$ value ($\tan\delta = G''/G'$), indicating that the plasticized potato starch is more elastic. This is due to the higher molecular weight of potato starch, thus longer chains and stronger ability to create entanglement.

High amylose maize starch has 70wt% amylose while waxy maize starch contains almost 100wt% amylopectin. The high amylose TPS has a much greater modulus than the waxy maize. The values of the complex modulus for the high amylose TPS are between 20 and 100 times greater than those obtained for the waxy maize or wheat TPS. In addition, the value of $\tan\ \delta$ of high amylose maize TPS is much lower than that of the waxy maize TPS (Valle and Buleon, 1998). In another paper, Valle *et al* (1996) reported the viscosities of maize starch with various amylose contents (0, 23.5, 47 and 70wt%). The greater the amylose content, the greater the viscosity, and the more pronounced the shear-thinning behavior. For the same moisture content, maize TPS with 70wt% amylose had a value of the shear thinning exponent of $n = 0.42$ and a value of consistency k of

3960 Pa.s^n (at 166°C), and the maize TPS with about 100% amylopectin had a n value of 0.87 and a k value of 580 Pa.s^n (at160°C). The similar results were reported by Lai *et al* (1990).

Effect of operating conditions on rheological properties

The processing temperature and thermo-mechanical treatment have an important impact on the rheological properties of thermoplastic starch. The apparent viscosity of starch melt is assumed to have an Arrhenius dependency on temperature:

$$\eta = \eta_0 \exp(E/RT). \tag{2-2}$$

Where, E = activation energy

R = gas constant, 1.987 cal/mol-K or 8.314 J/mol-K

Lai and Kokini (1990) reported the effect of extrusion temperature on the on-line apparent viscosity of 98wt% amylopectin and 70wt% amylose cornstarches. The viscosity of the thermoplastic starch decreases with increasing temperature. The shear thinning exponent, n, decreases as temperature decreases, indicating that the shear-thinning behavior is more pronounced at lower temperatures (less than 135°C). Valle *et al* (1998) and Willett *et al* (1995) reported similar results.

Biodegradability

You *et al* (2003) measured the biodegradability of plasticized cornstarch and found that the biodegradability of extruded starch was slightly better than that of native starch. After extrusion, the hydrogen bonds that stabilized the granular structure were destroyed. Therefore, enzyme could easily locate and disrupt the linkage between the glucose units. The addition of hydrophilic plasticizers and the degradation of starch molecules during extrusion were favorable to the attack of enzyme (e.g. amylase).

2.2 Structure and properties of poly (lactic acid)(PLA)

2.2.1 Stereo-chemistry and production technology of PLA

Lactic acid has two stereo-isomers, D- or L- lactic acid. Lactic acid produced by petrochemical route is a mixture consisting of 50/50 (mol%) D- and L- lactic acid. L- lactic acid is acquired from bacterial fermentation of starch or sugar beets. Lactic acid can form a cyclic dimer called lactide. PLA can be synthesized by the direct condensation polymerization of D- or L- lactic acid or by ring opening polymerization of the lactide. Since the condensation polymerization is an equilibrium reaction, and it is difficult to remove the water produced in the last stage of the polymerization, the molecular weight of PLA produced by this route is limited. Cargill Dow LLC has developed a solvent-free process to produce PLA with high molecular weight. A PLA pre-polymer with low molecular weight is produced by a condensation polymerization of lactic acid, and then the pre-polymer is depolymerized into lactide. This lactide remains in the melted state and is purified by distillation. The final PLA product with high molecular weight is produced by the catalytic opening ring polymerization of the lactide (Lunt, 1997). Mitsui Toatsu Chemicals produces PLA with high molecular weight by direct condensation through an azeotropic distillation process. A high-boiling solvent is used to remove water continuously in the esterification reaction so that high molecular weight product is acquired (Drumright *et al*, 2000).

2.2.2 Thermal, rheological and mechanical properties of PLA

PLA can exist in forms ranging from an amorphous glassy polymer to semi-crystalline / highly crystalline products depending on the ratio of two isomers in the polymer. Pure poly(D-lactic acid) or poly(L-lactic acid) has an equilibrium crystalline melting point of 207°C, but typical melting points are in the range of 170-180°C. The melting point range is due to small and imperfect crystallites, slight racemization and impurities (Garlotta, 2002). Introduction of meso-lactide decreases the melting point to as low as 130°C (Lunt, 1997). Dorgan *et al* (2000) analyzed the thermal properties of commercially available PLA from Cargill Dow LLC (the ratio of L to D isomer is 96:4). The glass transition temperature T_g was reported to be 58.4 ± 0.3°C and the melting point T_m was 151.7 ± 0.6°C. No crystallinity transition was observed in the DSC trace. Fang and Hanna (1999) reported the thermal properties of amorphous PLA (containing 82% L -lactide and 18% D -lactide) and semi-crystalline PLA (containing 95% L -lactide and 5% D -lactide). The glass transition temperature T_g and the melting point T_m were 58°C and 148°C, respectively, for the amorphous PLA, and 62°C and 151°C for semi-crystalline PLA.

Fang and Hanna (1999) measured the viscosities of amorphous PLA (containing 82% L -lactide and 18% D -lactide) and semi-crystalline PLA (containing 95% L -lactide and 5% D -lactide) at 150°C and 170°C at various shear rates using a tube rheometer on an extruder. The PLA melts behave as non-Newtonian fluids and the viscosity data can be fit to a power law equation. The amorphous PLA gave higher viscosities than semi-crystalline PLA. The viscosities measured at 150°C were higher than at 170°C. Lunt (1998) stated that PLA has low melt elasticity, which limits the application of the materials in some fields such as blown molding. The low melt elasticity can be improved by branching or low level of cross-linking of PLA molecules. An additional benefit of small degree of branching of PLA is a decrease in the viscosity.

Figure 2-5 shows the comparison of the mechanical properties of PLA with those of some common plastic packaging materials. PLA is a high performance biopolymer with high modulus and high strength but low elongation at break. The mechanical properties of PLA are comparable to those of polystyrene.

2.3 Structure and properties of starch/synthetic biopolymers blends

Starch can be blended with synthetic polymers in order to improve mechanical and moisture barrier properties. "First generation" biodegradable polymers started with starch filled polyethylene (PE). In some starch filled PE products, timed release photo- and thermo-degradable components were added to the starch/PE blends to trigger or accelerate the degradation process for the starch portion (Fringant *et al*, 1996). Other petroleum-based synthetic polymers which have been blended with starch include polystyrene (Riggle, 1998; Graaf and Janssen, 2001), polyurethane (Desai *et al*, 2000), poly(vinyl alcohol) (Ishigaki *et al*, 1999), and ethyl-vinyl acetate (Dell and Kohlman, 1994; George *et al*, 1994). However, these products could are not "completely biodegradable" since petroleum-based components cannot biodegrade at all in an amount

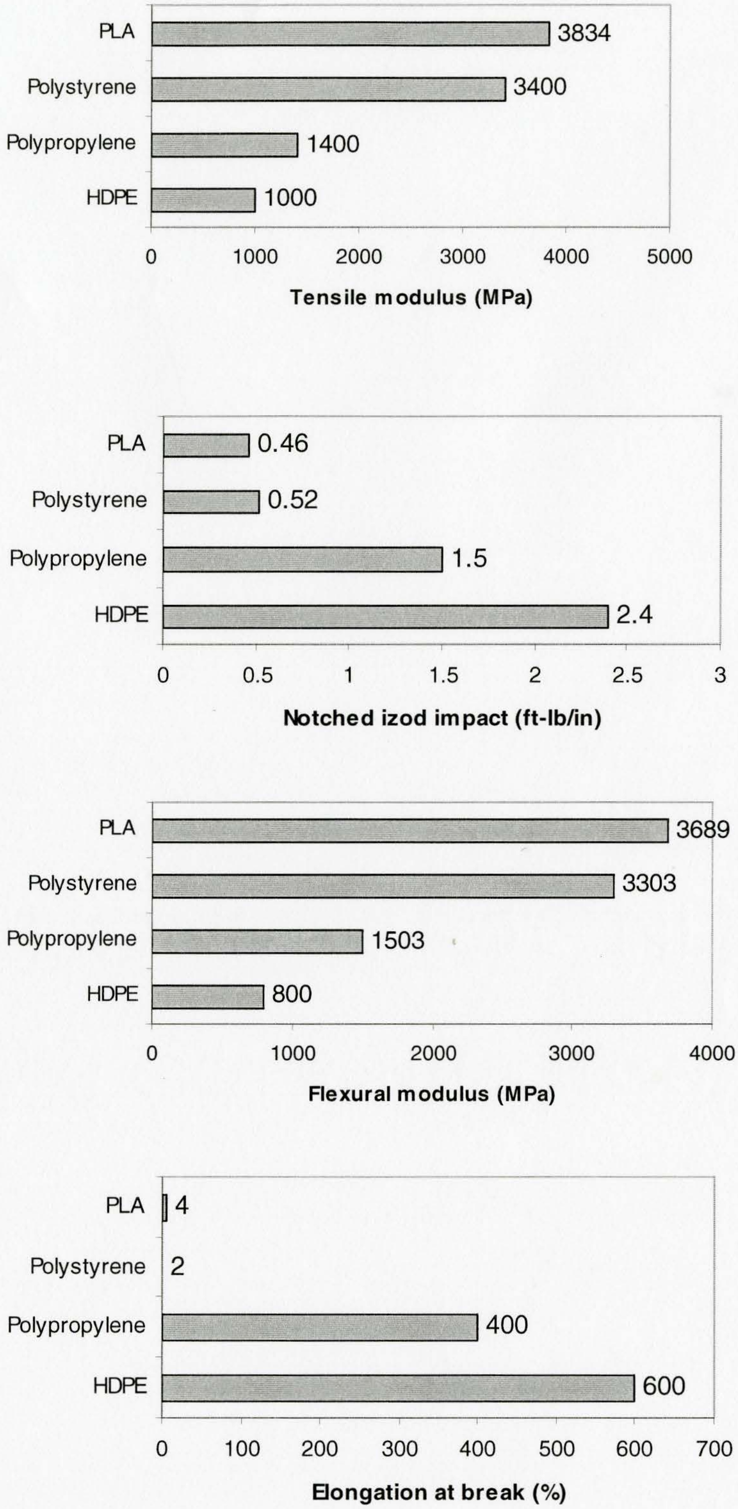

Figure 2-5. Comparison of mechanical properties of PLA with some common plastic packaging materials (Dorgan *et al*, 2000).

of time considered relevant, while the products may be reduced to minute fragments.

Complete biodegradation can be achieved by blending starch with biodegradable synthetic polymers such as polycaprolactone (PCL), polyester amide (PEA), poly hydroxybutyrate co hydroxyvalerate (PHBV), polylactic acid (PLA), polyester urethane (Stirna *et al*, 2002), and cellulose derivative (Averous *et al*, 2001a). Other aliphatic polyesters or copolyesters with aliphatic and aromatic blocks, such as polybutylene succinate/adipate and polybutylene adipate co terephtalate (Averous and Fringant, 2001b), have also been used.

2.3.1 Structure and properties of starch/PLA blends

Ke *et al* (2003) blended native cornstarches with different amylose content (approximately 0%, 28%, 50% and 70% by weight, respectively) and PLA in a twin-screw extruder and then investigated the morphology and mechanical properties of the samples. The SEM micrographs of the composites indicated that PLA was the continuous phase with starch granules appearing as filler in the two-phase structure. The blends made from other starches showed SEM micrographs with similar characteristics. The tensile strength and elongation of the blends decreased as the starch content increased regardless of starch type. The modulus increased slightly as starch content increased up to 40 wt%, and then decreased as starch content increased above 50 wt%. No significant differences in tensile strength were observed for the blends prepared from starches with 0 wt%, 28 wt% and 50 wt% amylose. The blends with high amylose cornstarch (containing 70 wt% amylose) had the lowest tensile strength. No explanation was given for different mechanical properties. Young's modulus and elongation of all blends prepared from starch with 30% moisture content ranged from 1540 to 1630 MPa and 4.2 to 4.4%, respectively.

Sun *et al* (2000) compared the morphology and mechanical properties of the composites prepared from blending native cornstarch and native wheat starch with PLA. The tensile strength and elongation at break decreased as the starch content increased at all compositions (ratio of starch to PLA ranged from 20:80 to 80:20) regardless of starch type. Nielsen and Nicolais-Narkin equations were used to study the relative mechanical properties of the starch/PLA composites. These equations relate filler content in the composite to the elongation at break and tensile strength of the composite. The Nielsen equation is given as:

$$\varepsilon_{\mathrm{comp}} = \varepsilon_0[1-(\phi_{\mathrm{f}})^{1/3}] \tag{2-3}$$

The Nicolais-Narkis equation is given as:

$$\sigma_{\mathrm{comp}} = \sigma_0[1-1.21(\phi_{\mathrm{f}})^{1/3}] \tag{2-4}$$

Where, $\varepsilon_{\mathrm{comp}}$ and ε_0 are the elongation at break of the composite and the matrix (PLA), respectively. σ_{comp} and σ_0 are the tensile strength of the composite and the matrix(PLA), respectively. ϕ_{f} is the volume fraction of the filler (starch). These equations assume that the filler particles are spherical, the matrix is homogenous, and there is no adhesion between the filler and the matrix. The relative mechanical properties indicate that some adhesion existed between PLA phase and starch granules, but the adhesion was poor. The wheat starch showed slightly better adhesion to PLA than the cornstarch did, but still poor, due to the greater granular size of the wheat starch that provided greater interface between two components. The adhesion forces between starch and PLA may be due to polar interactions between the two phases and hydrogen bonding between the carbonyl group of PLA and the hydroxyl group of starch.

Martin and Averous (2001a) reported the thermal and mechanical properties of thermoplastic wheat starch/PLA blends. Three thermoplastic wheat starches (the formulations are shown in Table 2-2), with T_g of 43, 10 and -20°C, were prepared and blended with PLA having a molecular weight of 49,000g/mol. The T_g of PLA phase in the blends decreased with an increase in the TPS component content, as shown in Table 2-3. The slight dependence of T_g of PLA phase on the composition indicated that thermoplastic wheat starch and PLA components may be partially miscible. The tensile modulus of the blends decreased as TPS content increased. The tensile strength, elongation at break and impact resistance of some of the blends are lower than those of two pure components as a result of poor compatibility.

Table 2-2. TPS formulations used in thermoplastic wheat starch/PLA blends by Martin and Averous (2001a)

Material	Starch content[a]	Water content[a]	Glycerol content[a]	Glycerol/starch ratio[a]	Density
TPS1	74	16 (8.5)	10 (11)	0.14 (0.14)	1.39
TPS2	70	12 (8.7)	18 (18)	0.26 (0.25)	1.37
TPS3	65	0 (12.6)	35 (30)	0.54(0.50)	1.34
PLA	/	/	/	/	1.25

[a] Starch, water and glycerol contents are given in wt% (wet basis), and values given in brackets are the glycerol and water contents or glycerol/starch ratio determined after processing.

Starch and PLA do not have readily reactive functional groups for each other, and interfacial adhesion arise from polar interactions between the two phases and hydrogen bonding between the carbonyl group of PLA and the hydroxyl group of starch, so the compatibility between two components is poor. In order to improve the compatibility, some coupling agents were added into starch/PLA blends. Wang *et al* (2002) reported the morphology and mechanical properties of native wheat starch / PLA composites with the addition of 0.5 wt% methylenediphenyl diisocyanate (MDI). The SEM micrographs of the composites showed a typical compatible structure where the starch granules were enveloped by the PLA matrix, indicating that highly reactive diisocyanate might react with both carboxyl and hydroxyl groups on PLA and with the hydroxyl groups on starch simultaneously. Mechanical properties of these composites supported this conclusion. The tensile properties of the composites at all compositions were similar to those of pure PLA. There was no significant change in elongation at break for composites compared to pure PLA until starch content reached 30 wt%. Between 30-60 wt%, elongation changes remained about 5%.

Table 2-3. Glass transition temperature of thermoplastic wheat starch/PLA blends reported by Martin and Averous (2001a)

Material	Starch/PLA ratio,wt/wt	Glycerol/starch ratio,wt%	T_g of PLA phase, °C
TPS/PLA	90/10	0.26	47
TPS/PLA	75/25	0.26	50
TPS/PLA	60/40	0.26	51
TPS/PLA	25/75	0.26	53
PLA	0/100	/	58

The water content and glycerol content in the TPS component are 12% and 18% by weight respectively.

2.3.2 Structure and properties of the blends of starch with other biopolymers

Starch / poly(β-hydroxylkanoate)s (PHAs) blends

PHAs are synthesized bio-chemically by microbial fermentation and may be produced in the future by transgenic plants. Poly-β-hydrobutyrate (PHB), which can be degraded to water and carbon dioxide under environmental conditions by a variety of bacteria, has similar material properties to polypropylene. However, it suffers from some disadvantages, such as brittleness and a narrow processability window (Tu *et al*, 1996). Various copolymers containing hydroxyalkanoate units other than 3-hydroxybutyrate (3HB) have been biosynthesized to improve mechanical and processing properties. Copolymers of hydroxybutyrate and hydroxyvalerate, commonly referred to as PHBV, were first manufactured by ICI in 1983 and have been marketed by Zeneca Biopolymers and Monsanto (Mohanty *et al*, 2000). PHBV still has disadvantages of high cost and low impact resistance, due to high crystallinity and relatively high glass transition, which prevented its larger commercial application.

Koller and Owen (1996) have investigated the structure and mechanical properties of melt-pressed sheet of PHB and PHBV filled with various amounts of maize starch. The addition of starch to the PHB and PHBV caused a decrease in the breaking strain and stress and an increase in the elastic modulus. Thus the PHB becomes even more brittle by the addition of the starch.

Avella *et al* (2000) studied the reactive blending of the PHBV and high-amylose starch with a small amount of organic peroxide [Bis(tert-butylperoxyisopropyl)benzene]. Bis(tert-butylperoxyisopropyl)benzene was selected because it has a $t_{½}$ of about 30 min at 190°C, which makes it possible to prevent too fast a reaction, to maintain homogeneous blending, and to avoid completely cross-linking the PHBV. The thermal properties of the blends were similar to those of the pure PHBV, showing that chemical interactions promoted during the PHBV/starch blending probably affected only a low percentage of chains. Without the addition of the peroxide to act as a compatibilizing agent, the addition of starch component led to a dramatic reduction of blend toughness. When the peroxide was used, 20 wt% starch increased toughness of the blend, whereas at a loading of 30 wt% starch the impact strength was similar to the PHBV.

Starch/PCL blends

Poly(ε-caprolactone) (PCL) is commercially available and partially crystalline aliphatic polyester with a T_g of –60 °C and a T_m of 60 °C. PCL is produced by a ring-opening condensation polymerization of cyclic ester monomer, ε-caprolactone. PCL is extensively used as a component in many polymer blends because of its toughness (due to low Tg) and good compatibility to many polymers. Averous *et al* (2000b) reported that PCL with a molecular weight of 69,000±1500 g/mol has a modulus of 190±6 MPa, a strength of 14.2±1.4 MPa and an elongation at break of >550%. The films and sheets based on thermoplastic starch/PCL blends were introduced into the market by Novamont in 1992. These products have reasonable mechanical properties and are truly biodegradable. Their degradation time is 20-45 days in composting conditions (Bastioli, 1998).

Koenig and Huang (1995) blended PCL with molecular weight of 40,000 and 80,000 g/mol with high amylose starch (containing 70% amylose) and waxy cornstarch granules as well as non-granular starch acetate derivatives. Those blends were found to be mechanically compatible but phase-separated. The modulus of the blends increased but the strength decreased as the starch content increased. The blends from high amylose starch showed the strongest mechanical properties, with about 15% decrease in tensile strength and about 50% increase in modulus compared with pure PCL with a starch content of 25 wt%. This result was considered to be due to the small size of high amylose starch granules and good dispersion of the granules in the PCL matrix.

Vikman *et al* (1999) evaluated the effect of processing conditions on the morphology and enzymatic degradation of thermoplastic potato starch/PCL blends with 50/50 (wt%/wt%) ratio. The blends were shown to be co-continuous and the thermoplastic starch had a particle-like, interconnected structure. The blends were very homogenous, and the size of the TPS pores in PCL matrix was very small, varying from 0.5 μm to 5μm. A thin layer of PCL formed on the surface of the blends during compression molding greatly reducing the rate of enzymatic hydrolysis.

Averous *et al* (2000b) reported the thermal, thermo-mechanical and mechanical properties of thermoplastic wheat starch/PCL blends. Phase separation was observed in those blends. In most of the blends, the thermal transitions of each component with a slight shift of the characteristic temperature were shown. The addition of PCL into TPS improves the mechanical properties of the pure thermoplastic starch. When the thermoplastic starch component with a glassy behavior was blended with PCL, the modulus of the blend decreased but the impact strength increased. When the thermoplastic starch component had a rubbery behavior (containing high plasticizer content), the addition of PCL resulted in an increase in the modulus of the blend.

2.3.3 Rheological properties of starch blends

The rheological behavior of starch blends has not been reported on to a great extent. Liu *et al* (1999) reported the effects of plasticizers (water, glycerol, ethylene glycol and propyl glycol), plasticizer amount and poly(vinyl acetate) (PVA) content on melt flow index (MFI) of wheat starch/polyvinyl alcohol blends. Of the investigated plasticizers, good flowability is best promoted by glycerol, and least by water. Addition of PVA into starch or starch into PVA decreases the MFI value, indicating a lowering effect on flow behavior. This negative deviation effect was related to phase-separation behavior of the blends. The influence of the PVA content on the viscosity is complicated. Addition of PVA component led to an increase in viscosity of the blend. However, the PVA thickening effect would be altered for the blends containing higher than 9% PVA. Flow behavior of the blend did not follow power law behavior, probably due to alteration in the continuous/discrete phase composition.

2.4 Application of starch-based materials

Products from starch-based plastics can be manufactured using conventional plastic production technologies such as injection molding, blow molding, film blowing, foaming, thermoforming and extrusion.

The market of starch-based plastics accounts for about 25,000 ton/year. The market share of these products accounts for about 75-80% of the global market of bio-plastics. 75 % of starch-based products are for packaging applications, including soluble foams for industrial packaging and film for bags and sacks (Bastioli, 2001). Specific applications of starch-based bio-plastics are given in Table 2-4. Some starch-based bio-plastics producers are given in Table 2-5 (Mohanty *et al*, 2000; Bastioli, 2001).

Table 2-4. Applications of bio-polymers

Segment	Specific items
Packaging	Washing bags, waste bags, carrier bags, eggcups, fast-food, drinking packaging, cosmetics, hygiene sector, pharmaceutics, washing & cleaning
Consumption	One-way cutlery, napkins, sanitary towels, litter products (e.g. golftees), flower pots, toys, CD trays, containers
Technical Utilisation	Denitrification of water, degradable carrier for chemicals
Plant protection	Herbicide bands, pesticide bands with controlledlay off, dispenser, gloves, label
Agriculture & Gardens	Fertilizer bags, films, cover films, harvest bounding yarn, rentilization as animal food after sterilization, bounding materials, sochets
Medicine	Medicine capsules, serving material, degradable carrier for medicines, fixing of fractures, orthopaedical surgery

BIOTEC of Germany (Lorcke, 1998) has conducted promising research and development along the lines of starch-based thermoplastic materials. The company's three production lines are:

- Blown film extrusion lines
- Flat film extrusion
- Injection molding lines

Under the Mater-Bi trademark, Novamont today produces four classes of biodegradable materials. They are all made from thermoplastic starch in combination with PCL, a cellulose derivative, or ethylene vinyl-alcohol copolymer. Their biodegradation rate is similar to that of cellulose and their mechanical properties close to those of traditional plastics like LDPE (Bastioli, 1998).

The main reasons why starch-based plastics cannot be applied extensively are high cost, insufficient market and performance limitations. The cost of starch-based plastics is 5 – 10 times higher compared to those of common synthetic petroleum-based plastics (Mohanty *et al*, 2000). Therefore, the real challenge lies in finding applications that would consume sufficiently large quantities of starch-based plastic products to lead to price reduction. The design of material formulation to achieve a balancing of mechanical properties, water absorption, biodegradability and cost is an important aspect of the research activities in this field. In the design of material formulation, it is important to understand the factors influencing material properties and performance as well as biodegradability.

Table 2-5. List of some starch-based plastics producers

Company	Products	Company	Products
Asian Pacific Basin			
Ajicello	Chitosan/Cellulose/starch	Japan Corn Starch	Starch-based derivatives
Chisso/Novon International	Starch /PVA or PCL blends	Nissei	Starch-based
Europe			
Avebe	Starch-based blends	Fluntera AG	Extrusionable starch materials
Biopac	Extrusionable starch materials	Novamont	Starch-based blends
Biotec	Starch-based blends	Novon Polymer AG	Extrusionable starch materials
EMS Chemie/Battelle	Polyethylene / Additives	storopack	foamable starch materials
USA			
Amylum	Extrusionable starch materials	Novon International	Starch-based derivatives
Archer Daniels	Extrusionable starch materials	St. Lawrence Starch	Extrusionable starch materials
BioPlastics	Starch / Polycaprolactone (PCL)	USDA - Agritech	Extrusionable starch materials
National Starch	Starch-based derivatives	Warner & Lambert	Extrusionable starch materials
National Starch & Chemical American Excelsior	Foamable starch materials	Willow Ridge	Polyethylene / Starch blends

Chapter 3

Experimental

3.1 Materials

The starches used in this work were:

- high amylose cornstarch (trade name: HYLON VII) containing approximately 70 wt% amylose,
- normal cornstarch (trade name: MELOJEL) with approximately 23 wt% amylose and
- waxy cornstarch (trade name: AMIOCA) containing almost 100 wt% amylopectin.

The starch samples were obtained from National Starch & Chemical Company (Bridgewater, New Jersey). All native starches are food grade and contain approximately 11 wt % moisture. Polylactic acid pellets (4042D) were provided by Cargill Dow LLC (Minnetonka, MN). Glycerol (99+% purity) was obtained from Sigma-Aldrich and has a boiling point of 182 °C. Pluronic F-108 block copolymer surfactant (polyoxypropylene-polyoxyethylene block copolymer), with an average molecular weight of 14,600, was obtained from BASF Corporation (Mount Olive, New Jersey), with a melting point of 57 °C.

3.2 Processing of thermoplastic starch (TPS) and starch/PLA blends

3.2.1 Preparation of thermoplastic starch

Each of three granular cornstarches was dried in a vacuum oven at 80°C for 24 hours prior to processing. Dried native starches were mixed with varying amounts of glycerol and water in a beaker by hand. The mixtures of starch, glycerol and water were loaded into a Haake Rheomix 3000 batch mixer with roller rotors for blending. In investigating effects of processing conditions on properties of thermoplastic starch, blending conditions (temperature, time and roller rolling rate) and the ratio of water to glycerol were set according to an experimental design at two levels, presented in Table 3-1. The ratio of starch to total plasticizer (water and glycerol) was fixed as 1/1(wt/wt). In the preparation of the thermoplastic starches, used in starch/PLA blends, the blending conditions were 120 °C at 45 rpm for 4 minutes and the ratio of water/glycerol/starch was 15/35/50 (wt/wt) for high amylose starch. The ratio of starch to plasticizer was increased for normal starch and waxy starch, and the ratio of water/glycerol/starch was 15/35/100 for normal starch and waxy starch.

3.2.2 Preparation of TPS/PLA blends

Thermoplastic starch/PLA blends were prepared according to a two-step procedure. Native starches were plasticized first by using water and glycerol as plasticzers. Five different of thermoplastic starches with different composition were prepared using different starches. Their compositions are listed in the Table 3-2. In the second step, the thermoplastic starches were blended with PLA in Haake Rheomix 3000 under 170 °C and 45 rpm for another 4 minutes.

Table 3-1. Experimental design for processing starch

No.	Run order	Code[1]	Temperature, °C, x_1	Ratio of water/glycerol, wt%, x_2	Rolling speed, rpm, x_3	Time, mins, x_4	Coded units			
							X_1	X_2	X_3	X_4
1	6	HAS-120-4-45-1-15/35	120	15/35	45	4	-	-	-	-
2	9	HAS-150-4-45-1-15/35	150	15/35	45	4	+	-	-	-
3	10	HAS-120-4-45-1-35/15	120	35/15	45	4	-	+	-	-
4	8	HAS-150-4-45-1-35/15	150	35/15	45	4	+	+	-	-
5	11	HAS-120-4-65-1-15/35	120	15/35	65	4	-	-	+	-
6	3	HAS-150-4-65-1-15/35	150	15/35	65	4	+	-	+	-
7	2	HAS-120-4-65-1-35/15	120	35/15	65	4	-	+	+	-
8	12	HAS-150-4-65-1-35/15	150	35/15	65	4	+	+	+	-
9	1	HAS-120-10-65-1-15/35	120	15/35	65	10	-	-	+	+
10	7	HAS-150-10-45-1-15/35	150	15/35	45	10	+	-	-	+
11	5	HAS-120-10-45-1-35/15	120	35/15	45	10	-	+	-	+
12	4	HAS-150-10-65-1-35/15	150	35/15	65	10	+	+	+	+
13	13	HAS-120-10-45-1-15/35	120	15/35	45	10	-	-	-	+
14	14	HAS-150-10-45-1-35/15	150	35/15	45	10	+	+	-	+

[1] Meaning of the code " HAS-120-4-45-1-15/35": HAS: high amylose starch, 120: processing temperature (°C), 4: processing time (minutes), 45: rpm of rollers, 1---ratio of starch to plasticizer (wt/wt%), 15/35 or 35/15: ratio of water to glycerol (wt/wt%).

Table 3-2. Composition of thermoplastic cornstarches used in thermoplastic starch/PLA blends

No	Name	Code	Starch type	Starch/plasticizers, wt/wt	Water/glycerol, wt/wt
1	TP-HAS1	HAS-120-4-45-1/1-15/35	High amylose starch	1/1	15/35
2	TP-HAS2	HAS-120-4-45-3/2-15/35	High amylose starch	3/2	15/35
3	TP-HAS3	HAS-120-4-45-2/1-15/35	High amylose starch	2/1	15/35
4	TP-NS	NS-120-4-45-2/1-15/35	Normal starch	2/1	15/35
5	TP-WS	WS-120-4-45-2/1-15/35	Waxy starch	2/1	15/35

Processing conditions: 120°C/4mins/45rpm.

3.3 Characterization of TPS and its blends with PLA

3.3.1 Rheological measurement

Shear viscosities of TPS and TPS/PLA blends at various shear rates were measured in a Rosand Precision Advanced Capillary Rheometer (Bohlin Instruments, UK) at different temperatures. The L/D of the long die is 16/1. Both Bagley correction and Rabinowitsch correction (Vlachopoulos, 2003) were used in calculating the shear viscosity and the shear rate.

3.3.2 Tensile testing

Two types of testing specimens were prepared. The fibers extruded through the Rosand capillary rheometer during the rheological measurement were cut to about 120mm in length. Those specimens were designated as post-extrusion molded specimens. The gauge length (the distance between the two holders) is set to be around 100mm. Compression-molded specimens were prepared using a lab-scale hot pressure machine. Thermoplastic starches and TPS/PLA blends were loaded in a square mold with a dimension of 85mm x 85 mm at 120°C for TPS and 160°C for starch/PLA blends, and held for 2 minutes, and then cooled naturally to around 60°C before removal from the molder. Molded samples were cut into dumbbell shape according to ASTM D638-91. The gauge length of the compression-molded specimens during tensile testing is around 50 mm. The specimens were stored in plastic bags for 3-5 weeks before tensile testing. All specimens were preconditioned at 50% relative humidity and 23°C for at least 24 hours prior to tensile testing.

Tensile testing was carried out on an Instron tensile testing machine (Series IX Automated Material Testing System) according to ASTM D882-91, with a crosshead speed of 25 mm/min. The diameters of the fiber specimens and the thickness and width of the compression-molded specimens were measured prior to testing. Elastic modulus, maximum tensile strength and the elongation at break were obtained with three replicates for each blend composition.

3.3.3 Scanning electron microscopy

Scanning electron microscopy (SEM) was performed on selected samples with a Philips Scanning Electron Microscope (Philips Scientific & Industrial Equipment, Eindhoven, The Netherlands). Two kinds of cross-section of test specimens were chosen. An etched cross-section was prepared by cutting compression-molded samples with a low speed saw (11-1180 ISOMET), and etching them with chloroform for 1 hour to remove PLA phase. A fractured cross-section came directly from broken surfaces of post-extrusion and compression molded specimens after tensile testing. All cross-sections were coated prior to observation.

3.3.4 Differential scanning calorimetry

Differential scanning calorimetry measurements were performed with a 2920 Modulated DSC equipped with a refrigerated cooling system (RCS) (TA Instruments, USA). About 10 mg of sample was sealed in an aluminum pan and heated from 5ºC to 180ºC at a thermal scan rate of 10ºC/min, then cooled to -30ºC at a rate of 10ºC/min, equilibrated at -30ºC and heated again to 200ºC at 10ºC/min scan rate. Other scan rates (thermal scan of 20ºC /min and cooling scan of 50ºC /min) were used to investigate the effects of scan rates on thermal properties of the materials. A nitrogen flow (150 ml/min) was maintained throughout thermal scan. Helium gas (50 ml/min) was used during cooling. Two kinds of pans were used because of the presence of water. Thermoplastic starch and starch/PLA blends were sealed in hermetic aluminum pans. Native starches and mixtures of native starches with plasticizers (water and/or glycerol) were sealed in Perkin-Elmer high volume stainless steel pans with sealing O-rings in order to prevent water volatilization and maintain the pressure in the pans (up to 3 MPa). Native starches were dried in a vacuum oven at 80ºC for 24 hours prior to usage. Melting temperature T_m and crystallization temperature T_c were taken at the peak value of respective endotherms and exotherms, and the glass transition temperature T_g at the mid-point of heat capacity changes. When multiple endothermic peaks were found, the peak temperature of the main endotherm was taken as T_m.

3.3.5 High performance size exclusion chromatography

Average molecular weights and molecular weight distributions were determined using high performance size-exclusion chromatography (HPSEC). The system consisted of four components including: Waters 515 pump, Waters column heater, Waters Refractive Index Detector 2410 and Viscotek Data Manager (DM400). The samples were first dissolved in DMSO (dimethyl sulfoxide) aqueous solution (0.9 mL DMSO + 0.1 mL water) under heating (100°C) and stirring for 1 hour. The solution stirred for 22 hours before the samples were precipitated using ethyl alcohol. The separated pellets were dissolved in the mobile phase before injection. The eluent was distilled deionized water consisting of 100 mM $NaNO_3$ and 5 mM NaN_3. The injection volume was 100μL. The columns used for SEC separation are from Rhenornenex and consisted of three parts: two PolySep-GFC-P Linear (300x 7.80 mm) and one guard column PolySep-GFC-P (35 x 7.80 mm). The eluent flow rate was 0.7 mL/min. TriSEC 3.0 GPC software was used to analyze data.

3.3.6 Density measurement

The density of thermoplastic starch and starch/PLA blends was measured by using an Electronic Densimeter MD-200S (Mirage Trading Co., Ltd, Osaka, Japan), which adopts Archimedes' principle. The determination of the (relative) density value is based on the density of water at 4°C: 1.000g/cm^3.

Chapter 4

Results and Discussion

4.1 Structure and properties of thermoplastic starch

4.1.1 Processing conditions

A full 2^3 factorial experimental design and a $\frac{1}{4}2^4$ factorial experiment design at two levels were carried out to investigate the effects of processing conditions and water/glycerol ratio on mechanical properties of thermoplastic high amylose starch, as shown in Table 3-1. Temperature (T, °C), ratio of water to glycerol (wt/wt), roller rolling rate (rpm) and processing time (t, minutes) are the considered variables. The ratio of native starch to total plasticizer (water and glycerol) was fixed as 1/1 (wt/wt). The variables can be transformed into coded units in order not to have to deal with the actual numerical measures of the variables.

Blending temperature: $x_1 = \frac{(T - 135^0 C)}{15}$

Ratio of water to glycerol: $x_2 = \frac{(R - 29/21)}{20/21}$

Blending RPM: $x_3 = \frac{(rpm - 55)}{10}$

Blending time: $x_4 = \frac{(t - 7\,mins)}{3}$

(135°C, water/glycerol ratio of 29/21, 55rpm, 7mins are variable values in the central region in the experimental design).

Mechanical properties of the post-extrusion molded thermoplastic starch were measured, as shown in Table 4-1. Sample No.1-8 in Table 3-1 constitutes a full 2^3 two-level factorial experimental design. The significance of factors (processing conditions) on responses (mechanical properties) at a 95% confidence interval was estimated according to the following statistical model:

$$y=\beta_0+\beta_1x_1+\beta_2x_2+\beta_3x_3+\beta_{12}x_1x_2+\beta_{13}x_1x_3+\beta_{23}x_2x_3+\beta_{123}x_1x_2x_3 \tag{4-1}$$

$$\beta_i=\frac{\sum x_i y}{\sum x_i^2} \tag{4-2}$$

y: responses (tensile strength, tensile modulus and elongation at break);

β_i: effect of changing variable i by one unit ; for example, β_0 is the average value of the responses; β_1 is the effect of changing variable 1 by one unit; ...; β_{12} is the effect of changing two-factor interaction of variable 1 and variable 2 by one unit; β_{123} is the effect of changing three-factor interaction of variables 1, 2 and 3 by one unit.

x_i: variables, x_1: processing temperature; x_2: ratio of water to glycerol; x_3: blending rpm; x_4: blending time.

The calculation process for assessing the significance of the effects at a 95% confidence interval is shown in Appendix B. The complete table of effects is shown in Table 4-2, which indicates that the ratio of water to glycerol has the most significant effects on tensile strength, modulus and elongation at break of the thermoplastic starch. The tensile strength, modulus and elongation at break of the thermoplastic high amylose starch change by 5.028 MPa, 104.4 MPa and 18.30 % respectively when the water/glycerol ratio

Table 4-1. The mechanical properties and moisture contents of the post-extrusion molded thermoplastic starch

No	Code	Water content [a], wt %	Plasticizers / starch after blending (wt/wt)	Mechanical properties [b]		
				Tensile strength (MPa)	Modulus (MPa)	Elongation at break (%)
1	HAS-120-4-45-1-15/35	14.2	0.98/1	0.866±0.147	17.17±0.65	9.69±2.31
2	HAS-150-4-45-1-15/35	7.5	0.84/1	1.12±0.14	16.58±0.57	12.3±2.57
3	HAS-120-4-45-1-35/15	23.0	0.69/1	3.73±1.22	88.03±30.13	21.8±10.3
4	HAS-150-4-45-1-35/15	12.3	0.48/1	7.60[c]	108.30[c]	36.2[c]
5	HAS-120-4-65-1-15/35	12.2	0.93/1	1.12±0.29	18.24±2.29	12.4±3.7
6	HAS-150-4-65-1-15/35	5.2	0.79/1	1.26±0.07	19.05±2.91	12.5±1.1
7	HAS-120-4-65-1-35/15	20.0	0.63/1	5.82±0.84	131.4±40.0	27.4±10.7
8	HAS-150-4-65-1-35/15	10.1	0.45/1	7.35±0.89	160.8±103.1	34.6±3.7
9	HAS-120-10-65-1-15/35	8.0	0.85/1	1.05±0.04	17.75±1.02	10.5±0.1
10	HAS-150-10-45-1-15/35	2.9	0.75/1	/[d]	/	/
11	HAS-120-10-45-1-35/15	10.7	0.46/1	8.94±1.54	292.7±99.4	35.7±4.6
12	HAS-150-10-65-1-35/15	1.6	0.32/1	/[d]	/	/
13	HAS-120-10-45-1-15/35	8.1	0.85/1	1.02±1.35	18.10±1.29	11.8±3.5
14	HAS-150-10-45-1-35/15	/	/	/[d]	/	/
15[e]	HAS-120-4-45-1-15/35	/	/	0.888±0.120	18.59±1.09	10.1±2.0
16	NS-120-4-45-2/1-15/35	/	/	2.81±0.32	55.09±18.09	76.0±33.8
17	WS-120-4-45-2/1-15/35	/	/	2.96±0.24	75.98±8.06	33.7±13.3

[a] The moisture content of blended samples.

[b] $X = \bar{X} \pm 1.96\sigma$ (95% confidence interval).

[c] Only one specimen was measured.

[d] No mechanical properties were obtained because the sample was degraded.

[e] Having same processing conditions and composition as No.1. Being used as TPS component in thermoplastic starch/PLA blends.

changes by one unit (from –1 to +1). The interaction of variable 1 (processing temperature) and variable 3 has a slight negative effect on tensile strength and a large negative effect on elongation at break of the samples. A change in one unit (from -1 to +1) of the temperature-blending rpm interaction causes a decrease of 0.6135 MPa in strength and 2.408 % in the elongation at break.

Table 4-2. Significance of factors on responses in a full 2^3 two-level factorial processing experimental design

Effect name	Estimated effects		
	Strength	Modulus	Elongation
Average, β_0	3.608	69.94	20.89
β_1	1.449	12.48	6.098
β_2	5.034	104.4	18.30
β_3	0.559	24.85	1.718
β_{12}	1.252	12.37	4.732
β_{13}	-0.6135	2.639	-2.408
β_{23}	0.3615	23.08	0.3320
β_{123}	-0.5565	1.938	-2.452

β_0 is the average value of the responses; β_1 is the effect of variable 1; ...; β_{12} is the effect of two-factor interaction of variable 1 and variable 2; β_{123} is the effect of three-factor interaction of variables 1, 2 and 3.

Samples No. 9, 11, 6, and 4 in Table 3-1 constitute a $\frac{1}{4}2^4$ two-level factorial experimental design. In this case, many effects are confounded, as shown in Table 4-3. The significance of effects of the factors was estimated. The calculation is shown in Appendix B. The complete table of effects at a 95% confidence interval is shown in Table 4-4, also indicating that the ratio of water to glycerol is statistically significant on the responses. In this experimental design, the tensile strength, modulus and elongation at break of the thermoplastic high amylose starch increase by 7.115 MPa, 182.1MPa and

Table 4-3. Signs and responses of a $\frac{1}{4}2^4$ two-level fractional factorial experiment design

Sample	$x_{234}=$ x_1	x_2	$x_{124}=$ x_3	$x_{123}=$ x_4	$x_{34}=$ x_{12}	$x_{24}=$ x_{13}	$x_{23}=$ x_{14}	x_{1234}	Strength, (MPa)	Modulus, (MPa)	Elongation, (%)
9	-	-	+	+	+	-	-	+	1.047	17.751	10.5
11	-	+	-	+	-	+	-	+	8.942	292.722	35.7
6	+	-	+	-	-	+	-	+	1.262	19.050	12.5
4	+	+	-	-	+	-	-	+	7.596	108.300	36.2

Table 4-4. Significance of factors on responses in an additional ¼ 2^4 two-level factorial processing experimental design

Effect name	Estimated effects		
	Strength	Modulus	Elongation
Average, β_0	4.712	109.46	23.73
1 + 234	-0.5655	-91.56	1.258
2	7.115	182.1	24.47
3 +124	-7.115	-182.1	-24.47
4+ 123	0.5655	91.56	-1.258
12 + 34	-0.7810	-92.86	-1.253
13 + 24	0.7810	92.86	1.253
14 + 23	-9.424	-218.9	-47.38
1234	9.424	218.9	47.38

24.47 % respectively when the water/glycerol ratio changes by one unit (from –1 to +1). The interaction of variable 1 (processing temperature) and variable 4 (blending time) has very obvious negative effects on the mechanical properties of thermoplastic amylose starch. The strength, modulus and elongation decrease by 9.424 MPa, 218.9 MPa and 47.38 % respectively when the confounded effect of the temperature-time two-factor interaction and water/glycerol-blending rpm two-factor interaction (14+23) increases by one unit. The effect of (water/glycerol ratio)-(blending rpm) two-factor interaction is small, which can be concluded from that the confounded effect of time and (temperature)-(water/glycerol ratio)-(blending rpm) three-factor interaction (4+123) is small (0.5655, 91.56 and –1.258 on tensile, modulus and elongation at break respectively). Time or temperature alone has a small significance on the responses. The confounded effects of temperature and (water/glycerol ratio)-(blending rpm)-(blending time) three-factor interaction (1+234) (0.5655, 91.56 and –1.258 on tensile, modulus and elongation at break respectively), as well as time and (temperature)-(water/glycerol ratio)-(rpm) three-factor interaction (4+123) are relatively small (0.5655, 91.56 and – 1.258 on tensile, modulus and elongation at break respectively).

4.1.2 Morphology

The morphology of native starch and thermoplastic starch was analyzed by using a scanning electron microscope, as shown in Figures 4-1 and 4-2. SEM images of native high amylose starch and normal starch show the morphology of individual cornstarch granules. High amylose starch exhibits different granular shapes and sizes compared to normal starch. The average diameter of individual high amylose starch granules varies from 7μm to 10μm for "large" and 1 μm to 4 μm for "small" granules. The average diameter of individual normal starch granules ranges from 15μm to 20μm for large and 1 μm to 7 μm for small granules. Both types of cornstarch particles are angular-shaped. After being plasticized, the individual granules were swelled or disrupted (compare images (a) and (b) in Figures 4-1 and 4-2).

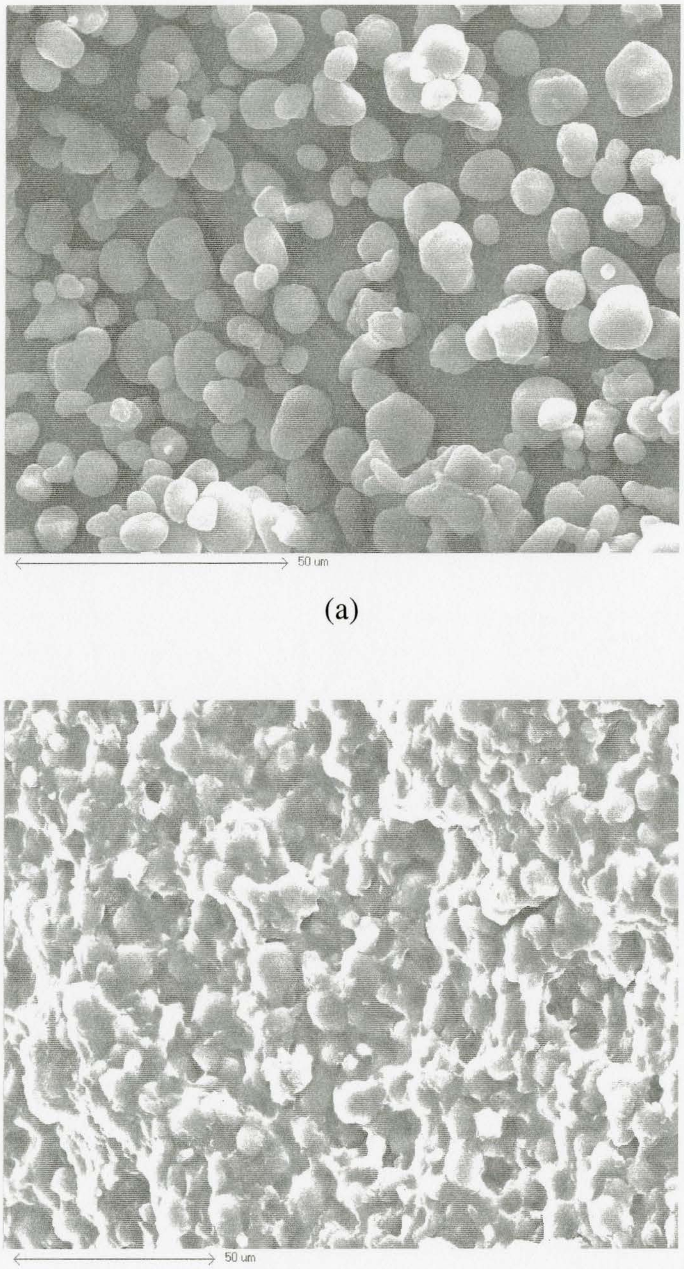

(a)

(b)

Figure 4-1. Comparison of SEM micrographs of native and thermoplastic high amylose starch: (a) native starch; (b) thermoplastic starch (starch/plasticizer: 1/1 wt/wt%, water/glycerol: 15/35wt/wt%, processing conditions: 120°C/4mins/45rpm).

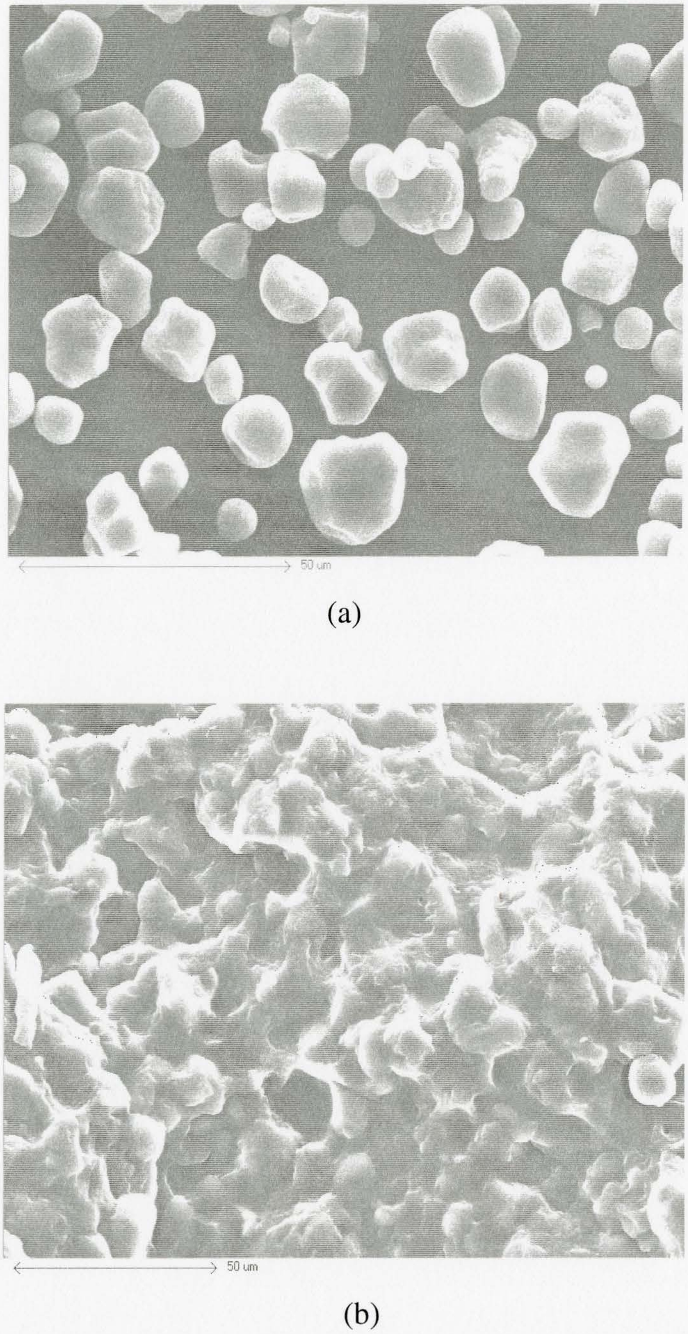

(a)

(b)

Figure 4-2. Comparison of SEM micrographs of native and thermoplastic normal starch: (a) native starch; (b) thermoplastic starch (starch/plasticizers: 2/1 wt/wt%, water/glycerol: 15/35 wt/wt%, processing conditions: 120ºC/4mins/45rpm).

4.1.3 Thermal properties

DSC thermograms of dry native high amylose starch are shown in Figure 4-3. In the first thermal scan, many small heat flow (for example, at 60.5°C, 83.1°C, 130.0°C, 154.8°C and 167.5°C) were observed. Those heat flow change, however, disappeared in second thermal scan, indicating that they may be attributed to thermal history in the starch drying. Neither a glass transition nor melting transition was observed in the first and second thermal scans. Poutanen and Forssell (1996) reported that the glass transition temperature T_g of dry amorphous starch is experimentally inaccessible because starch thermally degrades before it approaches its T_g. The T_g of dry starch was estimated to be in the range of 230-250°C, depending on the estimation methods used (for example,

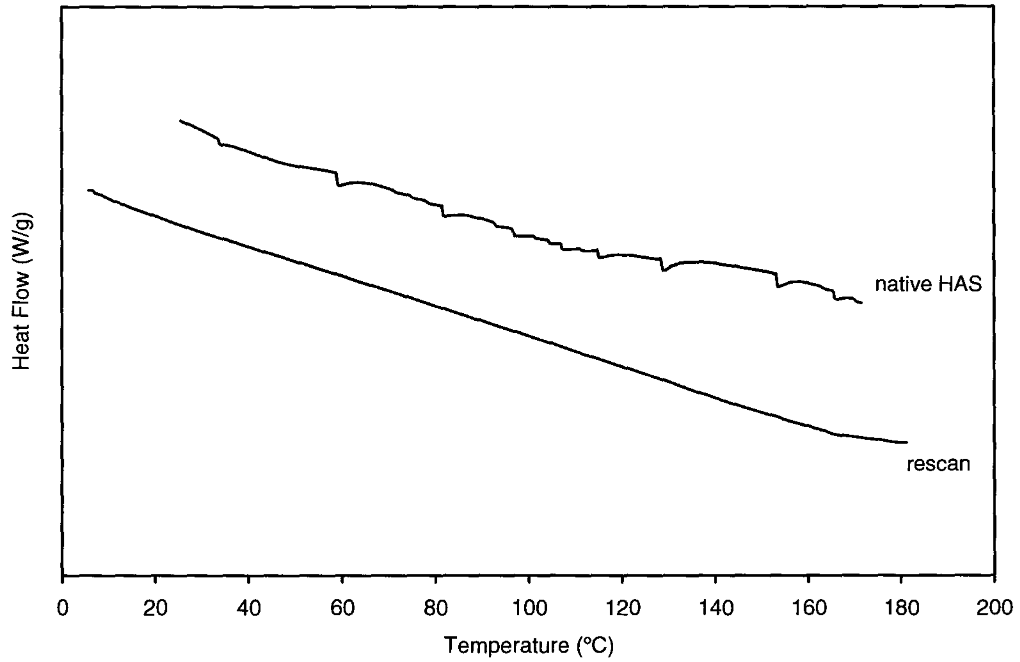

Figure 4-3. DSC thermograms of native high amylose starch.

study of the plasticizing effect of different amount of water, extrapolation to zero water content; and study of the oligomeric behavior, with extrapolation to high molar mass) (Poutanen and Forssell, 1996). The degradation temperature of high amylose starch was reported to be around 260°C (Avella *et al*, 2002).

DSC thermograms of the blends of native starches with plasticizers (water and/or glycerol) are shown in Figures 4-4 to 4-6 and the DSC thermal properties of the blends are summarized in Table 4-5.

Only one major plasticization exothermic peak occurred at a higher temperature in the DSC thermograms of the starch-glycerol blends in the first thermal scan. Same thermal behavior was observed for normal starch, high amylose starch and waxy starch. The peak temperature (T_p) of exothermic transition for high amylose starch, normal starch and waxy starch were 125.4°C, 133.6°C and 123.9°C respectively. The plasticization enthalpies were 36.33 J/g, 23.26 J/g and 39.32 J/g (based on dry starch) respectively. Waxy starch gives the highest enthalpy but the lowest T_p during plasticization. The high enthalpy of the waxy starch blend may be attributed to its high amylopectin content in the granules (almost 100%). Higher amylopectin content is responsible for a higher degree of amylopectin crystallinity. Higher enthalpy is a result of melting of more starch crystallites. Compared to waxy starch, normal starch with higher amylose content (23%wt) gives a lower enthalpy but a higher T_p. However, the melting enthalpy and T_p of high amylose starch are closer to those of waxy starch but higher than those of normal starch, probably attributed to its more amylose-lipid complexes. Part of the enthalpy change may come from destruction of the amylose-lipid complexes. No thermal transitions were observed in the second thermal scan in the temperature range

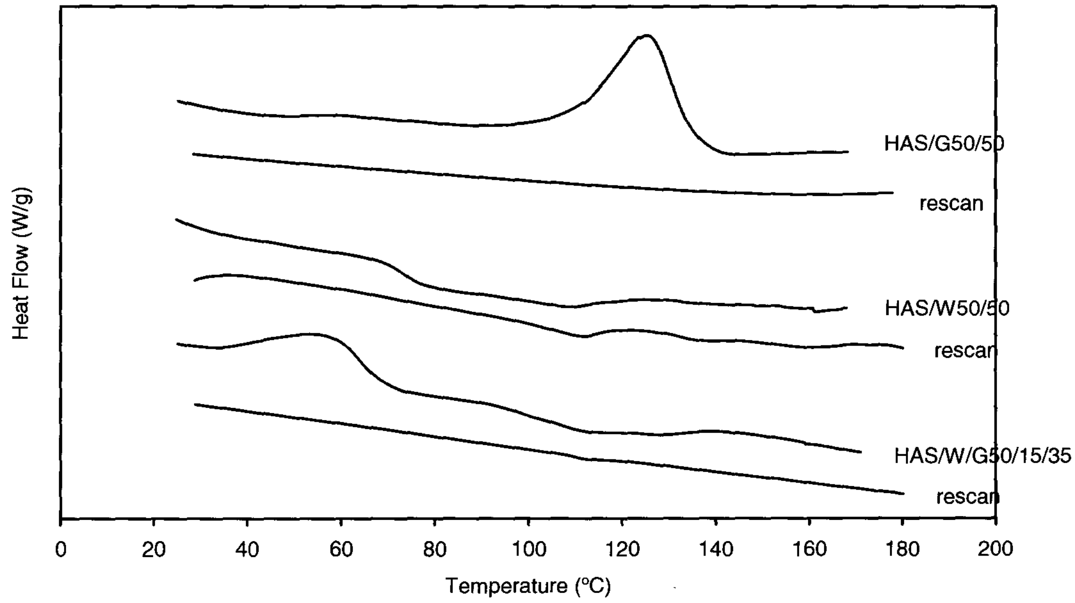

Figure 4-4. DSC thermograms of high amylose starch blends with plasticizers. The ratio of starch to plasticizer (wt/wt%): starch/glycerol =50/50; starch/water=50/50; starch/water/glycerol=50/15/35, respectively from top to bottom.

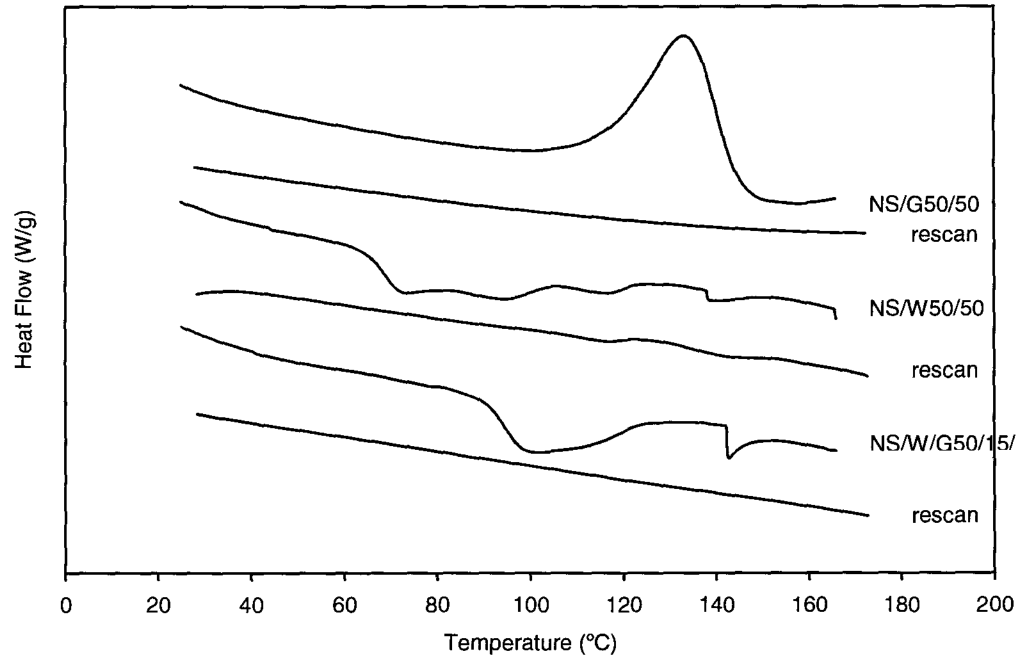

Figure 4-5. DSC thermograms of normal starch blends with plasticizers. The ratio of starch to plasticizer (wt/wt%): starch/glycerol =50/50; starch/water=50/50; starch/water/glycerol=50/15/35, respectively from top to bottom.

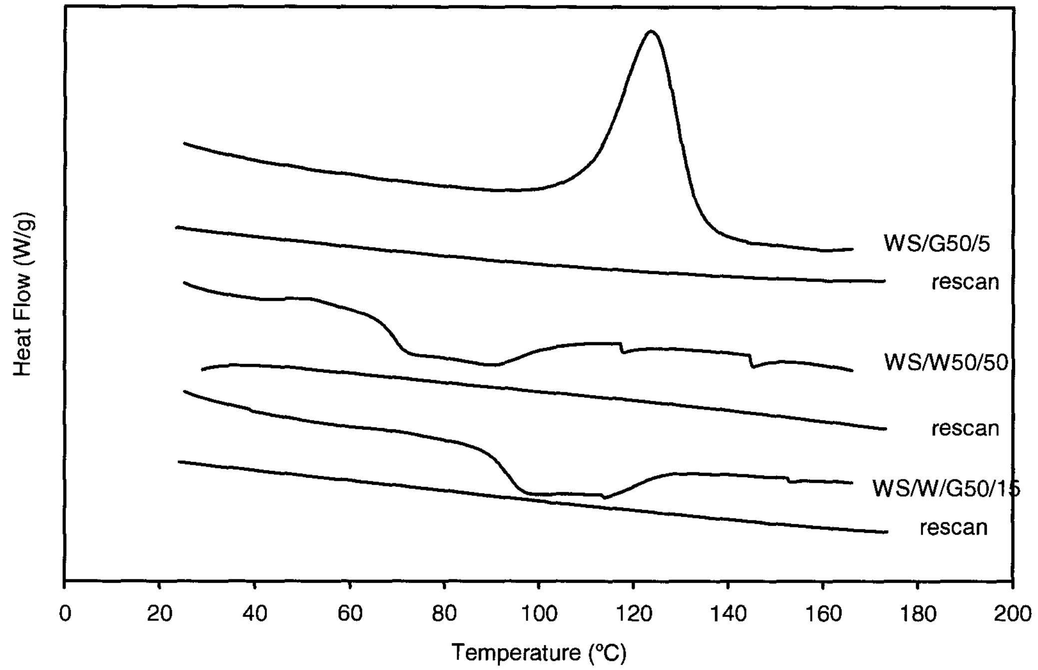

Figure 4-6. DSC thermograms of waxy starch blends with plasticizers. The ratio of starch to plasticizer (wt/wt%): starch/glycerol =50/50; starch/water=50/50; starch/water/glycerol=50/15/35, respectively from top to bottom.

Table 4-5. DSC parameters of starch blends with different plasticizers

Starch	Plasticizer	T_0(°C)	T_p(°C)	T_f(°C)	Enthalpy ΔH, (J/g)
HAS	Glycerol	87.8	125.4	144.1	(+) 36.33
NS	Glycerol	93.5	133.6	152.8	(+) 23.26
WS	Glycerol	85.8	123.9	144.6	(+) 39.32
HAS	Water	67.4	84.3	132.4	(-) 11.92
NS	Water	61.6	73.0	127.3	(-) 16.28
WS	Water	52.1	87.3	117.2	(-) 16.98
HAS	Water/glycerol(15/35)	28.3^a	56.3	76.3	(+) 11.14
		93.2^b	113.2	145.2	(-) 6.52
NS	Water/glycerol(15/35)	82.5	100.3	137.6	(-) 13.09
WS	Water/glycerol(15/35)	79.4	98.3	134.8	(-) 15.28

Enthalpy values are expressed in J/g of the dry starch; (+): exothermic, (-): endothermic; T_0= onset temperature; T_p=peak temperature; T_f=final temperature.

[a] The first exothermic peak in DSC thermogram of the blend of high amylose starch with plasticizers

[b] The second endothermic peak in DSC thermogram of the blend of high amylose starch with plasticizers.

measured, indicating that the crystalline structure in plasticized starch may be temperature resistant.

Gelatinization takes place when starch is heated in excess water. Starch gelatinization is accompanied by granular swelling, disappearance of crystallinity and diffusion of amylose molecules. The DSC thermograms of the blends of starch with water are shown in Figures 4-4 to 4-6. One broad gelatinization endothermic peak was observed in the DSC thermograms in the first thermal scan. Table 4-5 provides the onset temperature (T_o) and peak temperature (T_p) of the DSC thermograms of high amylose corn starch, normal corn starch and waxy corn starch, which are in agreement with data in the literature (Poutanen and Forssell, 1996). Waxy starch has the lowest T_o, but gives the highest T_p and enthalpy change. For the same reason as in the analysis of the starch-glycerol blends, the lower T_o, higher Tp and enthalpy change of the waxy starch blend with water can be attributed to its higher amylopectin content and its granular structure. Amylopectin crystallinity in waxy starch and amylose-lipid complexes in high amylose starch are more stable and more difficult to be destructurized. That is probably the reason why waxy starch and high amylose starch have a higher endothermic T_p in the gelatinization. From Table 4-5, it can be found that T_o and T_c of the gelatinization endotherms of the starch-water blends shift to higher temperature as the amylose content in the starches increases. The shifts of T_o and T_c with amylose content can be explained by the difference in average chain length of the outer chains of amylopectin and the presence of the intermediately branched, amylopectin-like molecules in the starches (Van

Soest and Borger, 1997; Jane *et al*, 1999). The molecular weight distribution indicates the presence of these intermediately branched, amylopectin-like molecules (see section 4.1.4).

In the second thermal scan, the DSC thermograms of the blends of high amylose starch and normal starch with water show a small exothermic peak and a small endothermic peak. The exothermic peak and endothermic peak correspond to the formation and melting of the amylopectin crystallinity. Very low enthalpies of the thermal transitions are attributed to weaker crystallinity. Higher enthalpies of the high amylose starch-water blend may be attributed to its higher amylose content. For high amylose starch, the onset temperature of the exotherm is 113.5°C and the onset temperature of the endotherm is 148.1°C. For normal starch, the onset temperature is 117.5°C and 137.7°C respectively. The crystallization enthalpy and melting enthalpy for the high amylose starch-water blend are 1.60 J/g and 0.74J/g (based on dry starch), respectively and for the normal starch-water blend, they are 0.54 J/g and 0.47 J/g (based on dry starch), respectively. The thermal transitions in the second thermal scan are probably related to retrogradation of gelatinized starch. After cooling of gelatinized starch, amylose molecules form helical associations of 40-70 glucose units whereas amylopectin crystallization occurs by association of the outermost short branches (Singh, 2003).

In the DSC thermogram of waxy starch-water blend in the second heating scanning, no thermal transition was observed due to the fact that waxy starch contains almost no amylose molecules.

When a mixture of water and glycerol (water/glycerol = 15/35, wt/wt) is used as a plasticizer, the high amylose starch blend with water and glycerol showed a different DSC thermogram as compared to that of normal starch and waxy starch blends. One exotherm and one endotherm appear in the DSC thermogram of the plasticized high amylose starch blend while only one broad endothermic peak is observed in the DSC thermograms of the plasticized normal starch blend and the waxy starch blend. When small amount of water is used as a plasticizer, water has been shown to act as the plasticizer of the amorphous part of starch granules (Poutanen and Forssell, 1996). Amylose molecules are responsible for the amorphous region of starch granules. High amylose starch has a totally different crystalline structure and molecular structure as compared to normal starch and waxy starch. As a result, an endothermic peak occurred at a higher temperature (T_p = 113.2°C), corresponding to the gelatinization or plasticization of crystalline component. Waxy starch contains little amylose and normal starch contains only 23% amylase; therefore, only broad endotherms were observed at lower temperature (T_p = 98.3 °C and 100.3°C, respectively) in the DSC thermograms of the waxy starch blend and the normal starch blend. Waxy starch gives higher enthalpy than normal starch because of its higher amylopectin content. No thermal transitions were observed in the DSC thermograms of starch-water-glycerol blends in the second thermal scan, indicating that no retrogradation occurred during cooling.

High amylose starch was blended with water and glycerol (ratio of water to glycerol = 15/35, wt/wt) in Haake Rheomix 3000. The thermal analysis of the thermoplastic starch was performed, as shown in Figure 4-7. No thermal transition is observed in first or second thermal scan, indicating that the starch granules in the blended starch were destructurized and the crystalline structure was temperature resistant. As a result, no melting transitions appear in the DSC thermograms. Averous and Boquillon (2004) reported that the glass transition temperature of thermoplastic starch is sometimes difficult to determine by DSC analysis because the heat capacity change is quite low at the glass transition temperature.

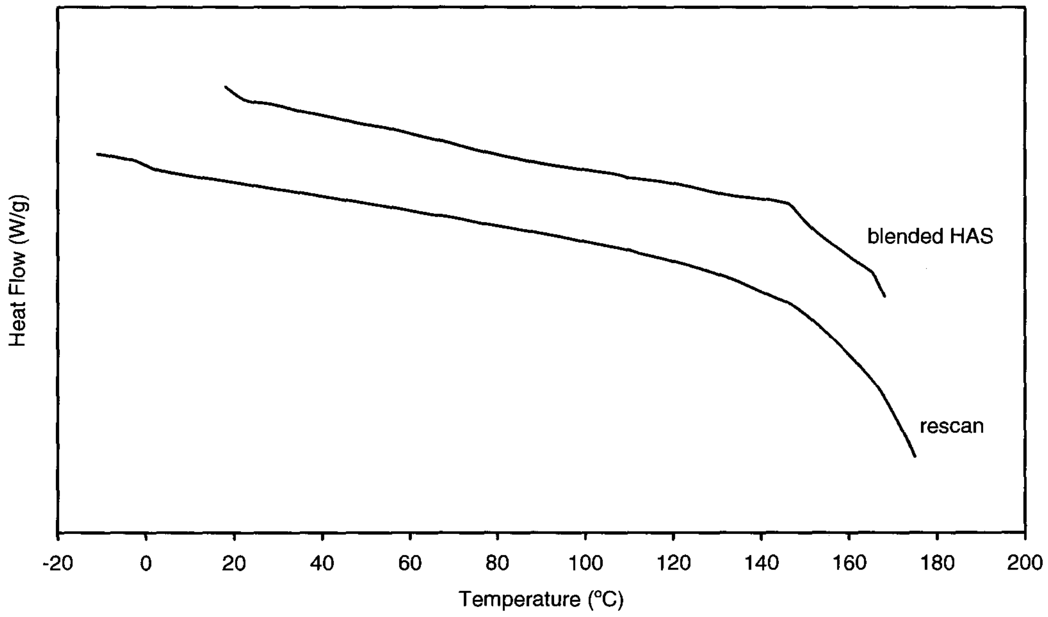

Figure 4-7. DSC thermograms of thermoplastic high amylose starch (starch/plasticizers ratio: 1/1 wt/wt%; water/glycerol ratio: 15/35 wt/wt%; blending conditions: 120°C/4mins/45rpm).

4.1.4 Molecular weight and molecular weight distribution

The molecular weights and molecular weight distributions of native high amylose starch, normal starch and waxy starch and their thermoplastic starches were measured using high performance size exclusion chromatography (HPSEC). The HPSEC chromatograms of the native starches are shown in Figure 4-8. The average molecular weights are summarized in Table 4-6.

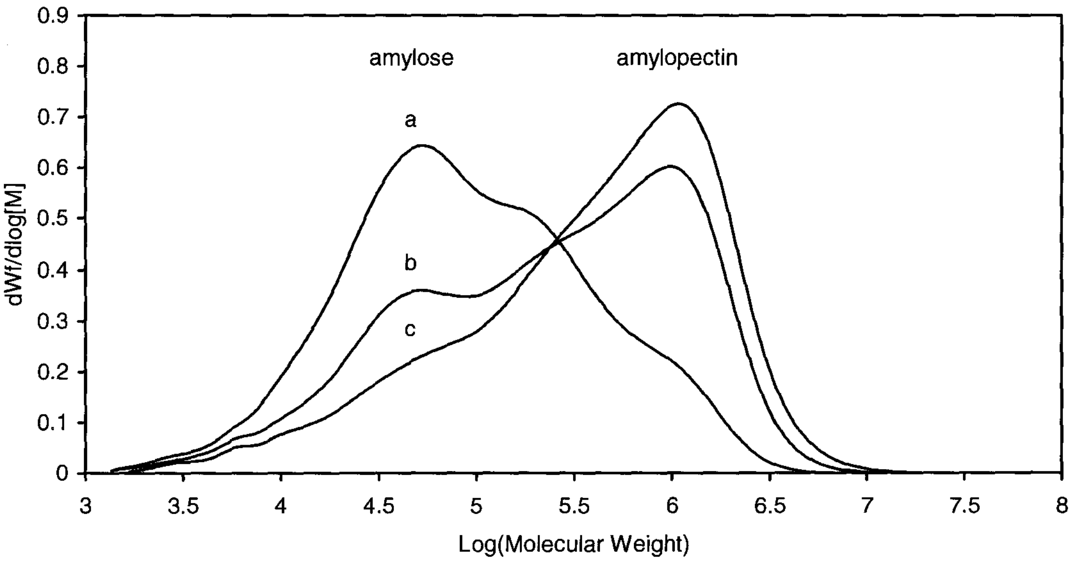

Figure 4-8. HPSEC chromatograms of native cornstarches: (a) high amylose starch, (b) normal starch, (c) waxy starch.

The molecular weight distributions of native starches in Figure 4-8 show a bimodal pattern, which is in agreement with that expected for a mixture of linear amylose and branched amylopectin. The major peak of the molecular weight distribution (MWD) profile of high amylose starch occurs at the same molecular weight of lower molecular weight portion of normal starch, which is attributed to amylose. The major peak of the MWD profile of waxy starch appears at the same place of higher molecular weight portion of normal starch, which is attributed to amylopectin. In the chromatogram of native high amylose starch, another peak between the amylose peak and amylopectin peak was observed. It can be attributed to the presence of intermediately branched,

Table 4-6. Average molecular weights of native and thermoplastic starches

Materials	Average molecular weights ($\times 10^{-3}$ g/mol)			
	Mn	Mw	Mz	Mw/Mn
Native HAS	41.0	214.5	463.7	5.23
Native NS	62.3	531.4	821.2	8.53
Native WS	90.1	722.2	1040.0	8.02
TP-HAS1	38.9	203.9	448.5	5.24
TP-NS	56.6	613.5	853.1	10.84
TP-WS	103.9	761.1	1000.0	7.33

amylopectin-like molecules. DSC studies showed their presence (see section 4.1.3). High amylose starch has the lowest average molecular weights while waxy starch shows the highest average molecular weights as a result of the difference of amylose contents in those starches, as shown in Table 4-6. Carvalho *et al* (2003) and Funke *et al* (1998) reported similar GPC-patterns of native starches. However, different values were obtained from Carvalho *et al* (2003) due to the difference in the experimental method and starch sources.

The molecular weight and its distribution of thermoplastic starch (starch/plasticizer ratio is 50/50 wt/wt%, water/glycerol ratio is 15/35 wt/wt%) were also investigated. The HPSEC chromatograms of native starches and thermoplastic starches are shown in Figures 4-9 to 4-11. The average molecular weights of the thermoplastic starches are presented in Table 4-6. The MWD curve of the plasticized high amylose starch shifts to a lower molecular weight compared to that of the native high amylose starch, indicating the starch underwent some extent of degradation during blending. However, comparing the chromatograms of the native normal starch and the thermoplastic normal starch (in Figure 4-9), as well as the chromatograms of the native waxy starch and the thermoplastic waxy starch (in Figure 4-10), it can be found that the amylose peaks of the thermoplastic starches are lower than those of the native starches while the amylopectin peaks of the thermoplastic starches are higher than those of native starches. It seems to indicate that amylose underwent degradation and amylopectin was more resistant to depolymerization. The amylopectin content in the thermoplastic normal starch and the thermoplastic waxy starch was increased compared to those of the native starches. The increase in the amylopectin contents of thermoplastic normal starch and waxy starch is probably attributed to the decrease of amylose content relative to amylopectin content in the materials.

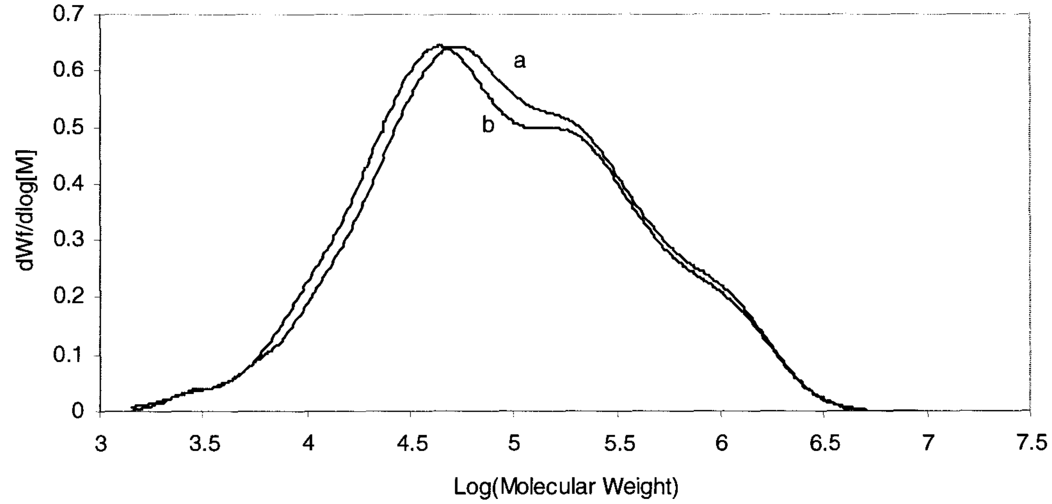

Figure 4-9. HPSEC chromatograms of the native high amylose starch (a) and thermoplastic high amylose starch (b) (starch/plasticizer ratio: 1/1 wt/wt%; water/glycerol ratio: 15/35 wt/wt%; blending conditions: 120°C/4mins/45rpm).

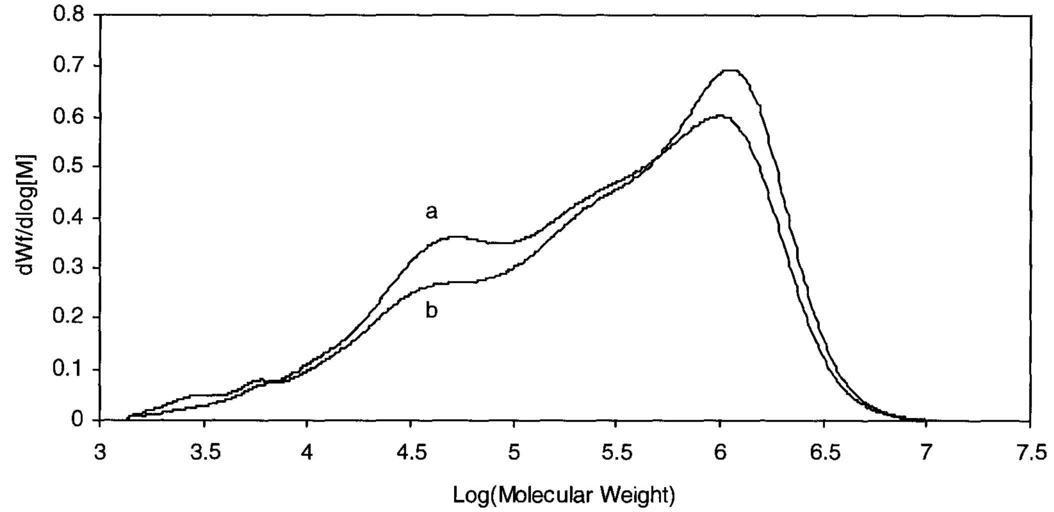

Figure 4-10. HPSEC chromatograms of the native normal starch (a) and thermoplastic normal starch (b) (starch/plasticizer ratio: 2/1 wt/wt%; water/glycerol ratio: 15/35 wt/wt%; blending conditions: 120°C/4mins/45rpm).

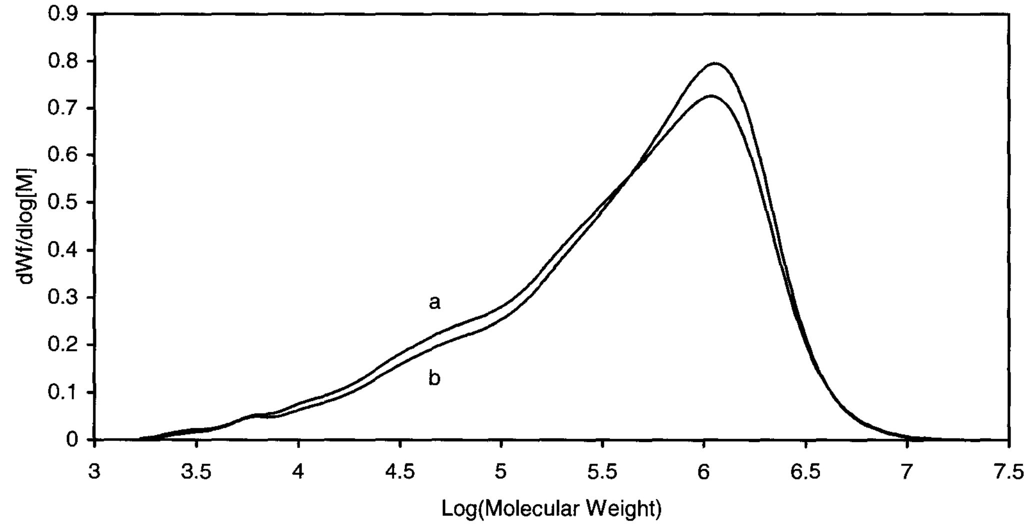

Figure 4-11. HPSEC chromatograms of the native waxy starch (a) and thermoplastic waxy starch (b) (starch/plasticizer ratio: 2/1 wt/wt%; water/glycerol ratio: 15/35 wt/wt%; blending conditions: 120°C/4mins/45rpm).

4.1.5 Mechanical properties

High amylose starch was blended with various amounts of plasticizers (water and glycerol) to obtain thermoplastic starch. The mechanical properties of thermoplastic starch were measured, as shown in Appendix A. The tensile strength of thermoplastic high amylose starch ranges from approximately 0.8 MPa to approximately 9 MPa, depending on processing conditions and plasticizer content. The elastic modulus varies from approximately 16 MPa to approximately 300 MPa. Elongation at break varies between around 10% and around 35%. Higher processing temperature, processing time, mixing rpm or water/glycerol ratio gives better whole mechanical properties. More water evaporates during blending at higher blending temperatures, times or ratios of water to glycerol; therefore, the total plasticizer content in the blended starch decreases. The ratio of glycerol to starch can be assumed to remain unchanged during blending (Averous and Fringant, 2001). The total plasticizer content is calculated after the water content is determined, as presented in Table 4-1. The relationship between mechanical properties and total plasticizer content is shown in Figures 4-12 to 4-14. The tensile strength, tensile modulus and elongation at break tend to decrease with increasing the ratio of total plasticizers to starch (i.e. increasing total plasticizer content in the blended starch). This result is in agreement with that obtained by You *et al* (2003) and Averous *et al* (2001b). However, when both higher blending temperature and longer blending time (150°C and 10 mins) were applied simultaneously, the water evaporated too quickly. As a result, the starch burned because of the rapid temperature rise in the mix chamber (up to 190°C) as well as the action of mechanical force (such as samples 10, 12 and 14). Lorcks (1998) pointed that plasticization process of starch is exothermic when dry starch is plasticized in compound extruders without water or water content is less than 5%(wt). Our DSC studies indicated that an exothermic transition took place when starch was blended with glycerol without water (shown in 4.1.3).

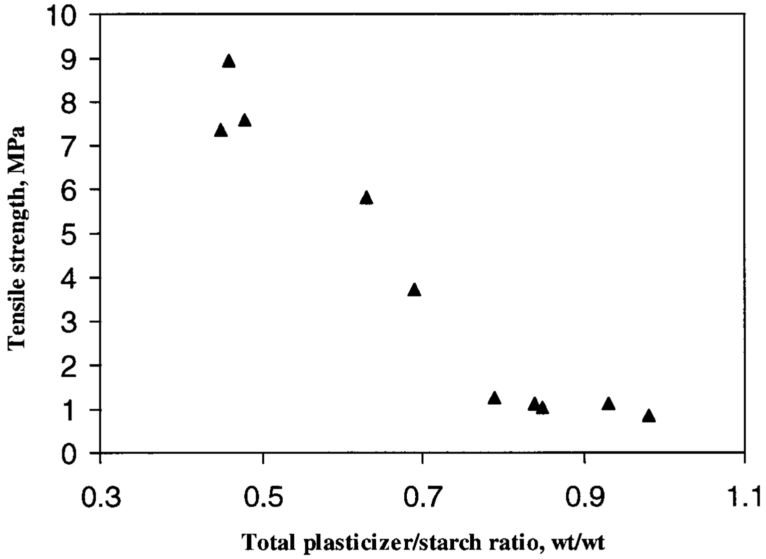

Figure 4-12. The effect of total plasticizer / starch ratio on tensile strength of thermoplastic high amylose starch.

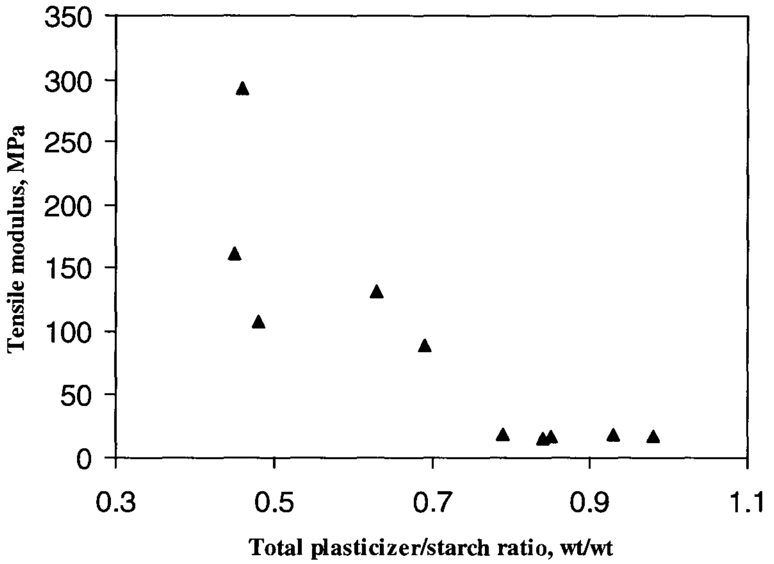

Figure 4-13. The effect of total plasticizer / starch ratio on tensile modulus of thermoplastic high amylose starch.

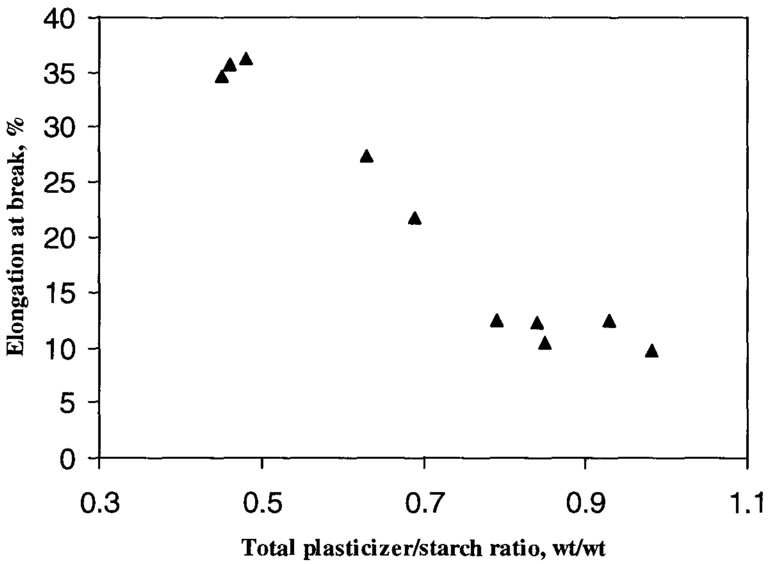

Figure 4-14. The effect of total plasticizer / starch ratio on elongation at break of thermoplastic high amylose starch.

Mechanical properties of the thermoplastic starch made by different processing methods were compared, as shown in Table 4-7. Post-extrusion molded thermoplastic high amylose starches, no matter what processing conditions and water/glycerol ratio, show higher tensile strength and elongation at break while compression-molded specimens have better tensile modulus. The difference in mechanical properties of thermoplastic high amylose starch prepared with different processing methods may be attributed to extending of starch molecular chains in the post-extrusion molded specimens through the die of a Rosand capillary rheometer. High amylose starch contains approximately 70% amylose. The linear amylose molecular chains probably were stretched or rearranged under the action of shear stress in the molding, which leads to higher tensile strength and elongation at break of the materials. In addition, the morphology studies of thermoplastic high amylose starch/PLA blends show an extended shape of starch phase in the blends (see 4.2.1).

Table 4-7. Influence of molding methods on the mechanical properties of thermoplastic starches

No	Code	Post-extrusion molded specimen			Compression-molded specimen		
		Tensile strength (MPa)	Tensile modulus (MPa)	Elongation at break (%)	Tensile strength (MPa)	Tensile modulus (MPa)	Elongation at break (%)
2	HAS-150-4-45-1-15/35	1.12±0.14	16.58±0.57	12.3±2.6	0.778±0.076	57.44±7.86	7.91±0.90
3	HAS-120-4-45-1-35/15	3.73±1.22	88.03±30.13	21.8±1.0	1.39±0.55	81.13±20.18	7.65±1.08
5	HAS-120-4-65-1-15/35	1.12±0.29	18.24±2.29	12.4±3.7	0.573±0.065	35.98±3.76	7.21±0.62
8	HAS-150-4-65-1-35/15	7.35±0.89	160.8±103.1	34.6±3.7	3.21±0.56	256.0±17.7	8.88±0.97
15	HAS-120-4-45-1-15/35	0.888±0.120	18.59±1.09	10.1±2.0	0.888±0.084	22.16±5.19	9.51±1.25
16	NS-120-4-45-2/1-15/35	2.81±0.32	55.05±18.09	76.0±33.8	5.83±0.07	175.6±13.7	21.6±1.2

---

[1] The specimens for tensile testing were post-extruded at 130°C in a Rosand capillary rheometer.

Both the tensile strength and modulus of post-extrusion molded thermoplastic normal starch are lower than those of samples from compression molding. But, post-extrusion molded thermoplastic normal starch shows higher elongation at break. The behavior of TP-NS is probably attributed to the low amylose content in normal starch granules (about 23%). In this case, the stretch effect of linear amylose molecular chains through the die of a Rosand capillary rheometer during processing is not significant. Extrusion molded thermoplastic waxy starch exhibits similar tensile strength (2.96MPa) but higher modulus (75.98MPa) and lower elongation at break (33.7%) compared to thermoplastic normal starch with same formula, whose tensile strength, modulus and elongation at break are 2.81 MPa, 55.09 MPa and 76.0% respectively, as presented in Table 4-1. Higher modulus and lower elongation of thermoplastic waxy starch may be attributed to its almost 100% amylopectin structure (see section 4.1.4).

4.1.6 **Rheological properties**

Rheological properties of some selected thermoplastic starch are shown in Figures 4-15 to 4-18. The thermoplastic starch materials exhibit shear thinning behavior that can be described by power law equation: $\eta = m\dot{\gamma}^{n-1}$. The power law parameters are presented in Table 4-8. The power-law index n values are in the range of 0.25 to 0.41. The consistency m changes between 12000 Pa.s^n and 37000 Pa.s^n.

The temperature dependency of shear viscosity of thermoplastic high amylose starch is complicated. In some cases, for example, the shear viscosity of sample HAS-

150-4-45-1-15/35 decreases with increasing temperature, as shown in Figure 4-15. The relationship between shear viscosity, shear rate and temperature can be described by:

$$\eta = m\,\mathrm{EXP}(\frac{E}{RT})\dot{\gamma}^{n-1} \qquad (4\text{-}3)$$

where E = activation energy, J/g

R = gas constant, 8.314 J/mol-K

m = consistency index, $Pa.s^n$

The model parameters are shown in Table 4-9.

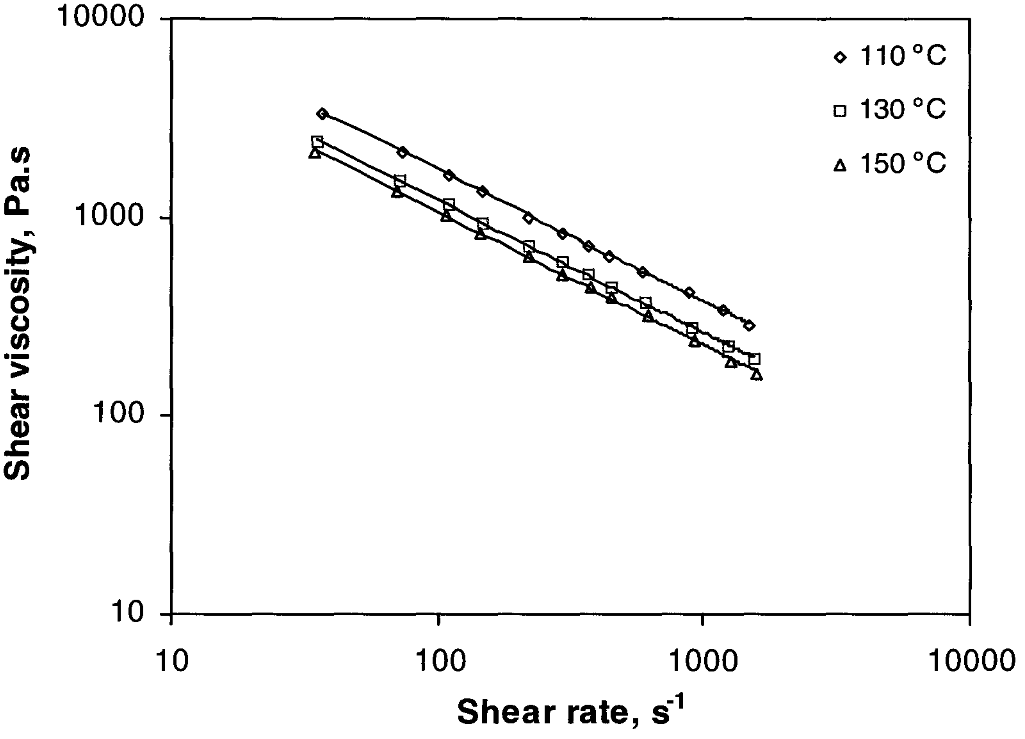

Figure 4-15. Shear viscosity of thermoplastic high amylose starch (HAS-150-4-45-1-15/35) at different temperature (starch/plasticizer ratio: 1/1 wt/wt%; water/glycerol ratio: 15/35 wt/wt%; blending conditions: 150°C/4mins/45rpm).

However, in other cases, the shear viscosity does not always decrease with increasing temperature. For example, sample HAS-120-4-45-1-15/35 has higher viscosity at 150°C than at 110°C and 130°C (as shown in Figure 4-16), and sample HAS-120-4-65-1-15/35 has higher viscosity at 130°C than at 110°C (as shown in Figure C3 in Appendix C). This is probably related to formation of new hydrogen bonds in those samples. The hydrogen bond increased the interaction of starch molecules, resulting in decreases in the shear viscosities of the samples.

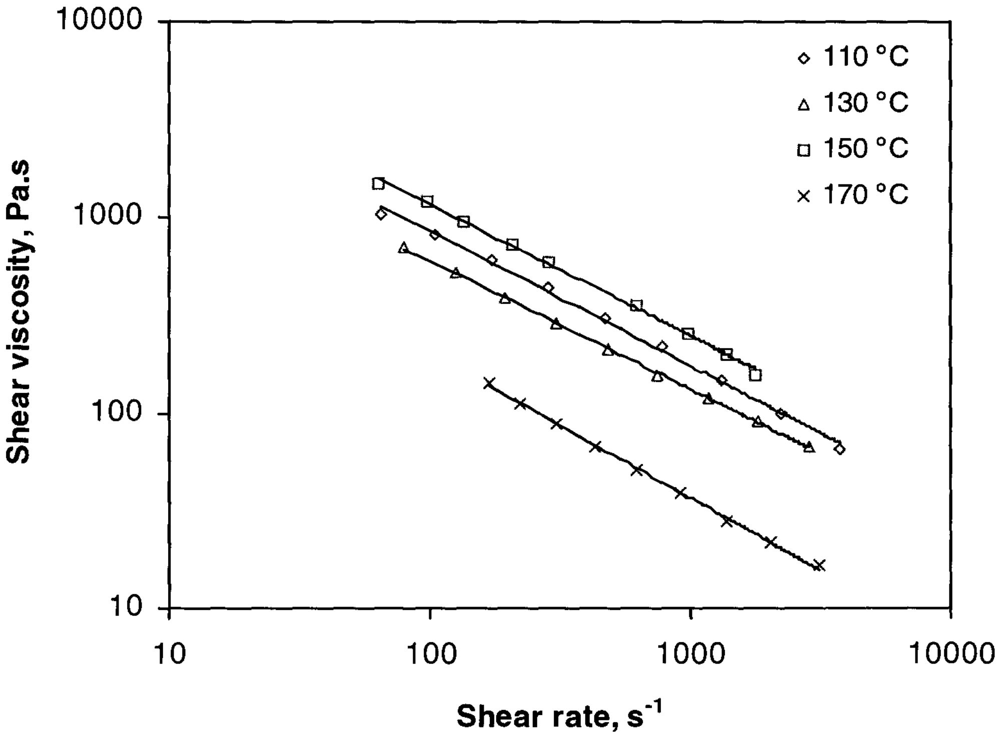

Figure 4-16. Shear viscosity of thermoplastic high amylose starch (HAS-120-4-45-1-15/35) at different temperature (starch/plasticizer ratio: 1/1 wt/wt%; water/glycerol: 15/35 wt/wt%; blending conditions: 120°C/4mins/45rpm).

The shear viscosities of thermoplastic normal starch and thermoplastic waxy starch decrease with increasing the temperature, as shown in Figures 4-17 and 4-18. The thermoplastic waxy starch exhibits higher shear viscosity under the same temperature compared to thermoplastic normal starch with the same composition (see Figure 4-19). The higher viscosity of thermoplastic waxy starch may be attributed to higher average molecular weight of waxy starch. The thermoplastic waxy starch also shows higher power law index n value (0.46) and activation energy (4949.0 J/mol) but a lower consistency index m_0 (206.1 Ps.s^n) than thermoplastic normal starch whose power-law index n, activation energy and consistency index m_0 are 0.34, 3695.5 J/mol and 1468 Ps.s^n, respectively. Normal starch contains about 23wt% of essentially linear amylose molecules while waxy starch almost consists of almost 100% highly branched amylopectin molecules.

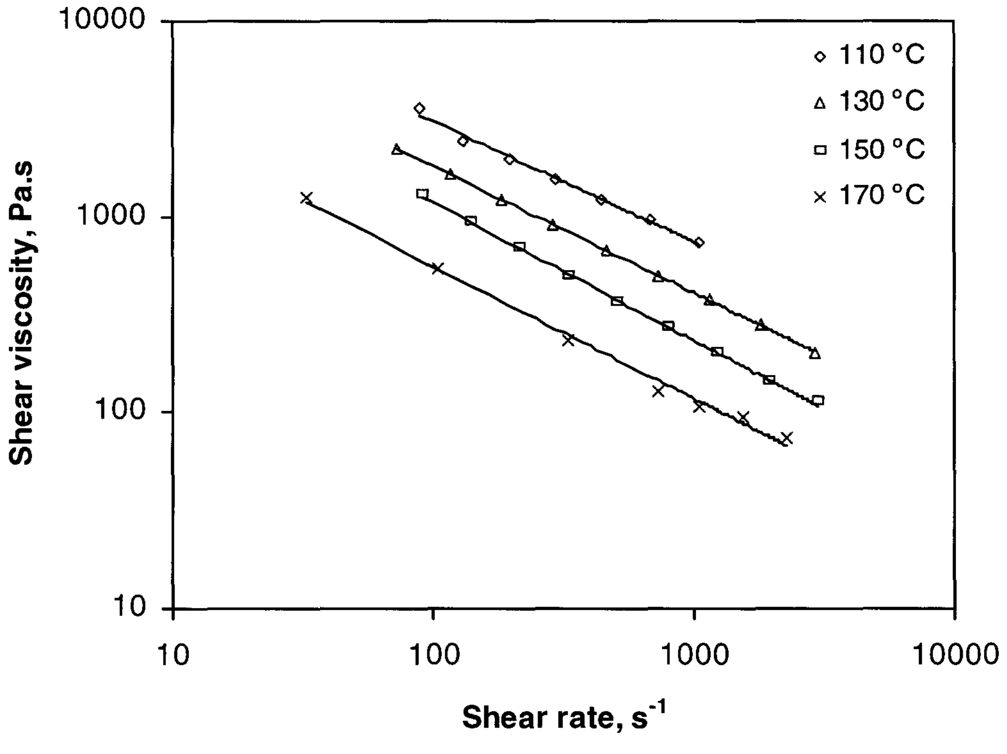

Figure 4-17. Shear viscosity of thermoplastic normal starch (NS-120-4-45-2/1-15/35) at different temperature (starch/plasticizer ratio: 2/1wt/wt%; water/glycerol: 15/35wt/wt%; blending conditions: 120°C/4mins/45rpm).

The entanglement of linear amylose molecules causes thermoplastic normal starch to be more viscous (higher consistency index m_0). Thermoplastic normal starch has a broader molecular weight distribution of (Mw/Mn of 10.84), compared to thermoplastic waxy starch (Mw/Mn of 7.33), as presented in Table 4-6. As a result, thermoplastic normal starch exhibits higher degree of non-Newtonian behavior (lower power-law index n) than thermoplastic waxy starch starch.

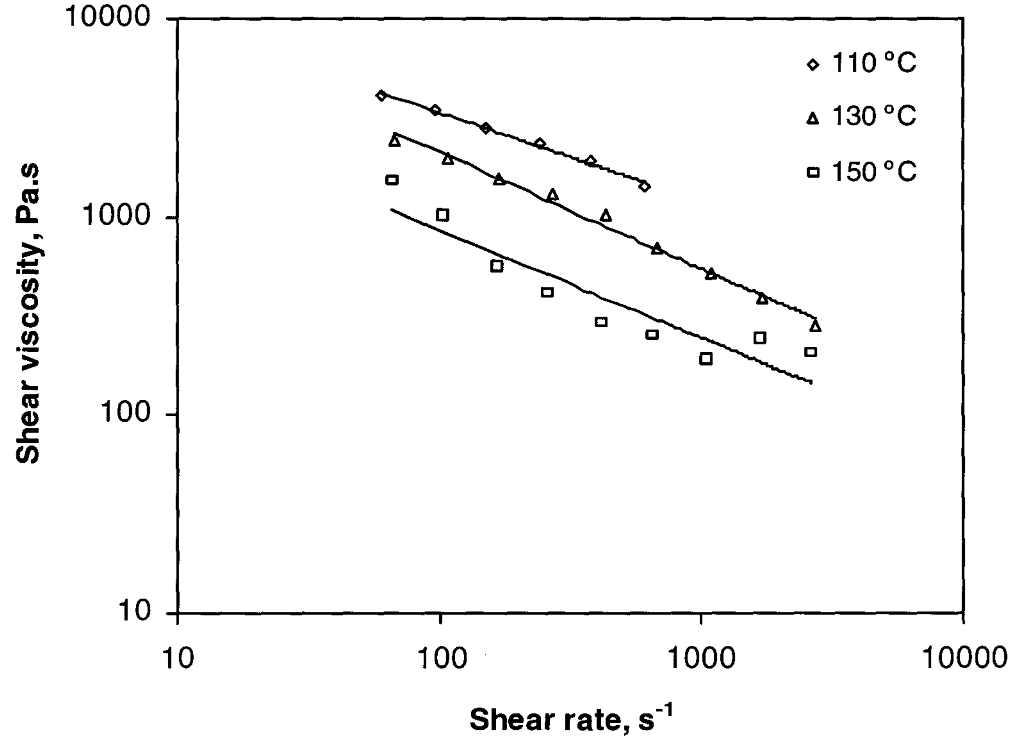

Figure 4-18. Shear viscosity of thermoplastic waxy starch (WS-120-4-45-2/1-15/35) at different temperature (starch/plasticizer ratio: 2/1wt/wt%; water/glycerol: 15/35wt/wt%; blending conditions: 120°C/4mins/45rpm).

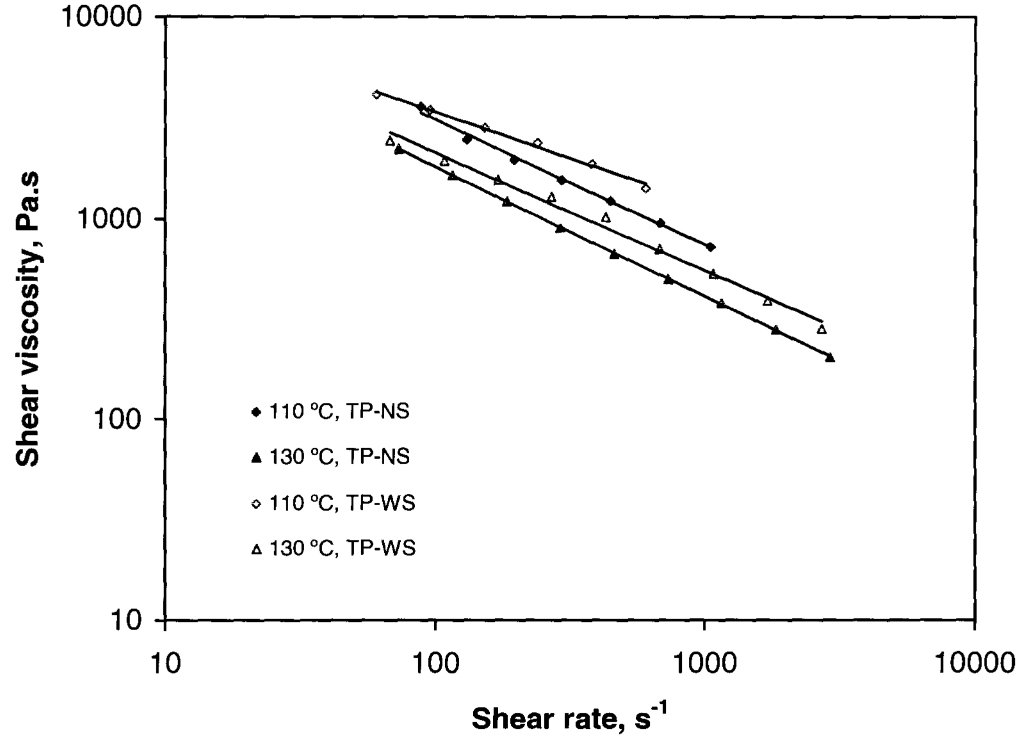

Figure 4-19. Comparison of shear viscosity of thermoplastic normal starch at 110°C and 130°C with those of thermoplastic waxy starch with same composition (starch/plasticizer ratio: 2/1wt/wt%; water/glycerol: 15/35wt/wt%; blending conditions: 120°C/4mins/45rpm).

The thermoplastic starches blended at higher processing temperature (150°C) give higher shear viscosity under same measurement conditions. For example, samples 2 and 6 show higher average values of consistency index m than other samples, as shown in Table 4-9. It may be attributed to the fact that higher processing temperature causes increased water evaporation and therefore a decrease in total plasticizer content. The shear viscosity increases with decreasing plasticizer content (Valle *et al*, 1998; Yu *et al*, 1996).

Table 4-8. Power law parameters for thermoplastic starch

No.	Code	Water/glycerol ratio, wt/wt	Blending conditions	Measurement temperature, (°C)	m (Pa.s ^{n})	n	R^2
1	HAS-120-4-45-1-15/35	15/35	120°C/4mins/45rpm	110	16959	0.34	0.9998
				130	14800	0.36	0.9978
				150	19666	0.35	0.997
2	HAS-150-4-45-1-15/35	15/35	150°C/4mins/45rpm	110	36332	0.34	0.9999
				130	26205	0.33	0.9997
				150	23517	0.33	0.9994
3	HAS-120-4-45-1-35/15	35/15	120°C/4mins/45rpm	110	17110	0.26	0.9983
				130	5622.3	0.37	0.9951
				150	/	/	/
5	HAS-120-4-65-1-15/35	15/35	120°C/4mins/65rpm	110	15742	0.34	0.9997
				130	23002	0.32	0.9990
				150	24171	0.25	0.9964
6	HAS-150-4-65-1-15/35	15/35	150°C/4mins/65rpm	110	36550	0.36	0.9985
				130	25222	0.36	0.9995
				150	24083	0.33	0.9997
9	HAS-120-10-65-1-15/35	15/35	120°C/10mins/65rpm	110	22848	0.37	0.9985
				130	14509	0.38	0.9986
				150	12536	0.41	0.9991

Starch/plasticizers ratio: 1/1 (wt/wt).

Table 4-9. Temperature and shear rate dependence model parameter of shear viscosity of thermoplastic starches

No.	Code	Starch/plasticizer ratio, wt/wt	Blending conditions	Consistency index m_0 (Pa.s ^{n})	Power law index, n	Activation energy E, J	R ^{2}
1	HAS-150-4-45-1-15/35	1/1	150°C/ 4mins/ 45rpm	199.8±83.3	0.34±0.02	16,878±1400	0.99
2	HAS-150-4-65-1-15/35	1/1	150°C/ 4mins/ 65rpm	99.92±38.65	0.35±0.02	19,046±1351	0.99
3	HAS-120-10-65-1-15/35	1/1	120°C/ 4mins/ 65rpm	611.3±382.1	0.40±0.02	11,407±2535	0.99
4	NS-120-4-45-2/1-15/35	2/1	120°C/ 4mins/ 45rpm	1468±157	0.34±0.01	3695.5±193.2	0.99
5	WS-120-4-45-2/1-15/35	2/1	120°C/ 4mins/ 45rpm	206.1±132.1	0.46±0.04	4949.0±410.8	0.95

Water/glycerol ratio in the thermoplastic starches: 15/35 (wt/wt %).

4.2 Structure and properties of thermoplastic starch/PLA blends

4.2.1 Morphology

The morphology of thermoplastic starch/PLA blends was analyzed using a Philips scanning electron microscope. The SEM images of compression-molded thermoplastic high amylose starch/PLA blends with different blend compositions are shown in Figure 4-20. Figure 4-20a shows the morphology of pure thermoplastic high amylose starch. There is no individual granule visible in the image, indicating that the high amylose starch granules are swollen or disrupted. In Figure 4-20b, PLA phases (black areas, as shown by an arrow) with a dimension of approximately 2 μm x 10 μm are distributed in a continuous TPS phase. The size of PLA phases in the blends increases as PLA content increases. In Figure 4-20c, the diameters of black hole-shaped PLA phases are approximately 2- 5 μm when the ratio of high amylose starch to PLA is 50/50 wt/wt%. The PLA phases in Figure 4-20d have approximate diameters of 5-10 μm when the ratio of high amylose starch to PLA is 30/70 wt/wt%. SEM micrographs of post-extrusion molded high amylose starch/PLA blends in Figure 4-21 also indicate that the size of PLA phases increases with increasing PLA content in the blends. Relatively smooth surfaces of both thermoplastic starch and PLA phases imply that the compatibility between TPS and PLA components is poor. The SEM micrographs of thermoplastic normal starch/PLA blends in Figure 4-22 show that the size of PLA phases in those blends increases as the PLA content increases and the comparability between the two components is poor.

Martin and Averous (2001a) reported that the PLA was partially miscible with thermoplastic wheat starch. In our analysis on thermal properties of thermoplastic corn starch/PLA blends (see section 4.2.2), the glass transition temperature T_g of PLA component in the blends shifted to lower values compared to T_g of pure PLA, indicating a slight degree of compatibility between TPS and PLA components.

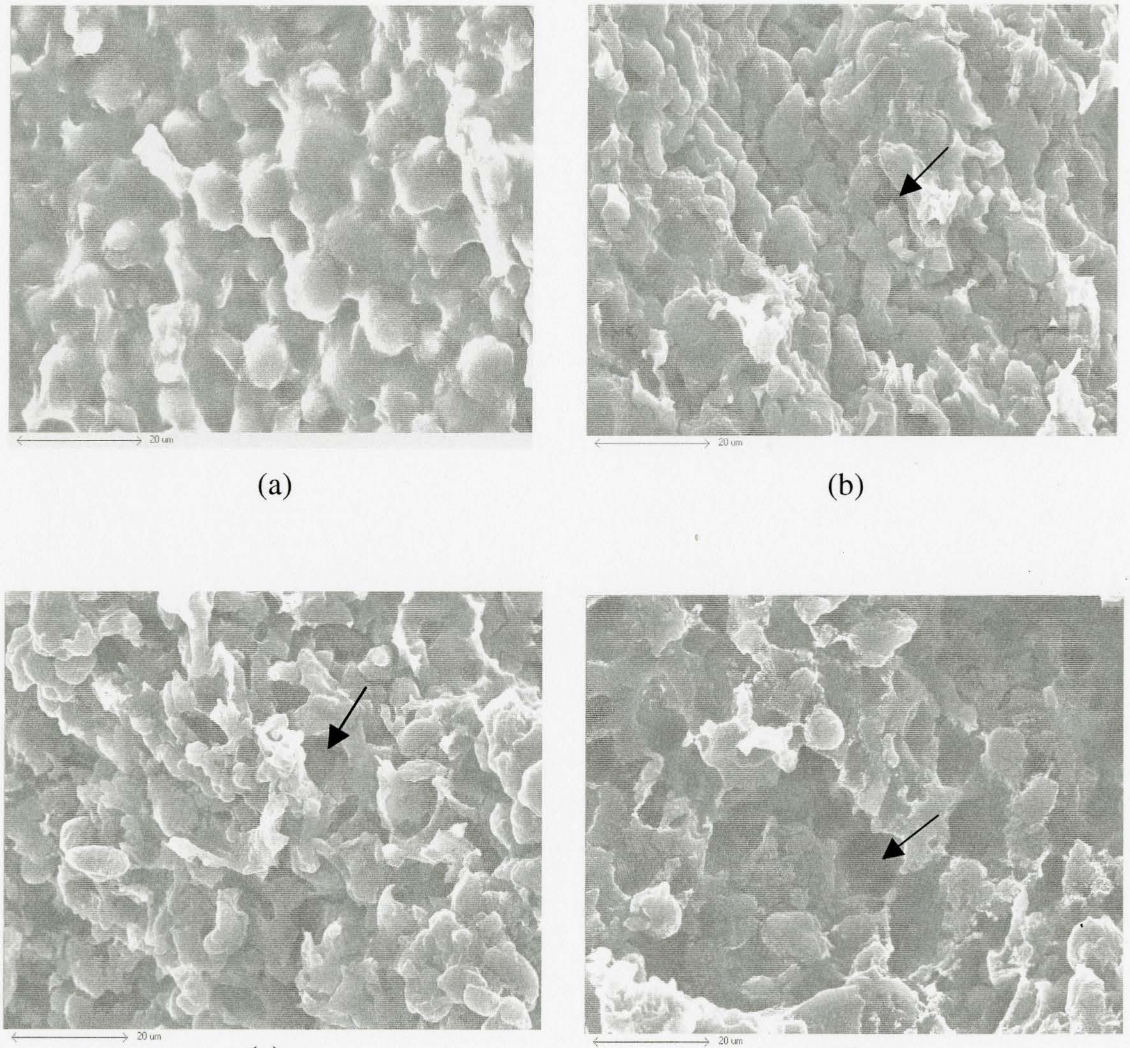

(a) (b)

(c) (d)

Figure 4-20. SEM images of compression molded thermoplastic high amylose starch/PLA blends with different ratio of starch to PLA (wt/wt%): (a) 100/0; (b) 70/30; (c) 50/50; (d) 30/70; Starch/plasticizer ratio: 1/1(wt/wt%); water/glycerol ratio: 15/35(wt/wt%).

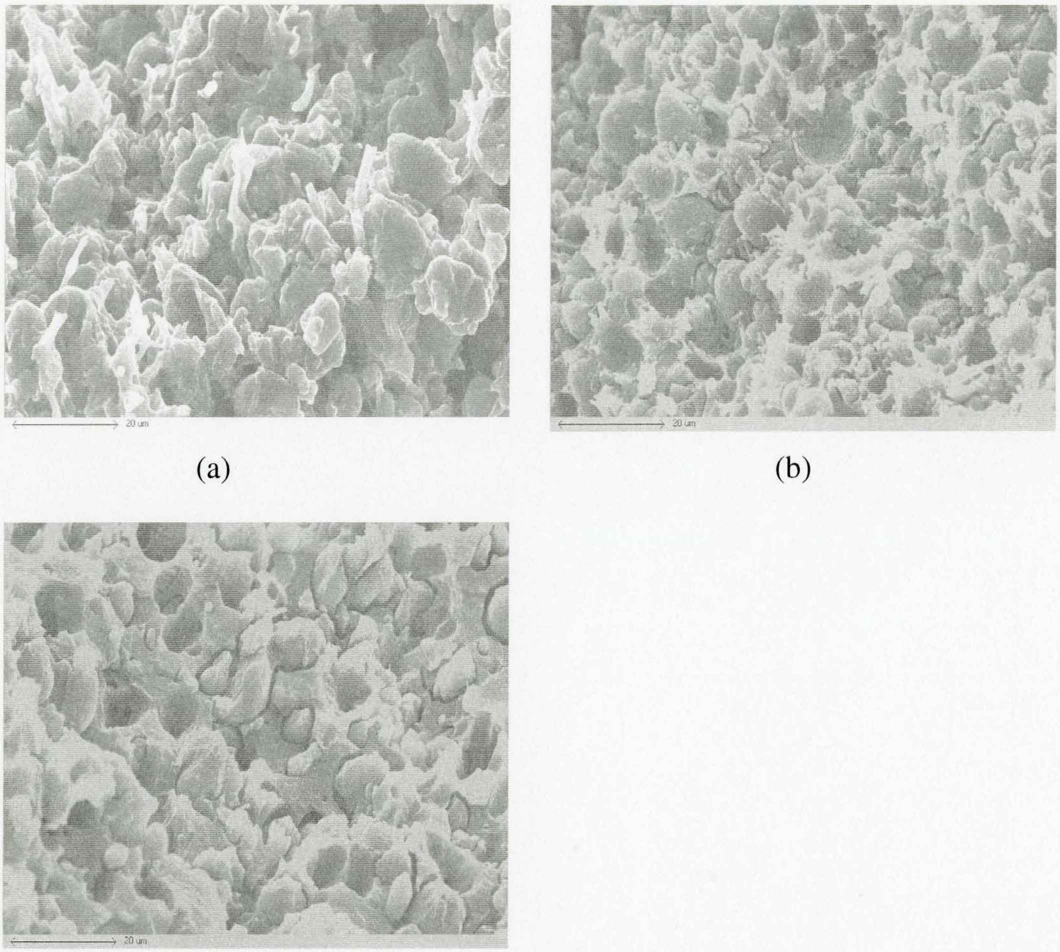

(a) (b)

(c)

Figure 4-21. SEM images of post-extrusion molded thermoplastic high amylose starch/PLA blends with different ratio of starch to PLA (wt/wt%): (a) 70/30; (b) 50/50; (c) 30/70; starch/plasticizer ratio: 1/1(wt/wt%); water/glycerol ratio: 15/35(wt/wt%).

The morphologies of compression molded and post-extrusion molded thermoplastic high amylose starch/PLA blends are compared, as shown in Figures 4-20 and 4-21. In Figure 4-21, the TPS phase shows an extended shape, indicating that the starch molecular chains were stretched under the action of shear stress during post-extrusion through the die of a Rosand capillary rhemometer. In Figures 4-21b and 4-21c, the black hole-shaped PLA phases with diameters of about 3-7μm appear in the continuous TPS phase. The size of those black holes is smaller than that of PLA phases observed in Figure 4-20, implying that the PLA molecular chains in the blends were also stretched during the post-extrusion molding.

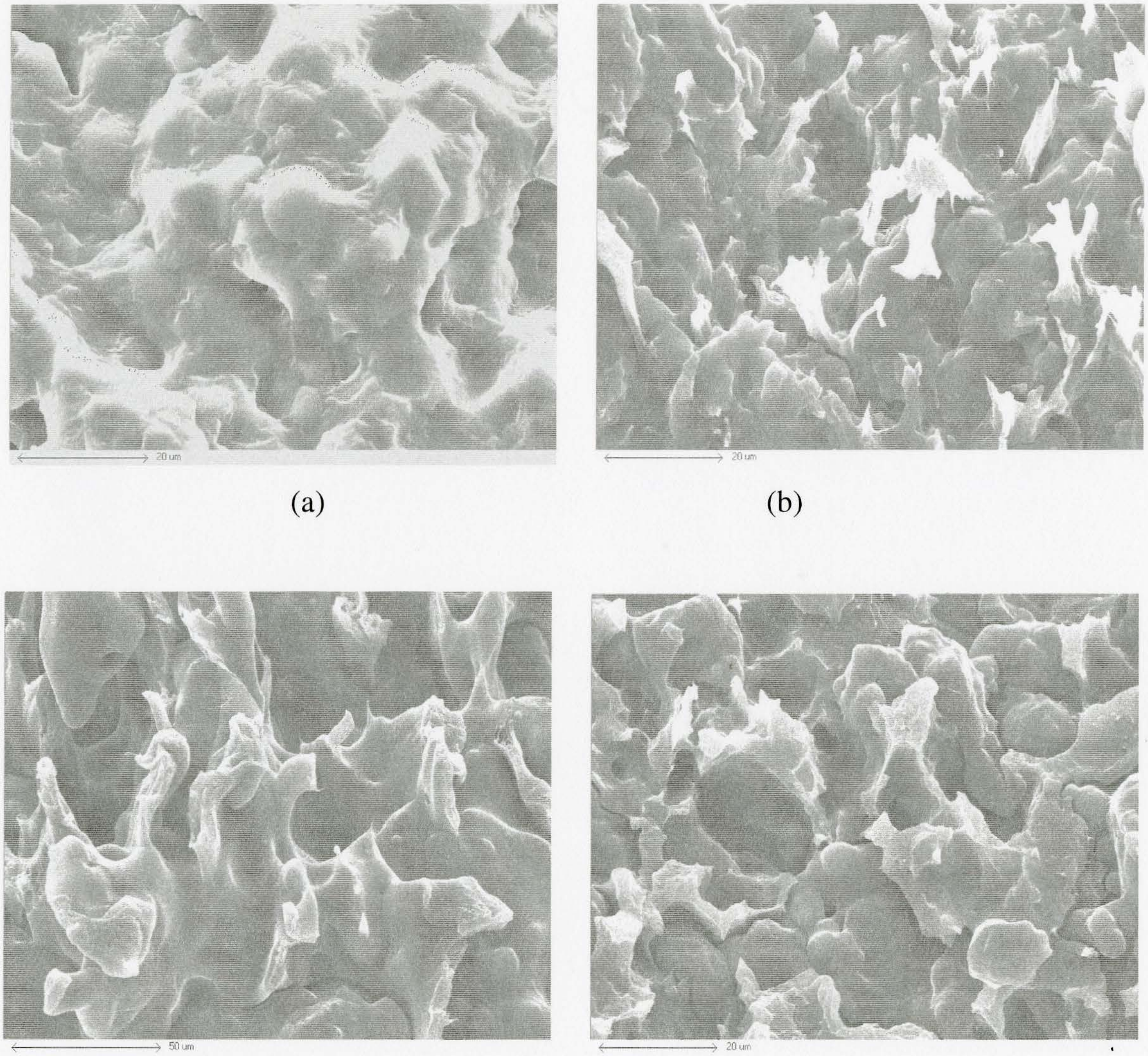

(a) (b)

(c) (d)

Figure 4-22. SEM images of compression molded thermoplastic normal starch/PLA blends with different ratio of starch to PLA (wt/wt%): (a) 100/0; (b) 70/30; (c) 50/50; (d) 30/70; starch/plasticizer ratio: 2/1(wt/wt%), water/glycerol ratio: 15/35(wt/wt%).

The SEM micrograph of the thermoplastic high amylose starch/PLA (70/30) blend, whose cross-section for SEM observation was prepared by etching the sample with chloroform, is shown in Figure 4-23. The dispersed PLA phases in the blend were removed and the continuous TPS phase was left. The SEM micrograph of the etched blend shows a clearer two-phase structure, compared to the SEM micrograph of the blend with the same blend composition [see Figure 4-20b].

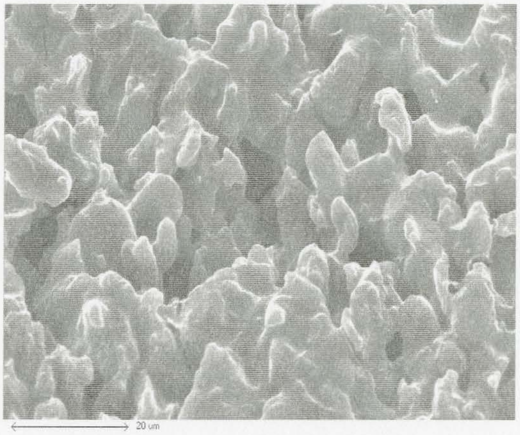

Figure 4-23. SEM image of the etched thermoplastic high amylose starch/PLA blend. The sample was etched in chloroform, and then coated; high amylose starch/PLA ratio: 70/30(wt/wt%); starch/plasticizer ratio: 1/1(wt/wt%); water/glycerol ratio: 15/35(wt/wt%).

A comparison of morphologies of thermoplastic starch /PLA blends prepared with different starches is shown in Figure 4-24. Some individual granules with angular shape appear in the micrograph of thermoplastic high amylose starch/PLA blend (starch/PLA ratio is 50/50 wt/wt%, starch/plasticizer ratio is 2/1 wt/wt%), as shown in Figure 4-24a, indicating that not all high amylose starch granules in the blend are plasticized. We observed that the high amylose starch was not plasticized in the processing when the starch/plasticizers ratio is 2/1 wt/wt% and water/glycerol ratio is 15/35 wt/wt% under the

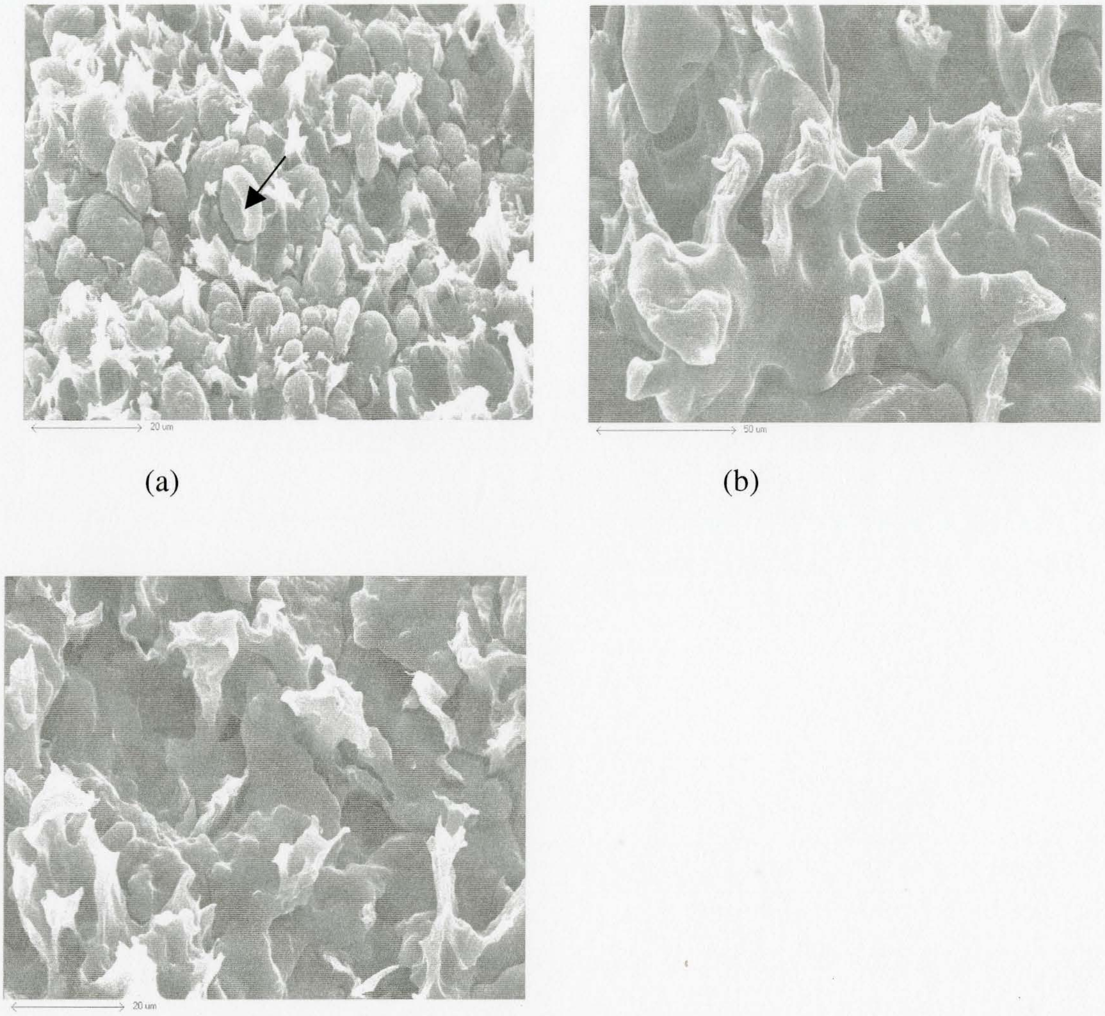

(a) (b)

(c)

Figure 4-24. Morphological comparison of thermoplastic starch/PLA blends prepared with different starches: (a): high amylose starch; (b): normal starch; (c): waxy starch; starch/PLA ratio: 50/50(wt/wt%); starch/plasticizer ratio: 2/1(wt/wt%); water/glycerol: 15/35(wt/wt%).

blending conditions of 120ºC at 45 rpm for 4 minutes. Figure 4-24b shows the morphology of thermoplastic normal starch/PLA blend with the same formula as the thermoplastic high amylose starch/PLA blend in Figure 4-24a, which gives very large and totally disrupted thermoplastic starch phases. No granular structure was observed in the micrograph shown in Figures 4-24c, indicating that the waxy starch granules were totally plasticized during the processing. The morphological comparison indicates that it is difficult for the high amylose starch to be plasticized. This result may be attributed to the difference in the amylose content, molecular structure and molecular organization in the starch granules.

4.2.2 Thermal properties

Thermoplastic high amylose starch, normal starch and waxy starch were blended with PLA and the thermal properties of the blends were analyzed using DSC. The first thermal scan is used to eliminate the effects of thermal history of samples. The DSC thermograms of extrusion-molded thermoplastic starch/PLA blends in a second thermal scan are shown in Figures 4-25 and 4-26. The thermal properties of the blends are presented in Table 4-10.

The DSC thermogram of pure PLA showed a glass transition at 58.4°C, a crystallization exotherm at 125.3°C and a melting endotherm at 153.3°C. Martin and Averous (2001a) reported that pure PLA showed a glass transition at 58°C, and a very small melting endotherm at 152°C, but no crystallization exotherm. PLA has slow crystallization kinetics and the raw materials may remain mainly amorphous. The PLA sample for our DSC analysis was obtained from the post-extrusion in a Rosand capillary rheometer. The shear stress through the die of rheometer may result in PLA molecular chains stretched. The stretched PLA molecular chains into a linear arrangement may allow the PLA molecules to form a crystalline phase. Compared to pure PLA, the glass temperature T_g of thermoplastic starch/PLA blends shift to lower temperatures, as presented in Table 4-10, indicating that a small degree of compatibility between

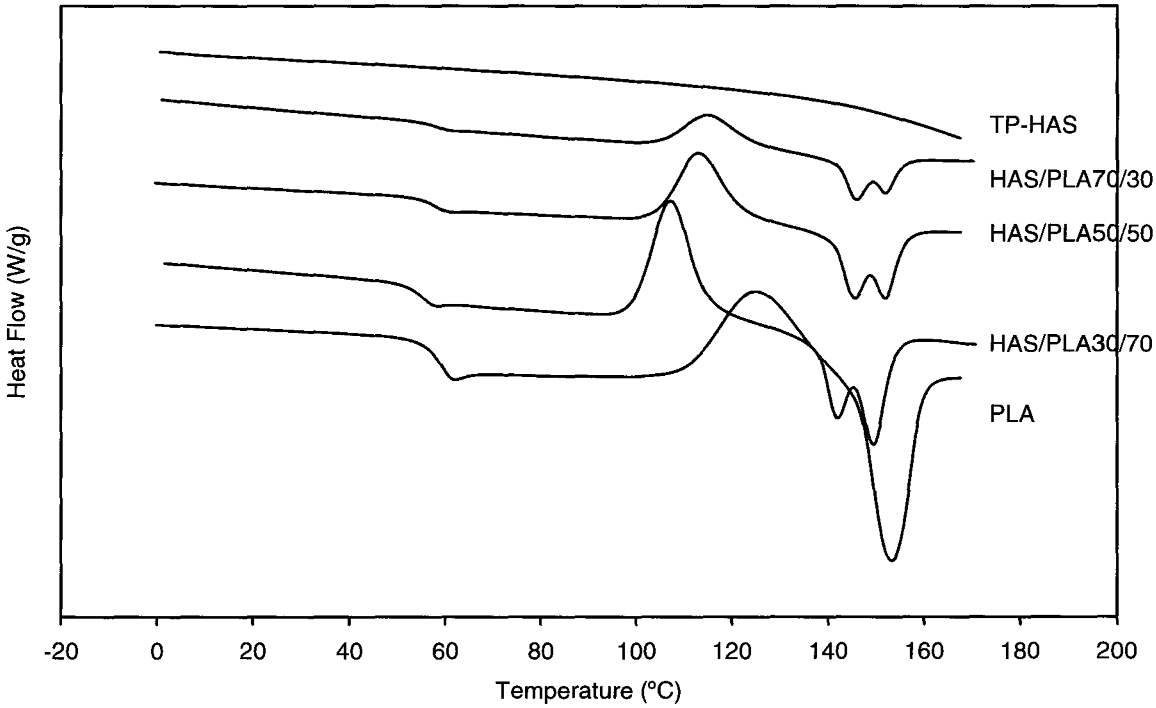

Figure 4-25. DSC thermograms of thermoplastic high amylose starch/PLA blends in a second thermal scan. Starch/PLA ratio (wt/wt%): 100/0, 70/30, 50/50, 30/70, 0/100, respectively from top to bottom.

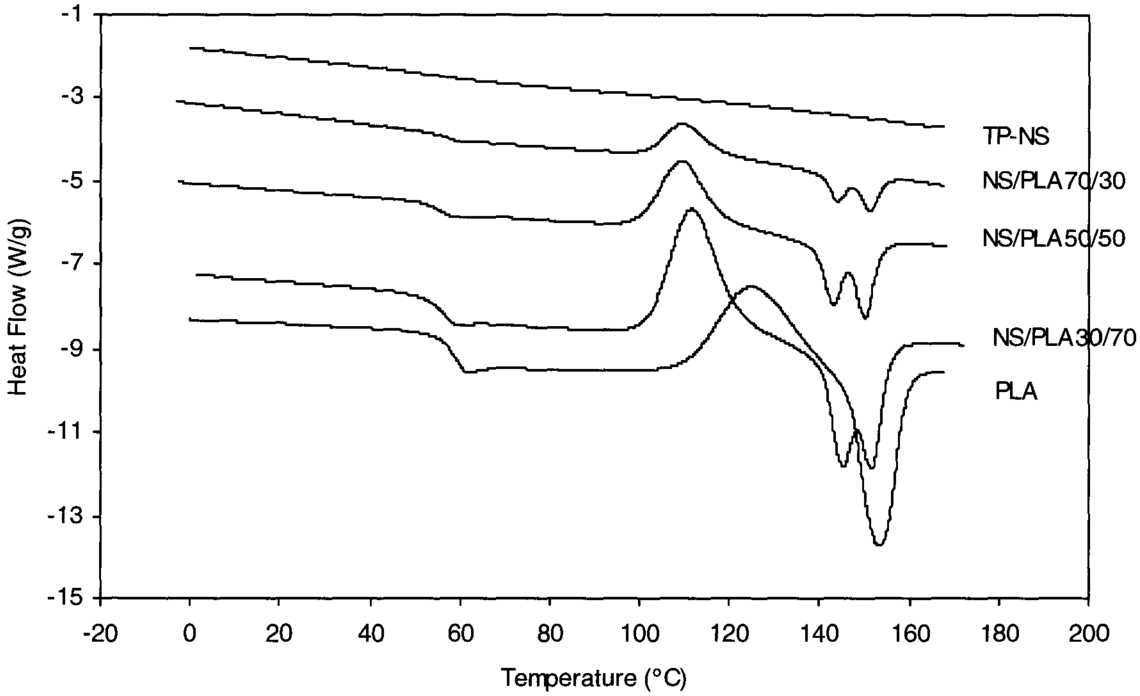

Figure 4-26. DSC thermograms of thermoplastic normal starch/PLA blends in a second thermal scan. Starch/PLA ratio (wt/wt%): 100/0, 70/30, 50/50, 30/70, 0/100, respectively from top to bottom.

Table 4-10. DSC parameters of thermoplastic starch/PLA blends

No.	Blends	Ratio of starch/PLA, wt.wt	Ratio of starch/plasticizers, wt/wt	T_g, °C	T_c, °C	Crystallization enthalpy, J/g	T_m, °C	Melting enthalpy, J/g
1	TP-HAS	100/0	1/1	/	/	/	/	/
2	HAS/PLA	70/30	1/1	58.1	114.9	24.74	146.0	26.57
3	HAS/PLA	50/50	1/1	57.8	113.1	31.92	145.7	31.95
4	HAS/PLA	30/70	1/1	55.2	107.2	30.27	149.5	30.07
5	Pure PLA	0/100	/	58.4	125.3	24.50	153.3	23.17
6	TP-NS	100/0	2/1	/	/	/	/	/
7	NS/PLA	70/30	2/1	57.0	109.7	26.15	140.4	25.26
8	NS/PLA	50/50	2/1	54.9	109.5	38.43	138.8	37.65
9	NS/PLA	30/70	2/1	56.1	111.7	36.40	140.2	35.82
10	Pure PLA	0/100	/	58.28	125.3	24.50	146.3	23.17

T_g , T_c , T_m are glass transition temperature, crystallization temperature and melting temperature respectively. Crystallization and melting enthalpies are based on PLA component. All parameters were obtained from DSC thermograms of starch/PLA blends in a second thermal scan.

thermoplastic starch and PLA components occurs. The crystallization enthalpy and melting enthalpy are higher than those of pure PLA. Crystallization temperature T_c and melting temperature T_m of the thermoplastic starch/PLA blends are lower than those of pure PLA. Higher thermal transition enthalpies and lower T_c and T_m indicate that the thermoplastic starch component may promote PLA crystallization as a result of enhancing the molecular chain mobility of PLA. The melting endotherms of thermoplastic starch/PLA blends showed two distinct peaks, as shown in Figures 4-25 and 4-26. This result is in agreement with Martin and Averous (2001). The thermal behavior could be due to the result of lamellar rearrangement during crystallization of PLA; the low-temperature peak was assigned to the melting endotherm of the original crystallites.

In comparing thermoplastic high amylose starch /PLA blends, the blends with same formula but prepared with normal starch gave a lower T_c and T_m, but higher crystallization enthalpies and thus melting enthalpies. That may be attributed to the difference in amylose content and the structure in the starches. The linear amylose molecules may form a more helical structure with PLA, which hampers the crystallization of PLA.

Comparison of the thermal properties of thermoplastic starch/PLA blends (starch/PLA ratio is 50/50 wt/wt%) prepared with different corn starches are shown in Figure 4-27. The thermal properties in the second thermal scan are presented in Table 4-11. The blends prepared by normal starch and waxy starch give higher crystallization enthalpies and thus higher melt enthalpies than high amylose starch. It may be attributed to higher amylose content in high amylose starch. The amorphous linear amylose

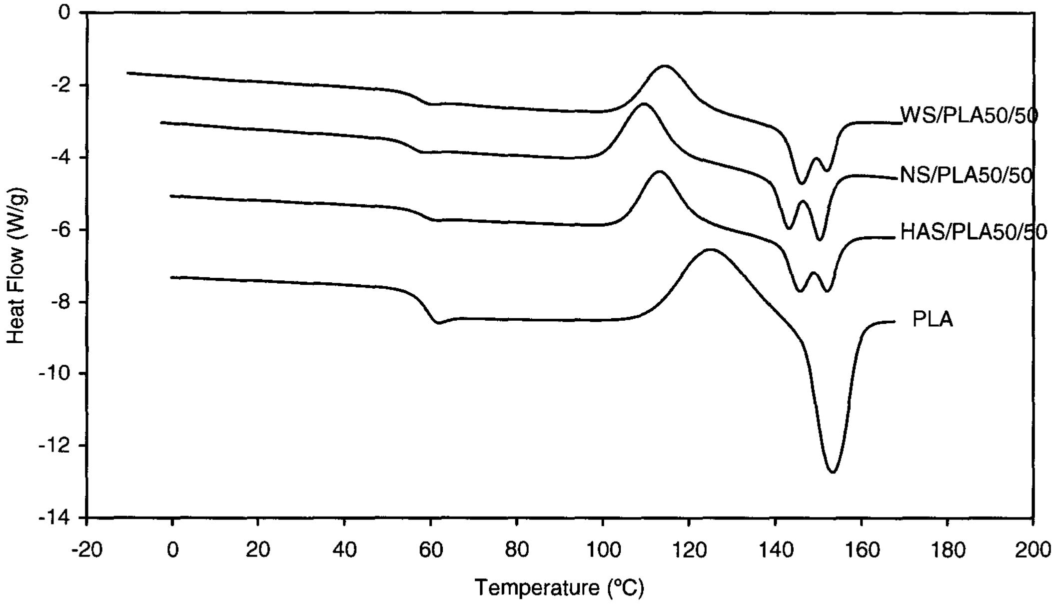

Figure 4-27. DSC thermograms of thermoplastic starch/PLA blends prepared with different cornstarches in a second thermal scan. Starch/PLA ratio (wt/wt%): 50/50, starches used: waxy starch, normal starch and high amylose starch respectively from top to bottom.

Table 4-11. DSC parameters of thermoplastic starch/PLA blends prepared with different cornstarches

No.	Blends	Ratio of starch/PLA (wt/wt)	Ratio of starch/plasticizers (wt/wt)	T_g, °C	T_c, °C	Crystallization enthalpy, J/g	T_m, °C	Melting enthalpy, J/g
1	WS/PLA	50/50	2/1	56.8	114.3	38.99	146.0	35.88
2	NS/PLA	50/50	2/1	55.2	109.5	38.43	138.8	37.65
3	HAS/PLA	50/50	2/1	57.8	113.1	31.92	145.7	31.95
4	Pure PLA	0/100	/	58.4	125.3	24.50	153.3	23.17

T_g, T_c, T_m are glass transition temperature, crystallization temperature and melting temperature respectively. Crystallization and melting enthalpies are based on PLA component. All parameters were obtained from DSC thermograms of starch/PLA blends in a second thermal scan.

molecules entangle with each other, which hinders the crystallization of PLA. Compared to the blends prepared with normal starch, the blend prepared with waxy starch shows higher T_c and T_m. That is probably due to the difference in average molecular weights of two starches. Waxy starch has a higher average molecular weight (see section 4.2.3.) and thus has less ability to promote chain mobility of the PLA component.

Effects of molding methods on thermal properties of thermoplastic starch/PLA blends were investigated, as shown in Figures 4-28 to 4-31. The DSC thermograms of pure PLA prepared by post-extrusion molding and compression molding are shown in Figure 4-28. No crystallization and melting peaks were observed in the thermogram of compression-molded PLA in the second thermal scan. Pure PLA has low crystallization kinetics. The time during DSC thermal scan is not long enough (about 20 minutes) for PLA to be crystallized. However, a broad and small crystallization exothermic peak and a melting endothermic peak appear in the DSC thermogram of the compression-molded PLA in the first scan. It may be attributed to the nucleation of small amount of crystalline material in the specimen. Small amount of PLA crystallites were formed during compression molding and specimen storage (about two months). The residual crystallites became crystalline nuclei during the DSC first thermal scan, leading to the appearance of a small crystallization exothermic peak and following a melting endothermic peak. The DSC thermograms of post-extrusion molded PLA in a first thermal scan and a second thermal scan gave exothermic crystallization and endothermic melting peaks. It may be attributed to the stretch of linear PLA molecular chains under action of shear stress through the die of a Rosand capillary rheometer. The stretch of PLA molecular chains into a linear arrangement is helpful for them to crystallize. The crystallization

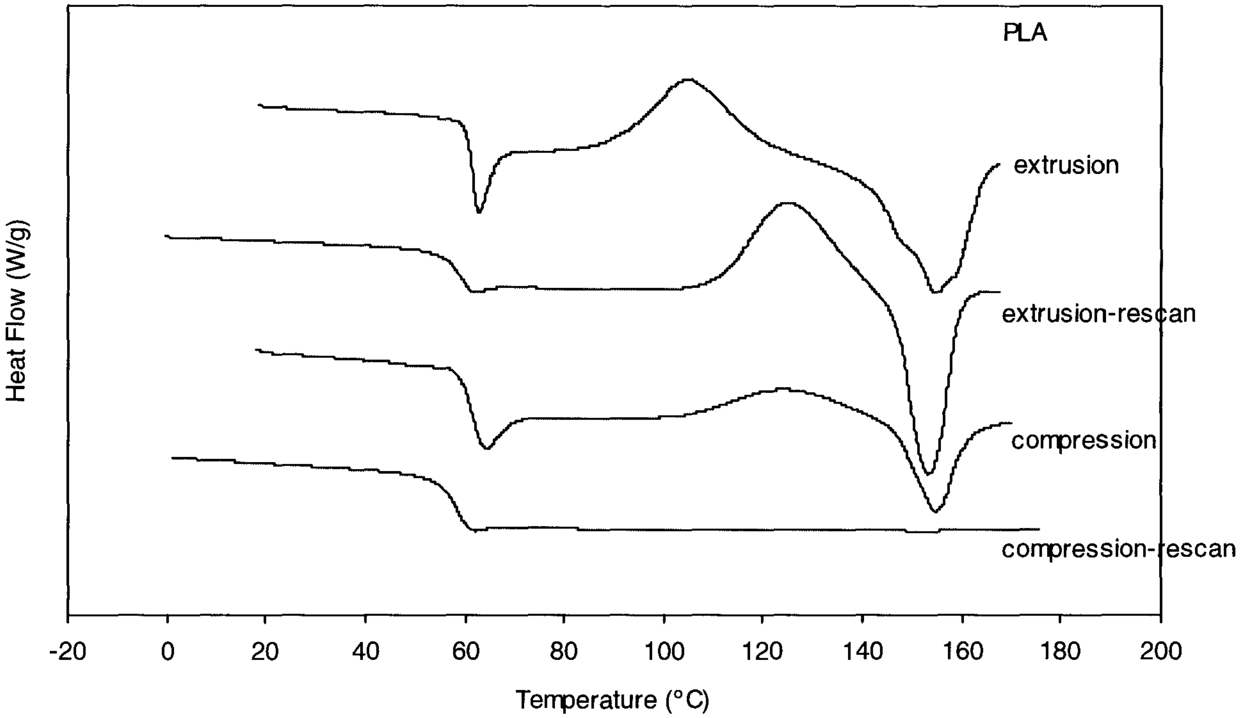

Figure 4-28. DSC thermograms of pure PLA prepared by different molding methods (post-extrusion molding and compression molding from top to bottom) in a first and a second thermal scan.

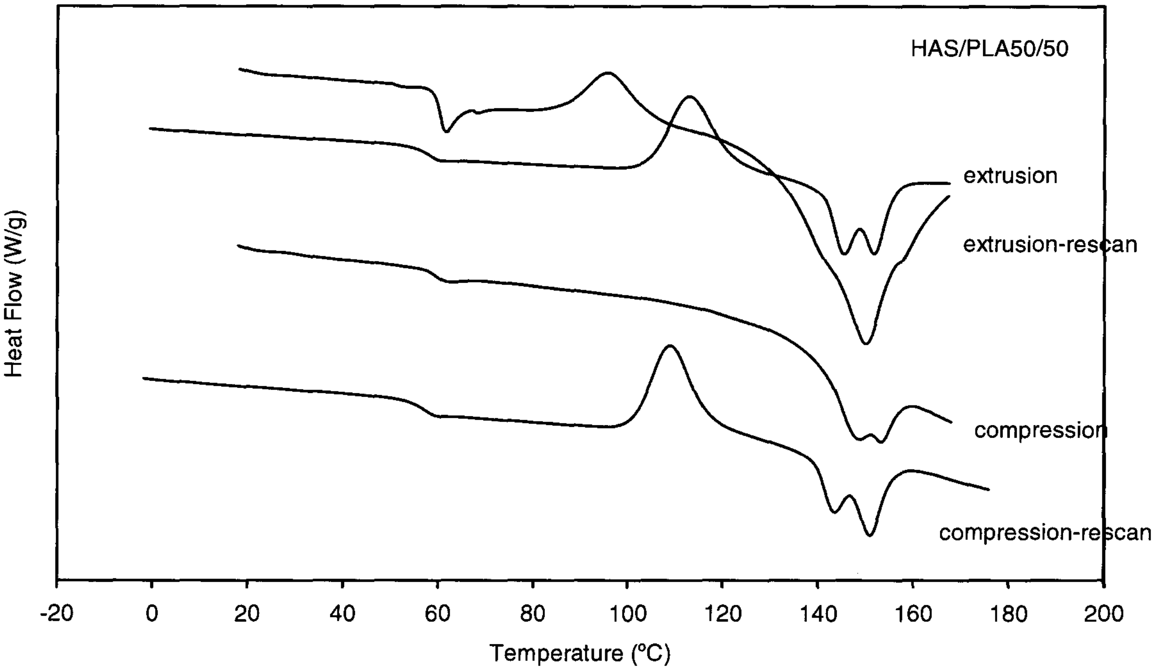

Figure 4-29. DSC thermograms of thermoplastic high amylose starch/PLA blends prepared by different molding methods (post-extrusion molding and compression molding from top to bottom) in a first and a second thermal scan scanning. Starch/PLA ratio: 50/50wt/wt%; starch/plasticizer ratio: 1/1 wt/wt%; water/glycerol ratio: 15/35wt/wt%.

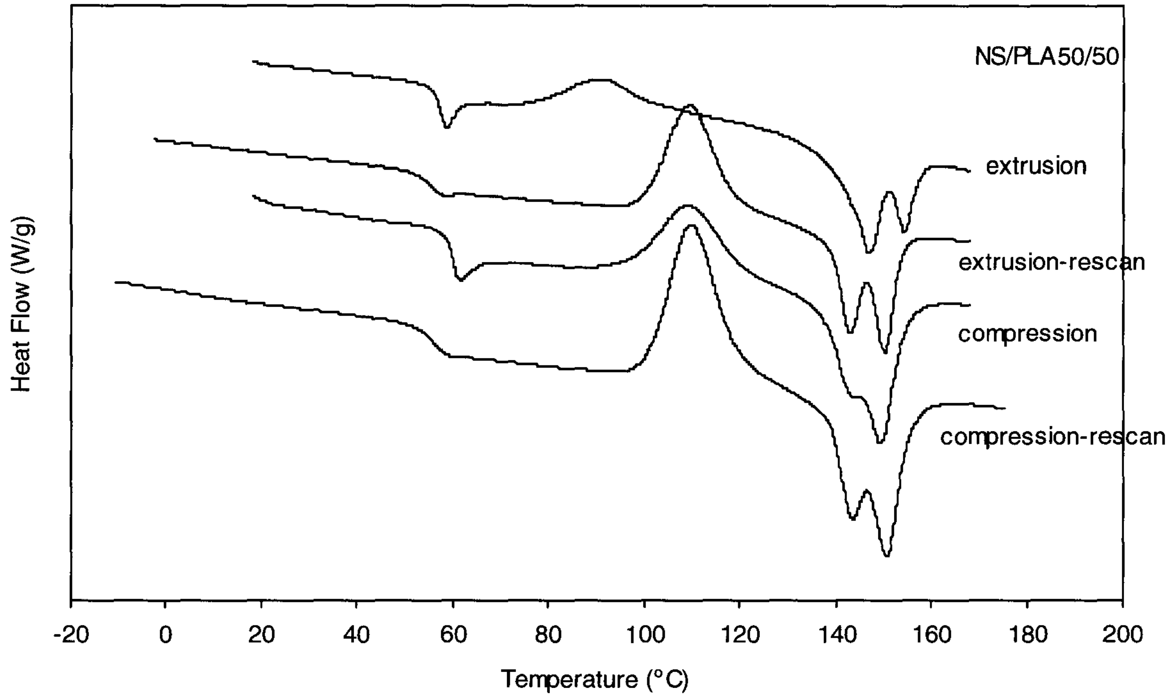

Figure 4-30. DSC thermograms of thermoplastic normal starch/PLA blends prepared by different molding methods (post-extrusion molding and compression molding from top to bottom) in a first and a second thermal scan. Starch/PLA ratio: 50/50wt/wt%; starch/plasticizer ratio: 2/1 wt/wt%; water/glycerol ratio: 15/35wt/wt%.

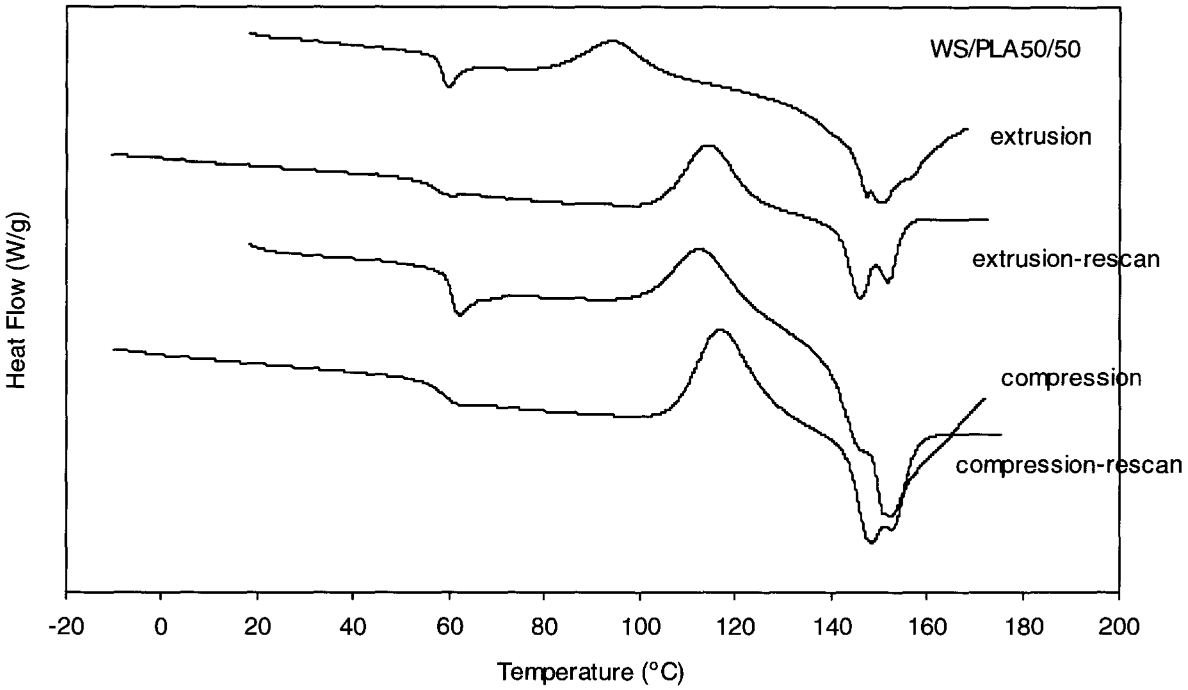

Figure 4-31. DSC thermograms of thermoplastic waxy starch/PLA blends prepared by different molding methods (post-extrusion molding and compression molding from top to bottom) in a first and a second heating scanning. Starch/PLA ratio: 50/50wt/wt%; starch/plasticizer ratio: 2/1 wt/wt%; water/glycerol ratio: 15/35wt/wt%.

temperature T_m in the first thermal scan was lower than that in the second thermal scan for the post-extrusion molded PLA. It is probably related to the nucleation of residual crystallites in the sample, which causes PLA molecules to be crystallized at a lower temperature in the first thermal scan. The degree of crystallinity ($X_{residual}$) in the residue can be calculated by following formulation:

$$\Delta H_{f,residual} = \Delta H_m - \Delta H_c \tag{4-4}$$

$$X_{residual} = \Delta H_{f,residual} / \Delta H_m^0 \tag{4-5}$$

where, ΔH_m : the melting enthalpy of the PLA component in the blend, J/g

ΔH_c : the crystallization enthalpy of the PLA component in the blend, J/g

ΔH_m^0 : the melting enthalpy of 100% crystalline PLA (97.3J/g) (Huda et al., 2004).

The degree of residual crystallinity of post-extrusion molded PLA is calculated to be 7.5%. The degree of residual crystallinity of compression-molded PLA is calculated to be 1.5%.

The same experimental results and conclusions as above can be obtained from the comparison of thermal properties of thermoplastic starch/PLA (50/50) blends prepared with different starches and by different molding methods. The degree of residual crystallinity of post-extrusion molded and compression-molded thermoplastic high amylose starch/PLA blends are 48% and 27% respectively. For normal starch/PLA (50/50) blends, the degree of residual crystallinity is approximately 27% for post-extrusion molded specimen and 16% for compression molded sample, respectively. The starch/plasticizer ratio in the thermoplastic high amylose starch/PLA blend was 1/1 wt/wt% while the starch/plasticizer ratio in the thermoplastic normal starch/PLA blend was 2/1 wt/wt%. Higher plasticizer content may be responsible for higher degree of the residual crystallinity in the blends.

Different thermal scan rate and cooling rate were also used to investigate the effects of scan rate on the thermal properties of thermoplastic starch/PLA blends. The DSC thermograms of the thermoplastic high amylose starch/PLA (50/50) blend at different thermal scan rates are shown in Figure 4-32. When the heating rate was increased to 20ºC/min (in thermogram B) from 10ºC/min (in thermogram A), the glass transition temperature T_g and crystallization temperature T_m shift to a higher temperature. The thermogram B only showed one melting endothermic peak, which is different from thermogram A where the melting endotherm showed two distinct peaks. Increase of thermal scan rate decreases the resolution of thermal analysis. The second thermal scan DSC thermogram of the thermoplastic high amylose starch/PLA (50/50) blend sample, which was heated at a scan rate of 10ºC/min, cooled at a scan rate of 50ºC/min and then reheated at 10ºC/min, is shown as thermogram C in Figure 4-32. Compared to the thermogram A, the thermogram C gave a lower T_g, T_c and T_m, indicating that fast cooling of the specimen is helpful for the crystallization of PLA.

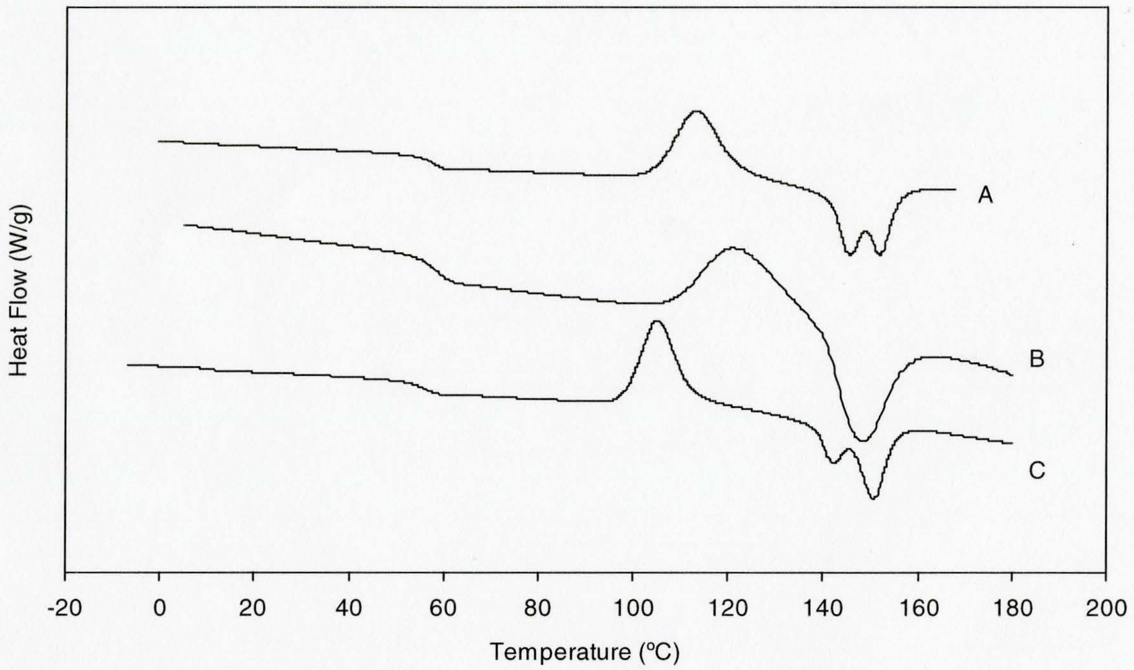

Figure 4-32. DSC thermograms of post-extruded thermoplastic high amylose starch/PLA (50/50wt/wt%) blend in a second thermal scan. Heating rate and cooling rate: (A) 10°C/min and 10°C/min, (B) 20C/min and 10°C/min, (C) 10°C/min and 50°C/min, respectively.

4.2.3 Molecular weight and molecular weight distribution

The high performance size exclusion chromatograms (HPSEC) of thermoplastic high amylose starch/PLA blends prepared using different molding methods are shown in Figure 4-33. The small peaks occurring at low molecular weight place are attributed to the molecular weight distribution of PLA residual materials after hydrolysis. The molecular weights of thermoplastic starch components in the blends shift to lower values compared to those of the native starches. The decrease in the molecular weights of starch and change of the molecular profile in the blends after processing may be attributed to partial degradation of the starch during processing.

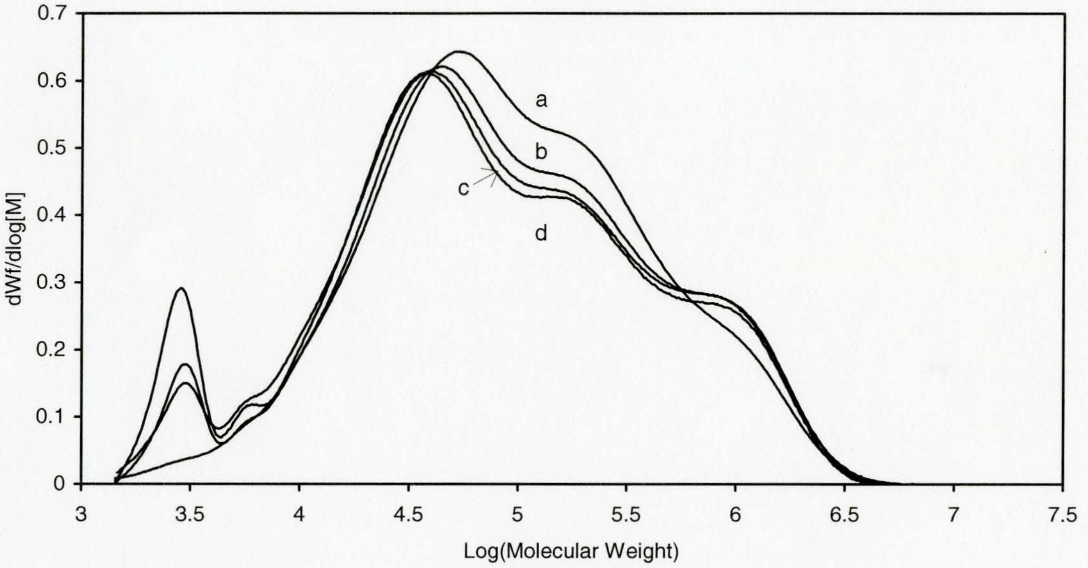

Figure 4-33. HPSEC chromatograms of the high amyloe starch/PLA blends prepared by different molding methods: (a) native starch, (b) blended, (c) post-extrusion molded and (d) compression-molded. Starch/PLA ratio: 50/50wt/wt%; starch/plasticizer ratio: 1/1 wt/wt%; water/glycerol ratio: 15/35 wt/wt%.

4.2.4 Mechanical properties

A series of thermoplastic starch/PLA blends with different blend composition were prepared using different type of starches. Their mechanical properties were measured, as presented in Table 4-12 for compression molded specimens and Table 4-13 for post-extrusion molded specimens.

PLA has high elastic modulus and tensile strength but low elongation at break. The addition of PLA into thermoplastic starch causes a substantial increase in modulus

Table 4-12. Mechanical properties of compression-molded thermoplastic starch/PLA blends

No.	Starch/PLA	Starch type	Starch/ plasticizer ratio, wt/wt	Content 0f F-108,wt%	Density, g/cm^3	Tensile properties		
						Strength (MPa)	Modulus (MPa)	Elogation at break (%)
1	100/0	HAS	1/1	0	1.360	0.888±0.084	22.16±5.19	9.51±1.25
2	70/30	HAS	1/1	0	1.356	3.10±0.77	184.6±40.6	4.35±1.31
3	50/50	HAS	1/1	0	1.340	6.68±1.80	585.8±261.3	2.30±0.58
4	30/70	HAS	1/1	0	1.311	18.1±0.8	1750±27	1.93±0.29
5	70/30	HAS	1/1	5	1.355	1.95±0.14	173.4±28.2	2.73±1.17
6	50/50	HAS	1/1	5	1.327	6.34±0.95	496.7±53.1	2.65±0.59
7	30/70	HAS	1/1	5	1.305	13.8±1.4	1417±125	3.60±3.53
8	20/80	HAS	1/1	5	1.293	23.2±2.6	2023±274	3.15±2.44
9	50/50	HAS	3/2	5	1.351	12.0±1.1	976.8±75.1	2.46±0.25
10	50/50	HAS	2/1	5	1.350	12.7±1.4	1496±53	1.50±0.09
11	50/50	HAS	2/1	10	1.349	10.9±1.1	1754±186	1.15±0.13
12	0/100	/	/	0	1.251	67.8±3.7	3336±133	3.07±0.64
13	0/100	/	/	5	1.256	51.2±3.9	3141±202	2.77±0.85
14	100/0	NS	2/1	0	1.426	5.83±0.07	175.6±13.7	21.6±1.2
15	70/30	NS	2/1	0	1.407	7.11±2.51	717.9±35.3	1.90±0.26
16	50/50	NS	2/1	0	1.362	14.7±2.8	1335±51	1.91±0.18
17	30/70	NS	2/1	0	1.318	25.5±0.6	1852±120	2.60±0.28
18	50/50	HAS	2/1	0	1.356	15.7±2.1	1255±221	2.03±0.25
19	50/50	WS	2/1	0	1.354	12.8±0.4	1249±341	1.84±0.11

and strength of the thermoplastic starch/PLA blends for each blend composition, as shown in Figure 4-34 to 4-37. For example, the tensile strength of the compression molded thermoplastic high amylose starch/PLA blend (starch/PLA ratio is 50/50 wt/wt%, starch/plasticizer ratio is 1/1 wt/wt%) increases to 6.68 MPa from 0.888 MPa for pure thermoplastic high amylose starch. The elastic modulus of the blend increases to 585.8 MPa from 22.16 MPa for thermoplastic high amylose starch. The tensile strength and modulus of the compression molded thermoplastic normal starch/PLA blend (starch/PLA

Table 4-13. Mechanical properties of post-extrusion molded thermoplastic starch/PLA blends

Sample	Starch/PLA	Starch type	Starch/ plasticizer ratio, wt/wt	Content Of F-108	Density, g/cm^3	Tensile properties ^{a,b}		
						Strength (MPa)	Modulus (MPa)	Elongation at break (%)
1	100/0	HAS	1/1	0	1.367	0.888±0.120	18.59±1.09	10.1±2.0
2	70/30	HAS	1/1	0	1.341	3.72±0.72	162.3±23.7	10.1±3.7
3	50/50	HAS	1/1	0	1.311	9.70±1.60	629.1±158.2	6.59±3.42
4	30/70	HAS	1/1	0	1.296	22.8±2.5	1522±76	7.59±2.07
5	70/30	HAS	1/1	5	1.345	3.03±1.07	134.5±36.1	11.0±3.8
6	50/50	HAS	1/1	5	1.315	8.73±0.47	568.9±41.0	7.30±0.58
7	30/70	HAS	1/1	5	1.296	17.6±0.3	1327±82	20.1±3.5
8	20/80	HAS	1/1	5	1.295	22.4±0.3	1700±45	19.4±7.0
9	50/50	HAS	3/2	5	1.344	14.8±0.8	1067±43	3.46±0.86
10	50/50	HAS	2/1	5	1.346	16.8±2.3	1740±384	2.17±1.19
11	50/50	HAS	2/1	10	/	12.9±3.2	1149±169	2.23±0.42
12	0/100	/	/	0	1.251	68.2±5.8	3119±125	4.80±2.20
13	0/100	/	/	5	1.240	61.4±5.3	3220±521	5.95±3.28
14	100/0	NS	2/1	0	1.417	2.81±0.32	55.09±18.09	76.0±33.8
15	70/30	NS	2/1	0	1.391	5.08±1.19	250.6±57.2	13.0±2.9
16	50/50	NS	2/1	0	1.367	15.1±2.3	926.2±220.3	6.22±2.59
17	30/70	NS	2/1	0	1.324	24.5±1.1	1557±49	5.30±2.90
18	50/50	HAS	2/1	0	1.353	13.9±1.3	937.5±171.1	3.32±1.97
19	50/50	WS	2/1	0	1.363	13.8±1.2	784.8±68.4	7.03±0.62

ratio is 50/50 wt/wt%, starch/plasticizer ratio is 2/1 wt/wt%) increase to 14.7 MPa and 1335 MPa from 5.83 MPa and 175.6 MPa for pure thermoplastic normal starch. The tensile strength and modulus of post-extruded thermoplastic high amylose starch/PLA blend (starch/PLA ratio is 50/50 wt/wt%, starch/plasticizer ratio is 1/1 wt/wt%) increase to 9.70 MPa and 629 MPa from 0.888 MPa and 18.59 MPa for pure thermoplastic high amylose starch. The tensile strength and modulus of post-extruded thermoplastic normal starch/PLA blend (starch/PLA ratio is 50/50 wt/wt%, starch/plasticizer ratio is 2/1

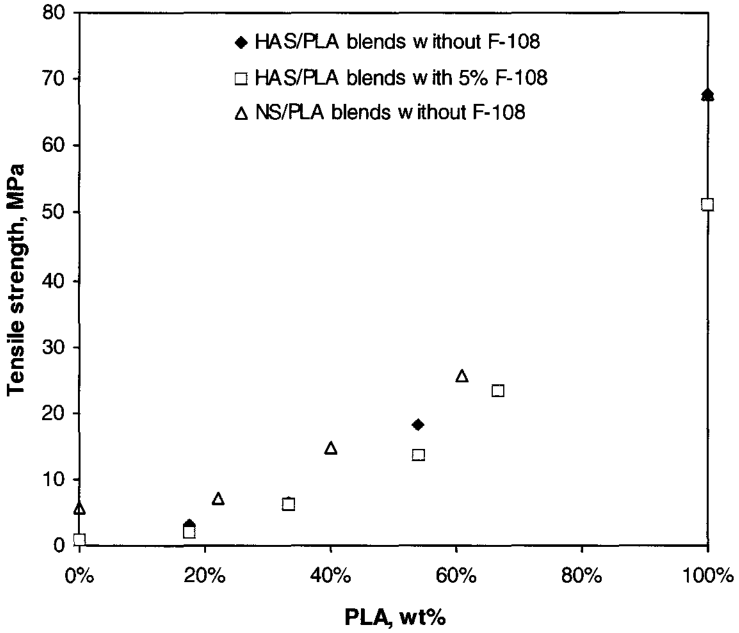

Figure 4-34. Tensile strength of compression-molded starch/PLA blends (starch/plasticizer ratio: 1/1wt/wt% for TP-HAS/PLA blends and 2/1 wt/wt% for TP-NS/PLA blends; water/glycerol ratio: 15/35wt/wt% for all blends].

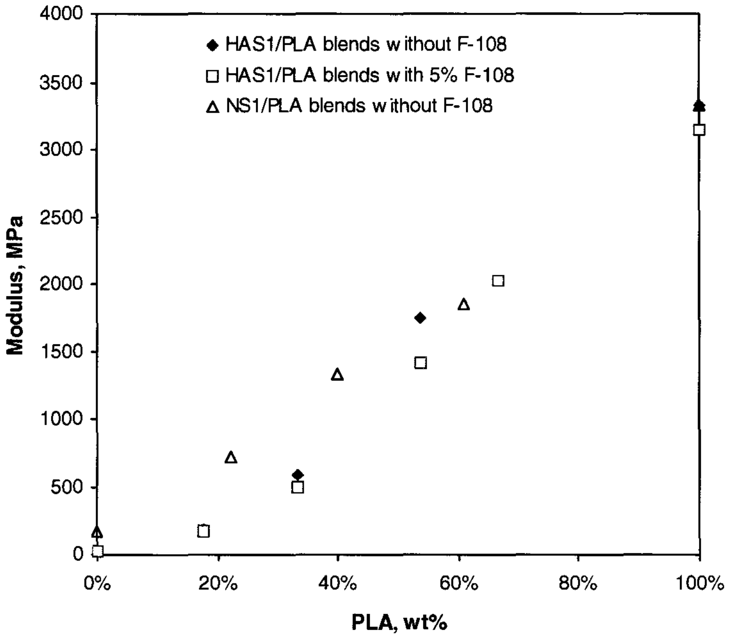

Figure 4-35. Elastic modulus of compression-molded thermoplastic starch/PLA blends (starch/plasticizer ratio: 1/1wt/wt% for TP-HAS/PLA blends and 2/1 wt/wt% for TP-NS/PLA blends; water/glycerol ratio: 15/35wt/wt% for all blends).

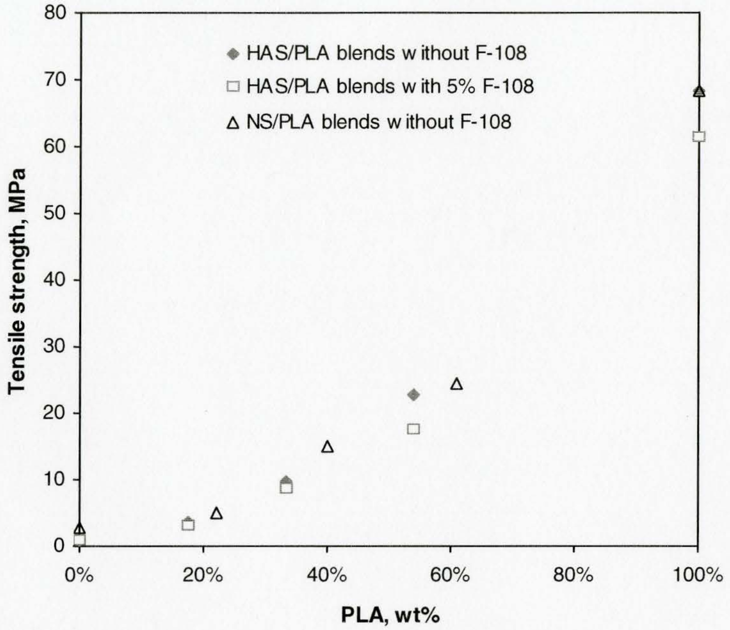

Figure 4-36. Tensile strength of post-extrusion molded thermoplastic starch/PLA blends (starch/plasticizer ratio: 1/1wt/wt% for TP-HAS/PLA blends and 2/1 wt/wt% for TP-NS/PLA blends; water/glycerol ratio: 15/35wt/wt% for all blends).

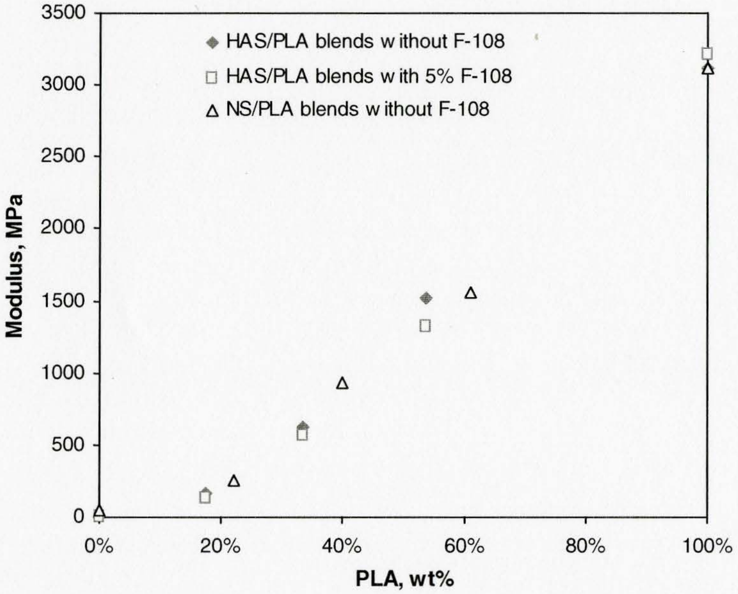

Figure 4-37. Elastic modulus of post-extrusion molded thermoplastic starch/PLA blends (starch/plasticizer ratio: 1/1wt/wt% for TP-HAS/PLA blends and 2/1 wt/wt% for TP-NS/PLA blends; water/glycerol ratio: 15/35wt/wt% for all blends).

wt/wt%) increase to 15.1 MPa and 926.2 MPa from 0.2.81MPa and 55.09 MPa for pure thermoplastic high amylose starch. Figure 4-38 shows the elongation at break of the thermoplastic starch/PLA blends. For compression-molded thermoplastic starch/PLA blends, addition of a small amount of PLA causes a sharp decrease in elongation at break of the materials, indicating that PLA plays a dominant role in the elongation at break of the blends. As to the extrusion-molded thermoplastic starch/PLA blends, the elongation at break decreases as the PLA content increases. The elongations at break of the blends lie between those of two pure components.

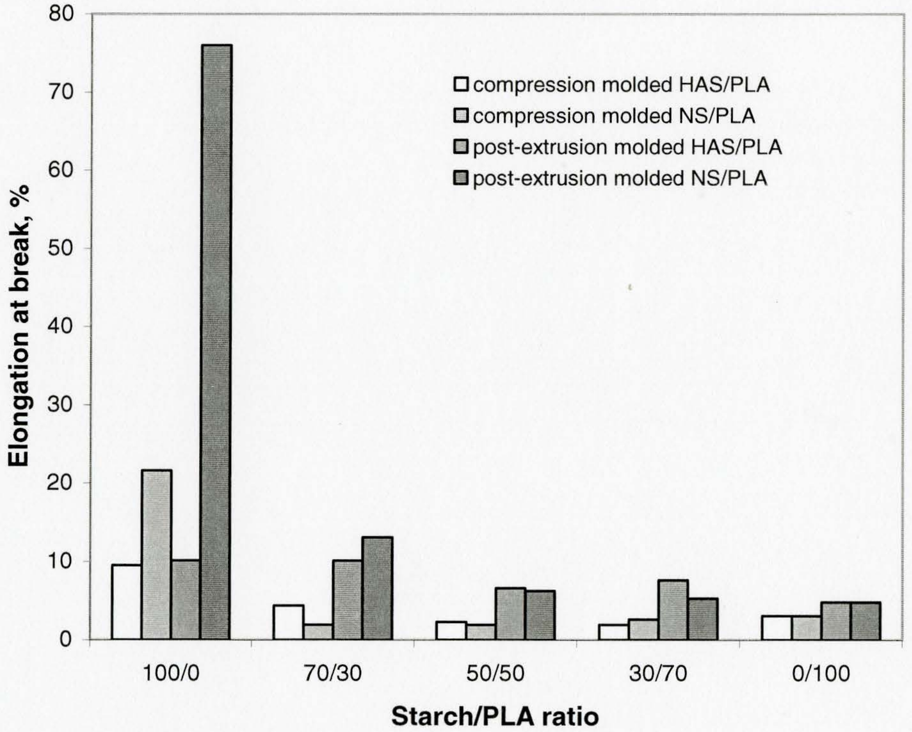

Figure 4-38. Elongation at break of compression-molded and post-extrusion molded thermoplastic starch/PLA blends with starch/PLA ratio (wt/wt%): (a) 100/0; (b) 70/30; (c) 50/50; (d) 30/70; and (e) 0/100 (starch/plasticizer ratio: 1/1wt/wt% for TP-HAS/PLA blends and 2/1 wt/wt% for TP-NS/PLA blends; water/glycerol ratio: 15/35wt/wt%).

The modulus of polymer blends generally range between an upper bound, Eu, given by the parallel model:

$$E_U = \phi_1 E_1 + \phi_1 E_2 \tag{4-6}$$

and a lower bound, E_L, given by the series model:

$$\frac{1}{E_L} = \frac{\phi_1}{E_1} + \frac{\phi_2}{E_2} \tag{4-7}$$

where, E_i and ϕ_i are the modulus and the volume fraction of phase *i*.

For co-continuous polymer blends, a different equation for the elastic modulus as a function of the composition has been proposed as following by Davies (Willemse *et al*, 1999).

$$E_D^{1/5} = E_1^{1/5}\phi_1 + E_2^{1/5}\phi_2 \tag{4-8}$$

In Figures 4-39 and 4-40, the elastic modulus of compression-molded and extrusion-molded thermoplastic starch/PLA blends are plotted as a function of the volume fraction of PLA, and compared with the parallel and Davies model. The experimental modulus of the blends are between the limits provided by parallel model and Davies model. The modulus of compression-molded thermoplastic starch/PLA blends show good agreement with the values predicted by parallel model, indicating that the PLA component control the modulus of the blends. The modulus of the post-extrusion molded thermoplastic starch/PLA blends are close to predicted values by the Davies model, indicating that post-extrusion molding caused the formation of a phase structure which is approximately co-continuous in the blends.

The mechanical properties of thermoplastic high amylose starch/PLA blends prepared using different starch/plasticizer ratio were investigated. The results are shown

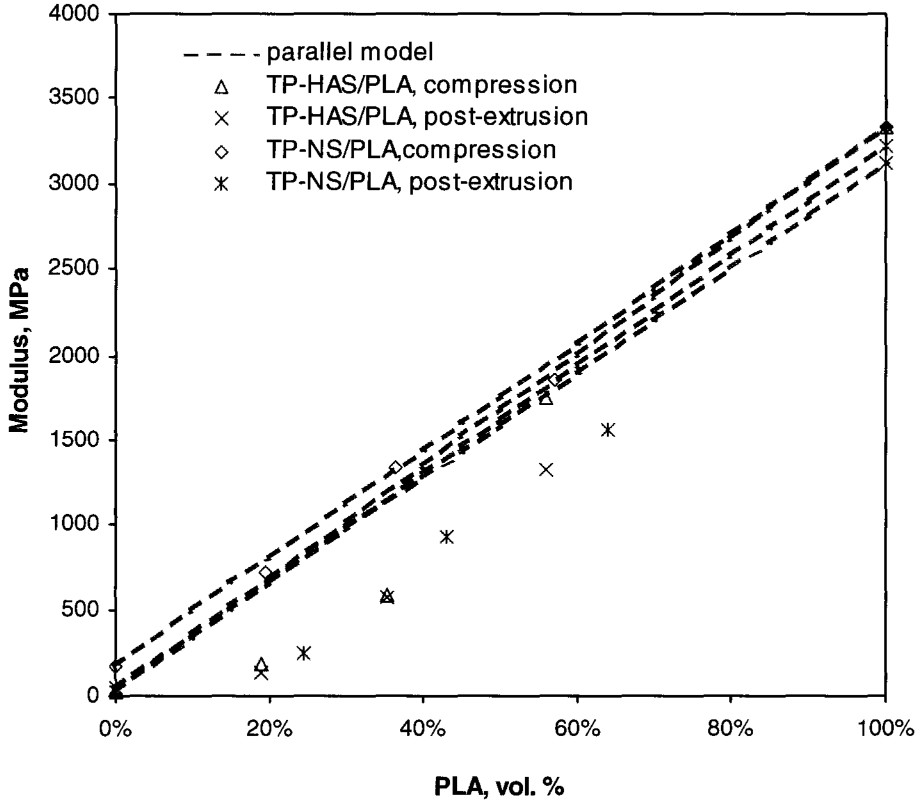

Figure 4-39. Experimental elastic modulus of thermoplastic starch/PLA blends compared with the parallel model (starch/plasticizer ratio: 1/1wt/wt% for thermoplastic high amylose starch and 2/1 wt/wt% for thermoplastic normal starch; water/glycerol ratio: 15/35wt/wt%).

in Table 4-14. The tensile strength and modulus of the blends increase with increasing the starch/plasticizer ratio while elongation at break decreases with increasing the starch/plasticizer ratio. For example, the tensile strength and modulus of compression molded thermoplastic high amylose starch/PLA blend with a starch/plasticizer ratio of 2/1 wt/wt% (starch/PLA ratio is 50/50 wt/wt%) increase to 12.7 MPa and 1496 MPa from 6.34 MPa and 496.7 MPa for the blend with a starch/plasticizer ratio of 1/1 wt/wt%. The elongation at break decreases to 1.50% from 2.65%. The usage of plasticizers softens the materials and improves the toughness of the materials.

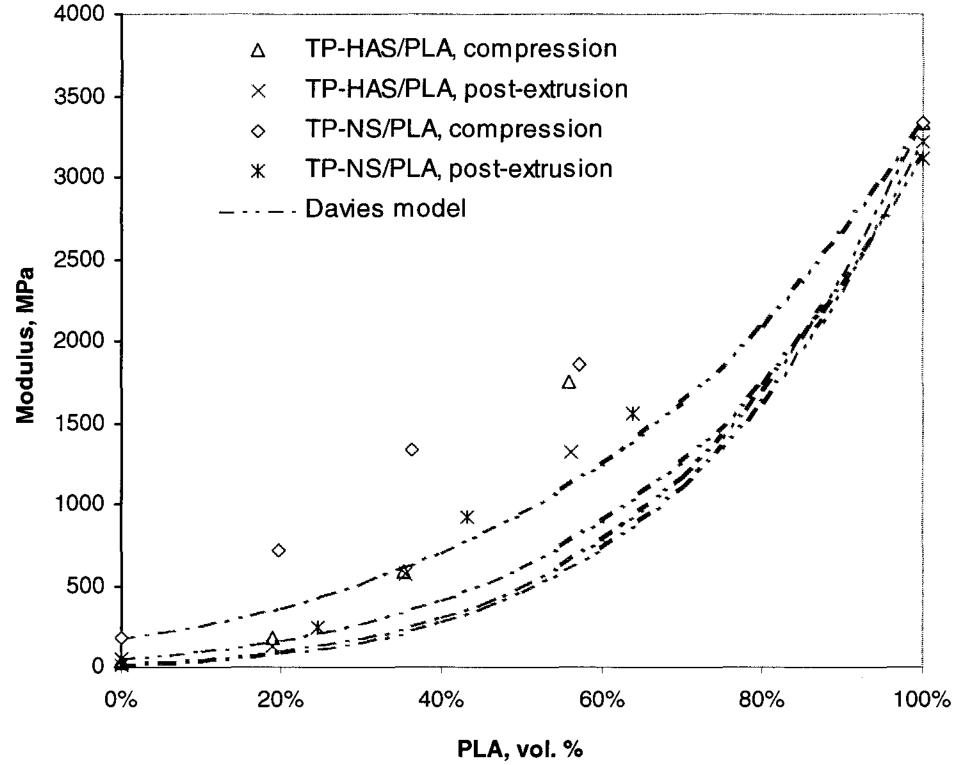

Figure 4-40. Experimental elastic modulus of thermoplastic starch/PLA blends compared with the Davies model (starch/plasticizer ratio: 1/1wt/wt% for thermoplastic high amylose starch and 2/1wt/wt% for thermoplastic normal starch; water/glycerol ratio: 15/35wt/wt%).

Table 4-15 presents the mechanical properties of thermoplastic starch/PLA blends, with a starch/plasticizer ratio of 2/1wt/wt% and a starch/PLA ratio of 50/50wt/wt%, prepared with three different corn starches. When the blends were molded by same molding method (compression molding or post-extrusion molding), tensile strength and modulus of the thermoplastic starch/PLA blends show no big difference caused by starch type. In other words, the mechanical properties of the thermoplastic starch/PLA blends are not dependent on starch type, indicating that the tensile strength and modulus of the blends are mainly determined by the PLA. The thermoplastic starch/PLA blends prepared by compression molding also show no big difference in elongation at break. However, the post-extrusion molded normal starch/PLA and waxy starch/PLA blends result in better elongation at break than the post-extrusion molded blends prepared with high amylose starch. The elongations at break of the post-extruded thermoplastic normal starch/PLA blend and the thermoplastic waxy starch/PLA blend

Table 4-14. Mechanical properties comparison of thermoplastic high amylose starch/PLA (50/50) blends with different starch/plasticizer ratio.

No.	Starch/ plasticizer ratio, wt/wt	Molding method	Density, g/cm^3	Tensile properties [a,b]		
				Strength (MPa)	Modulus (MPa)	Elongation at break (%)
1	1/1	Compression	1.327	6.34±0.95	496.7±53.1	2.65±0.59
2	3/2	Compression	1.351	12.0±1.1	976.8±75.1	2.46±0.25
3	2/1	Compression	1.350	12.7±1.4	1496±53	1.50±0.09
4	1/1	Post-extrusion	1.315	8.73±0.47	568.9±41.0	7.30±0.58
5	3/2	Post-extrusion	1.344	14.8±0.8	1067±43	3.46±0.86
6	2/1	Post-extrusion	1.346	16.8±2.3	1740±384	2.17±1.19

Specimens containing 5% F-108 were post-extruded in a Rosand capillary rheometer at 150°C (water/glycerol ratio: 15/35 wt/wt%).

Table 4-15. Mechanical property comparison of thermoplastic starch/PLA blends prepared with different starches.

No .	Starch/PLA	Molding type	Density, g/cm^3	Tensile properties		
				Strength (MPa)	Modulus (MPa)	Elogation at break (%)
1	HAS/PLA	Compression	1.356	15.65±2.10	1255±221	2.03±0.25
2	NS/PLA	Compression	1.362	14.70±2.78	1335±51	1.91±0.18
3	WS/PLA	Compression	1.354	12.79±0.39	1249±341	1.84±0.11
4	HAS/PLA	Post-extrusion	1.353	13.85±1.33	937.5±171.1	3.32±1.97
5	NS/PLA	Post-extrusion	1.367	15.10±2.30	926.2±220.3	6.22±2.59
6	WS/PLA	Post-extrusion	1.363	13.79±1.22	784.8±68.4	7.03±0.62

All specimens were post-extruded in a Rosand capillary rheometer at 150°C, starch/PLA ratio: 50/50; starch/plasticizer ratio: 2/1 (wt/wt); water/glycerol: 15/35(wt/wt).

(starch/PLA ratio is 50/50 wt/wt% and starch/plasticizer ratio is 2/1 wt/wt%) are 6.22% and 7.03% while the elongation of the thermoplastic high amylose starch/PLA blend with the same composition is 3.32%. In the thermoplastic high amylose starch/PLA blend, not all starch granules were plasticized (see Figure 4-25 and section 4.2.1). Thus, some part of granules exists in the blends as filler. The elongations at break of thermoplastic high amylose starch/PLA blends are almost same as that of pure PLA. In post-extrusion molded thermoplastic normal starch/PLA and waxy starch/PLA blends, the starch granules are plasticized completely and the starch phases were stretched under the action of shear stress during processing in a Rosand capillary rheometer, which caused an increase in elongation at break of the thermoplastic normal starch/PLA and thermoplastic waxy starch/PLA blends.

The comparison of mechanical properties of thermoplastic starch/PLA blends molded by different molding method is shown in Table 4-16 and Figures 4-41 to 4-44. The thermoplastic high amylose starch/PLA blends prepared by post extrusion molding exhibit higher tensile strength, modulus and elongation at break than the blends with same composition prepared by compression molding. The tensile strength, modulus and elongation at break of the post-extruded thermoplastic high amylose starch/PLA(50/50) blend with starch/plasticizer ratio of 1/1 wt/wt% increased to 8.73 MPa, 568.9 MPa and 7.30 % from 6.34 MPa, 496.7 MPa and 2.65% for the compression molded blend with the same composition. The tensile strength, modulus and elongation at break of the post-extruded blends with starch/plasticizer ratio of 3/2 wt/wt% and 2/1 wt/wt% increases to 14.8MPa and 16.8MPa, 1067MPa and 1740 MPa, 3.46% and 2.17% respectively from

Table 4-16. Comparison of mechanical properties of thermoplastic starch/PLA blend prepared by different molding methods

No.	Starch/PLA	Starch type	Starch/ plasticizer ratio, wt/wt	Molding method	Density, g/cm^3	Tensile properties		
						Strength (MPa)	Modulus (MPa)	Elogation at break (%)
1	100/0	HAS	1/1	Compression	1.360	0.888±0.084	22.16±5.19	9.51±1.25
2	70/30	HAS	1/1	Compression	1.356	3.10±0.77	184.6±40.6	4.35±1.31
3	50/50	HAS	1/1	Compression	1.340	6.68±1.80	585.8±261.3	2.30±0.58
4	30/70	HAS	1/1	Compression	1.311	18.1±0.8	1750±27	1.93±0.29
5	0/100	/	/	Compression	1.251	67.8±3.7	3336±133	3.07±0.64
6	100/0	HAS	1/1	Extrusion	1.367	0.888±0.120	18.59±1.09	10.1±2.0
7	70/30	HAS	1/1	Extrusion	1.341	3.72±0.72	162.3±23.7	10.1±3.7
8	50/50	HAS	1/1	Extrusion	1.311	9.70±1.60	629.1±158.2	6.59±3.42
9	30/70	HAS	1/1	Extrusion	1.296	22.8±2.5	1522±76	7.59±2.07
10	0/100	/	/	Extrusion	1.251	68.2±5.8	3119±125	4.80±2.20
11	100/0	NS	2/1	Compression	1.426	5.83±0.07	175.6±13.7	21.57±1.20
12	70/30	NS	2/1	Compression	1.407	7.11±2.51	717.9±35.3	1.90±0.26
13	50/50	NS	2/1	Compression	1.362	14.70±2.78	1335±51	1.91±0.18
14	30/70	NS	2/1	Compression	1.318	25.51±0.61	1852±120	2.60±0.28
15	100/0	NS	2/1	Extrusion	1.417	2.81±0.32	55.09±18.09	76.0±33.8
16	70/30	NS	2/1	Extrusion	1.391	5.08±1.19	250.6±57.2	13.0±2.9
17	50/50	NS	2/1	Extrusion	1.367	15.1±2.3	926.2±220.3	6.22±2.59
18	30/70	NS	2/1	Extrusion	1.324	24.5±1.1	1557±49	5.30±2.90

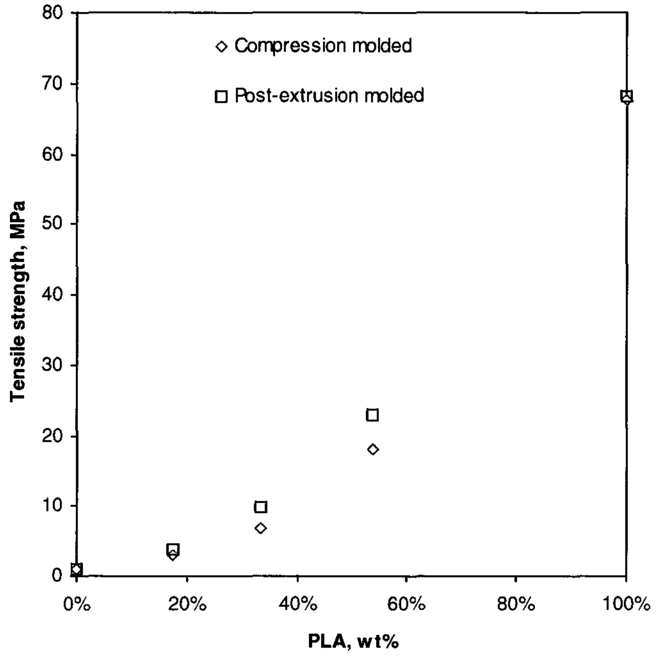

Figure 4-41. The effect of molding method on the tensile strength of thermoplastic high amylose starch/PLA blends (starch/plasticizer ratio: 1/1wt/wt%; water/glycerol ratio: 15/35wt/wt%).

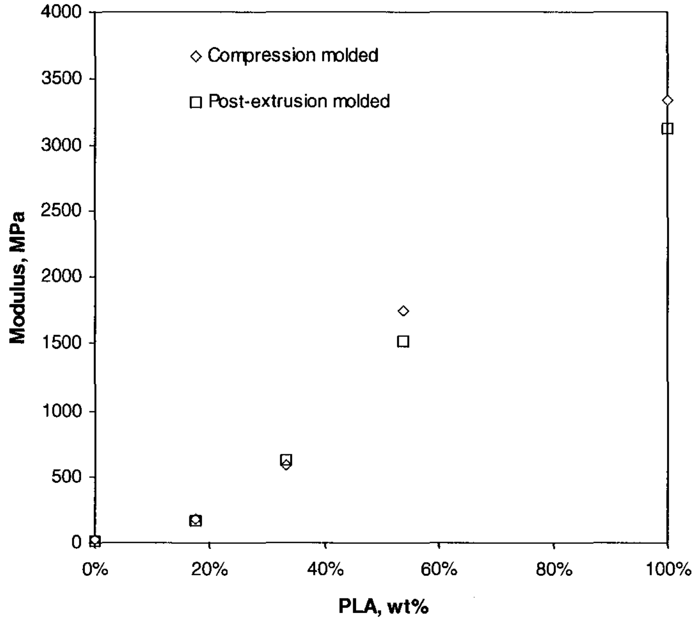

Figure 4-42. The effect of molding method on the tensile modulus of thermoplastic high amylose starch/PLA blends (starch/plasticizer ratio: 1/1wt/wt%; water/glycerol ratio: 15/35wt/wt%).

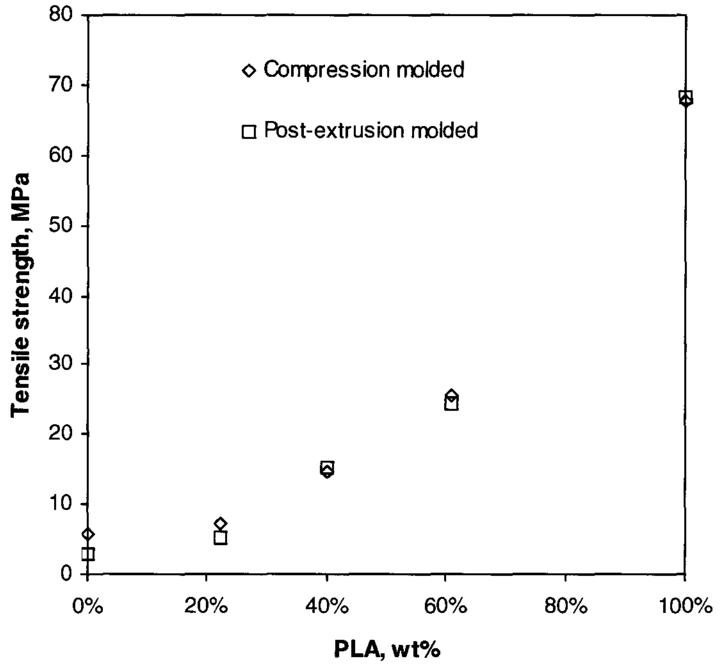

Figure 4-43. The effect of molding method on the tensile strength of thermoplastic normal starch/PLA blends (starch/plasticizer ratio: 2/1wt/wt%; water/glycerol ratio: 15/35 wt/wt%).

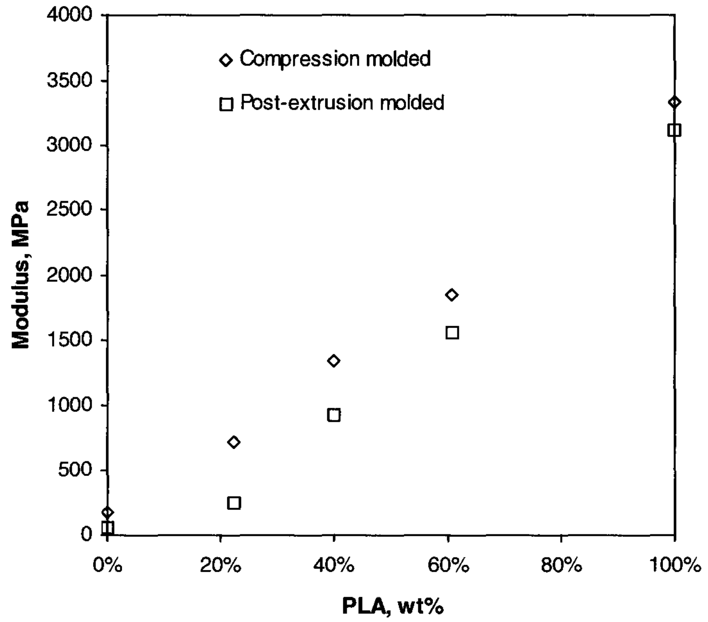

Figure 4-44. The effect of molding method on the elastic modulus of thermoplastic normal starch/PLA blends (starch/plasticizer ratio: 2/1wt/wt%; water/glycerol ratio: 15/35 wt/wt%).

12.0 MPa and 12.7 MPa, 976.8 MPa and 1496 MPa, 2.46% and 1.50% for the compression molded samples with the same composition. The improved tensile and elongation at break for blends prepared by post extrusion molding may be attributed to difference in the degree of crystallinity of the blends. DSC studies indicate that PLA in the post-extrusion molded high amylose starch/PLA blends has higher degree of crystallinity than the compression molded blends (see section 4.2.2). The increase in the degree of PLA crystallization may be contributed to the extension of PLA phase in the thermoplastic starch/PLA blends (see section 4.2.1). However, thermoplastic normal starch/PLA blends showed different results. The thermoplastic normal starch/PLA blends prepared by post extrusion molding exhibit lower tensile strength and modulus but higher elongation at break than the blends prepared by compression molding.

The effects of the post-extrusion temperature in the Rosand capillary rheometer on the mechanical properties of post-extruded starch/PLA blends were also investigated. The results are shown in Figures 4-45 to 4-48. For all thermoplastic starch/PLA blends measured, the samples extruded at 170°C had lower mechanical properties, indicating the blends underwent a small degree of degradation at higher extrusion molding temperature.

Jun (2000) reported that Pluronic F-108 (polyethylene-polypropylene glycol copolymer) from BASF was a good PLA plasticizer and the addition of a small amount of F-108 caused a large increase in elongation at break of the starch/PLA blend with 25% starch component (for example, elongation at break increases to 306% for the blend containing 6.7 wt% F-108 from 3.6% for the blend without F-108). In the present study, Pluronic F-108 has little influence on elongation at break for compression molded thermoplastic high amylose starch/PLA blends. However, F-108 seems to improve the

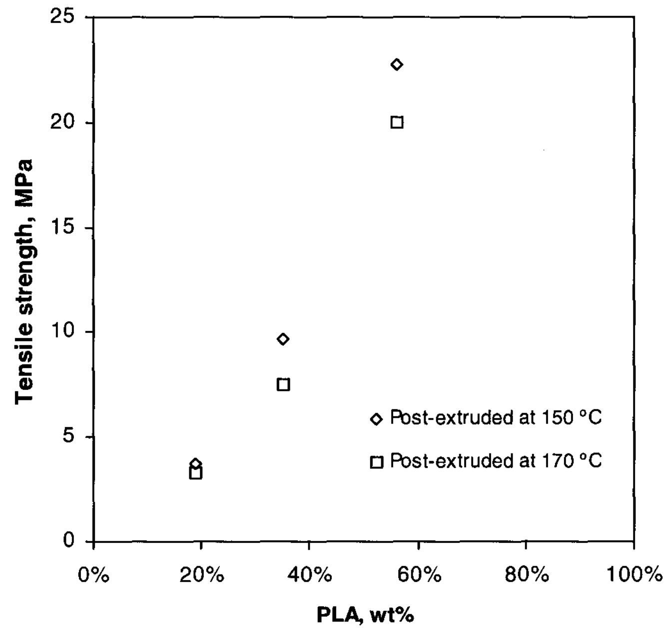

Figure 4-45. Tensile strength of thermoplastic high amylose starch/PLA blends post-extruded at different temperature: 150°C and 170°C (starch/plasticizer ratio: 1/1wt/wt%; water/glycerol ratio: 15/35wt/wt%).

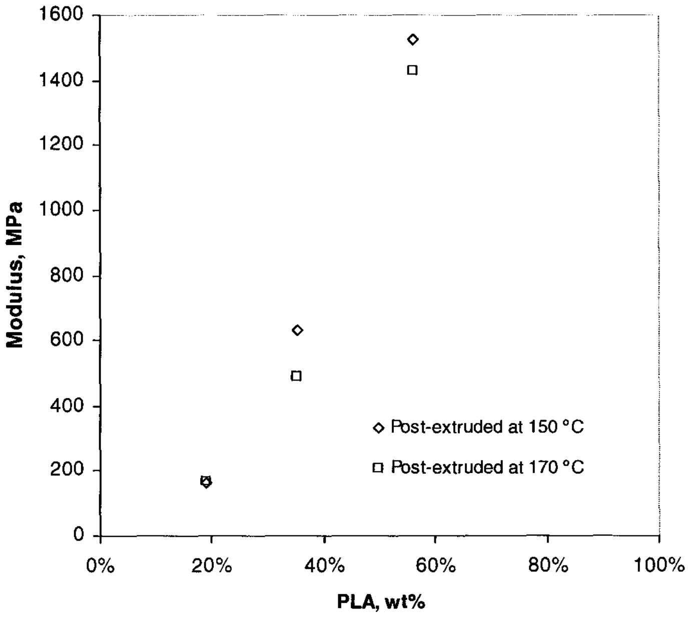

Figure 4-46. Elastic modulus of thermoplastic high amylose starch/PLA blends post-extruded at different temperature: 150°C and 170°C (starch/plasticizer ratio: 2/1wt/wt%; water/glycerol ratio: 15/35wt/wt%).

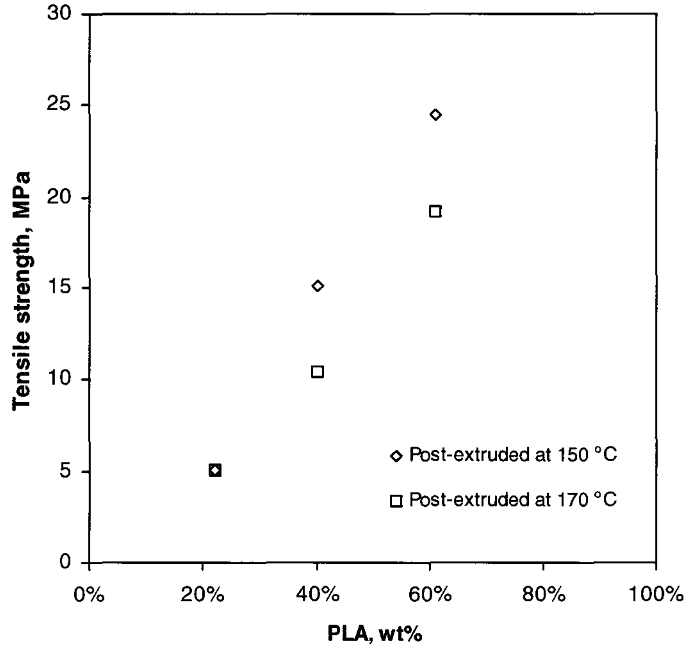

Figure 4-47. Tensile strength of thermoplastic normal starch/PLA blends post-extruded at different temperature: 150°C and 170°C (starch/plasticizer ratio: 2/1wt/wt%; water/glycerol ratio: 15/35wt/wt%).

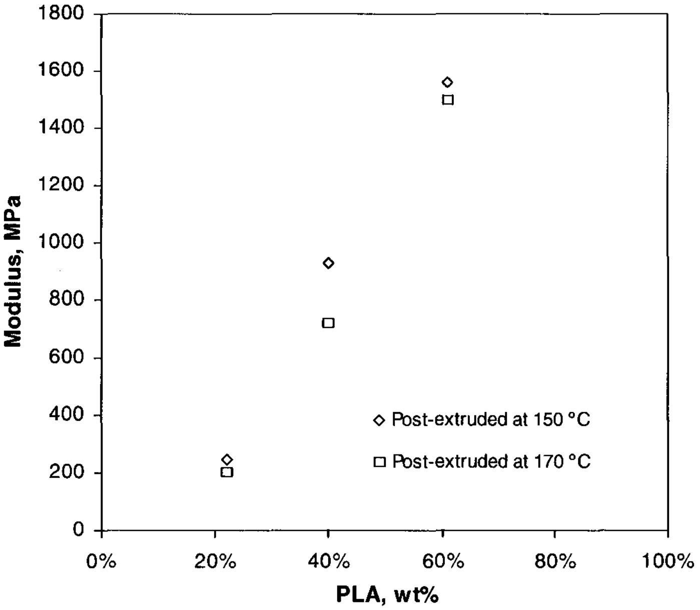

Figure 4-48. Tensile modulus of thermoplastic normal starch/PLA blends post-extruded at different temperature: 150°C and 170°C (starch/plasticizer ratio: 2/1wt/wt%; water/glycerol ratio: 15/35wt/wt%).

elongation at break of the post-extrusion molded thermoplastic high amylose starch/PLA blends with high PLA content, as shown in Table 4-17. The effects of F-108 on the mechanical properties of thermoplastic starch/PLA blends need to be further investigated.

Table 4-17. Effects of plasticizer F-108 on the mechanical properties of thermoplastic starch /PLA blends

No.	Blends	Starch/PLA ratio, wt/wt	Starch/ plascizer ratio, wt/wt	Content Of F-108,wt%	Molding method	Density, g/cm^3	Tensile properties		
							Strength (MPa)	Modulus (MPa)	Elogation at break (%)
1	HAS/PLA	70/30	1/1	0	Compression	1.356	3.10±0.77	184.6±40.6	4.35±1.31
2	HAS/PLA	70/30	1/1	5	Compression	1.355	1.95±0.14	173.4±28.2	2.73±1.17
3	HAS/PLA	50/50	1/1	0	Compression	1.340	6.68±1.80	585.8±261.3	2.30±0.58
4	HAS/PLA	50/50	1/1	5	Compression	1.327	6.34±0.95	496.7±53.1	2.65±0.59
5	HAS/PLA	30/70	1/1	0	Compression	1.311	18.1±0.8	1750±27	1.93±0.29
6	HAS/PLA	30/70	1/1	5	Compression	1.305	13.8±1.4	1417±125	3.60±3.53
7	HAS/PLA	0/100	/	0	Compression	1.251	67.8±3.7	3336±133	3.07±0.64
8	HAS/PLA	0/100	/	5	Compression	1.256	51.2±3.9	3141±202	2.77±0.85
9	HAS/PLA	70/30	1/1	0	Extrusion	1.341	3.72±0.72	162.3±23.7	10.1±3.7
10	HAS/PLA	70/30	1/1	5	Extrusion	1.345	3.03±1.07	134.5±36.1	11.0±3.8
11	HAS/PLA	50/50	1/1	0	Extrusion	1.311	9.70±1.60	629.1±158.2	6.59±3.42
12	HAS/PLA	50/50	1/1	5	Extrusion	1.315	8.73±0.47	568.9±41.0	7.30±0.58
13	HAS/PLA	30/70	1/1	0	Extrusion	1.296	22.8±2.5	1522±76	7.59±2.07
14	HAS/PLA	30/70	1/1	5	Extrusion	1.296	17.6±0.3	1327±82	20.1±3.5
15	HAS/PLA	20/80	1/1	5	Extrusion	1.295	22.4±0.3	1700±45	19.4±7.0

The mechanical properties of thermoplastic high amylose starch/PLA blends (after storage in plastic bags for 180 days) were measured and presented in Table 4-18. After storage for 180 days, pure thermoplastic high amylose starch had higher tensile strength and modulus, but lower elongation at break. The tensile strength and modulus of the thermoplastic high amylose starch after a storage of 180 days increase to 1.11 MPa

Table 4-18. The change in the mechanical properties of thermoplastic high amylose starch /PLA blends after storage for 180 days.

No.	Blends	Ratio of starch/PLA, wt/wt	Ratio of starch to plasticizers, wt/wt	Mechanical properties					
				First measurement			Second measurement		
				Tensile strength, MPa	Modulus, MPa	Elongation at break, %	Tensile strength, MPa	Modulus, MPa	Elongation at break, %
1	HAS	100/0	1/1	0.888±0.120	18.59±1.09	10.1±2.0	1.11±0.24	29.06±2.49	5.9±1.5
2	HAS /PLA	70/30	1/1	3.72±0.72	162.3±23.7	10.1±3.7	4.36±0.23	200.3±19.2	7.8±3.7
3	HAS /PLA	50/50	1/1	9.70±1.60	629.1±158.2	6.59±3.42	8.41±1.78	571.8±132.9	4.6±2.5
4	HAS /PLA	30/70	1/1	22.8±2.5	1522±76	7.59±2.07	20.3±2.0	1566±100	7.0±1.8
5	PLA	0/100	/	68.2±5.8	3119±125	4.80±2.20	63.5±5.4	3034±292	4.2±3.4
6	HAS /PLA	50/50	3/2	14.8±0.8	1067±43	3.46±0.86	12.6±1.1	974±128	3.4±2.3
7	HAS /PLA	50/50	2/1	16.8±2.3	1740±384	2.17±1.19	13.3±1.5	1141±163	1.8±0.1

and 29.06 MPa from 0.888 MPa and 18.59 MPa for the original sample while the elongation at break of the sample decreases to 5.9% from 10.1%. This result may be attributed to the post-crystallization (retrogradation) of the starch molecules during the storage. However, the effect of storage on the mechanical properties of thermoplastic high amylose starch/PLA blends is different from pure thermoplastic starch. When the starch component dominates (ratio of starch to PLA was 70/30 wt/wt%), the tensile strength and modulus of the blend increased but the elongation decreased. When PLA component dominates (ratios of starch to PLA were 50/50, 70/30 or 0/100 wt/wt%), the mechanical properties of the blends after storage are lower than those of fresh blends, no matter what the ratio of starch to plasticizer is. For example, the tensile strength, modulus and elongation at break of the thermoplastic high amylase starch/PLA (50/50wt/wt) blend

after the storage of 180 days decrease to 8.41 MPa, 571.8 MPa and 4.6% from 9.70 MPa, 629.1 MPa and 6.59% for the original sample.

4.2.5 Rheological properties

The rheological properties of thermoplastic starch/PLA blends at different temperature were investigated, as shown in Figures 4-49 to 4-57. The thermoplastic starch/PLA blends exhibit a shear-thinning behavior. The shear rate dependence of shear viscosity of the blends at lower temperature (for example, 130°C and 150°C) might be described by the power law equation: $\eta = m\dot{\gamma}^{n-1}$. The power law parameters are shown in Table 4-19. At higher temperatures (for example, 170°C); however, some of thermoplastic starch/PLA blends with higher PLA content (starch/PLA ratio was 50/50 or 30/70 wt/wt%) exhibited a Newtonian plateau at low shear rates (i.e. the power-law model does not fit). A Cross model can be used in this case (Vlachopoulos, 2003):

$$\eta = \frac{\eta_0}{1+(\lambda\dot{\gamma})^m} \tag{4-9}$$

$$\mathrm{Ln}\left(\frac{\eta_0}{\eta}-1\right) = m\mathrm{Ln}(\lambda) + m\mathrm{Ln}(\dot{\gamma}) \tag{4-10}$$

where, η_0 = zero shear viscosity, Pa.s

λ = relaxation time, s^{-1}

m = 1-n (n = power-law index)

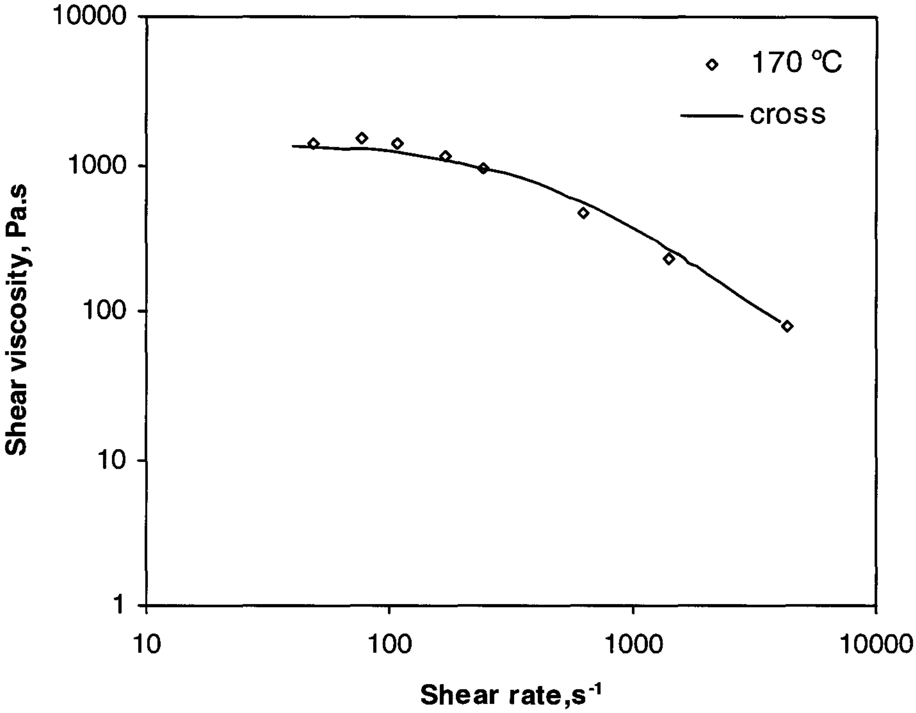

Figure 4-49. Rheological properties of pure PLA.

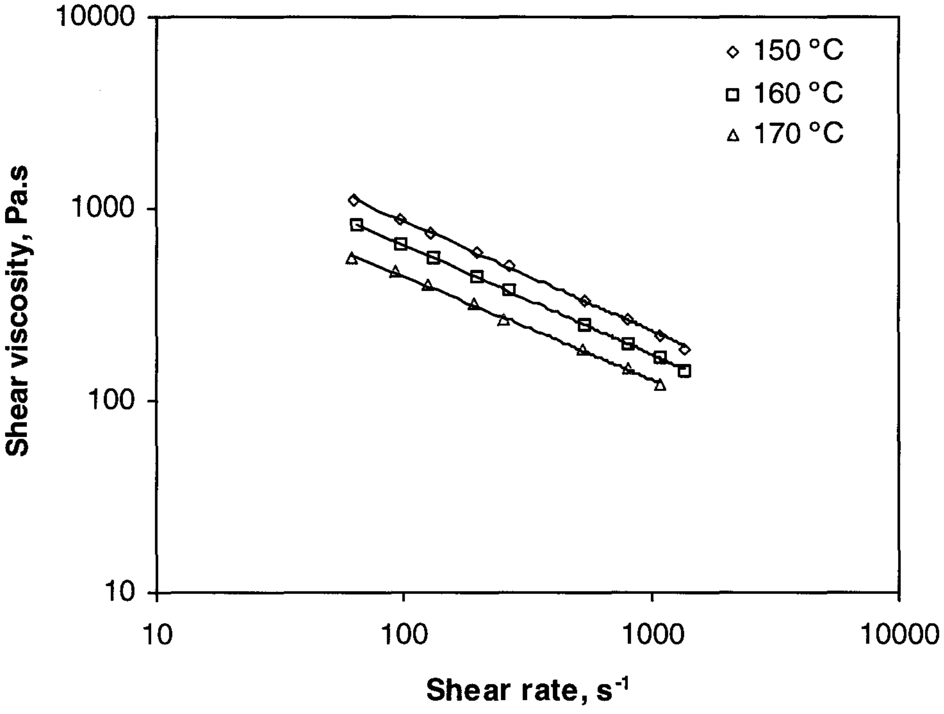

Figure 4-50. Rheological properties of thermoplastic high amylose starch/PLA (70/30) blend (starch/plasticizer ratio: 1/1wt/wt%; water/glycerol: 15/35wt/wt%).

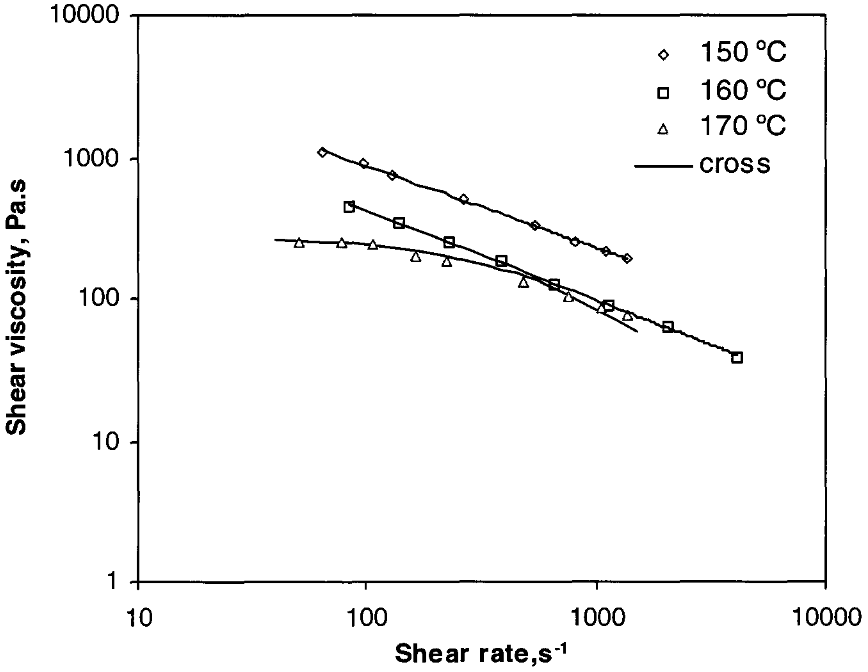

Figure 4-51. Rheological properties of thermoplastic high amylose starch /PLA (50/50) blend (starch/plasticizer ratio: 1/1wt/wt%; water/glycerol: 15/35wt/wt%).

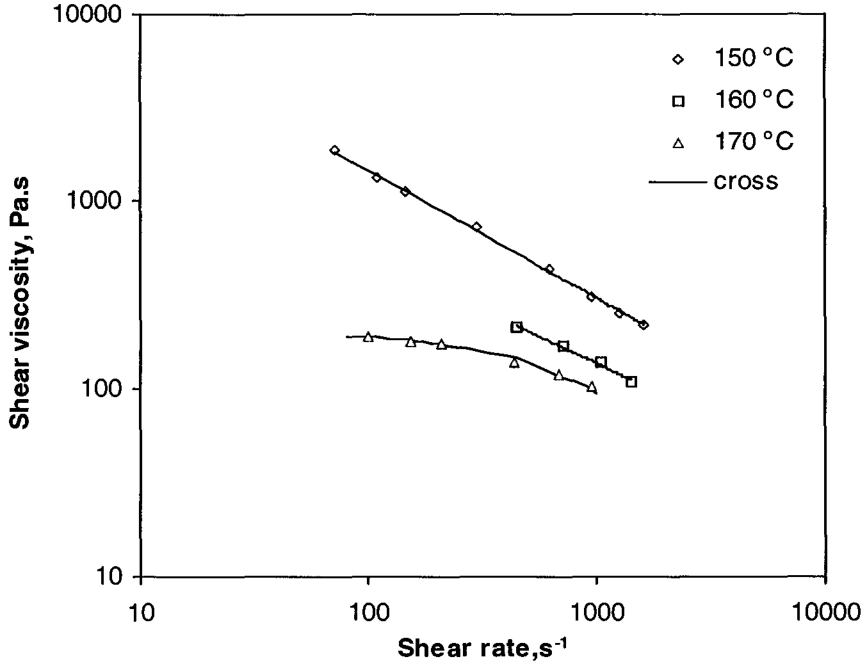

Figure 4-52. Rheological properties of thermoplastic high amylose starch/PLA (30/70) blend (starch/plasticizer ratio: 1/1wt/wt%; water/glycerol: 15/35wt/wt%).

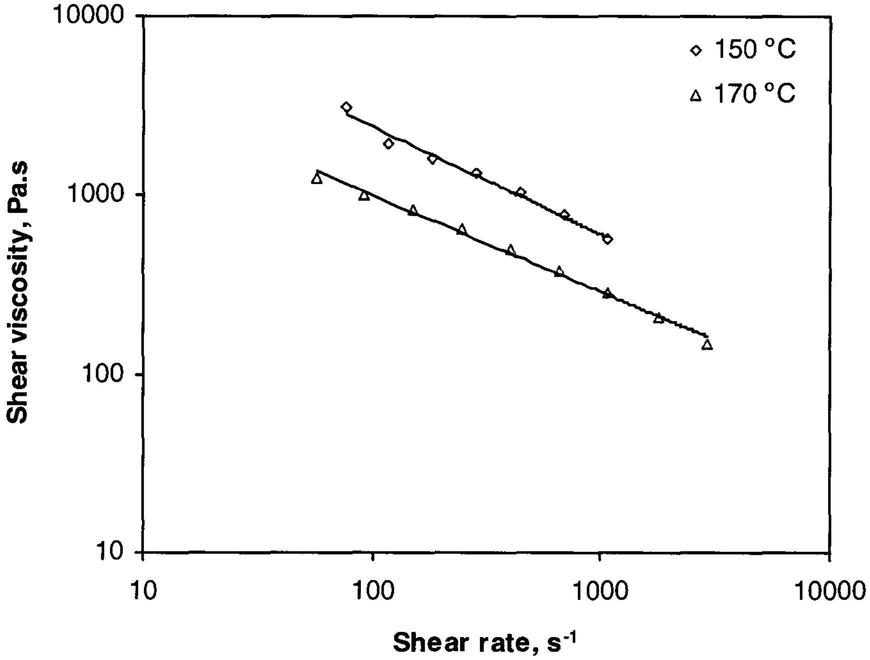

Figure 4-53. Rheological properties of thermoplastic normal starch/PLA (70/30) blend (starch/plasticizer ratio: 2/1wt/wt%; water/glycerol: 15/35wt/wt%).

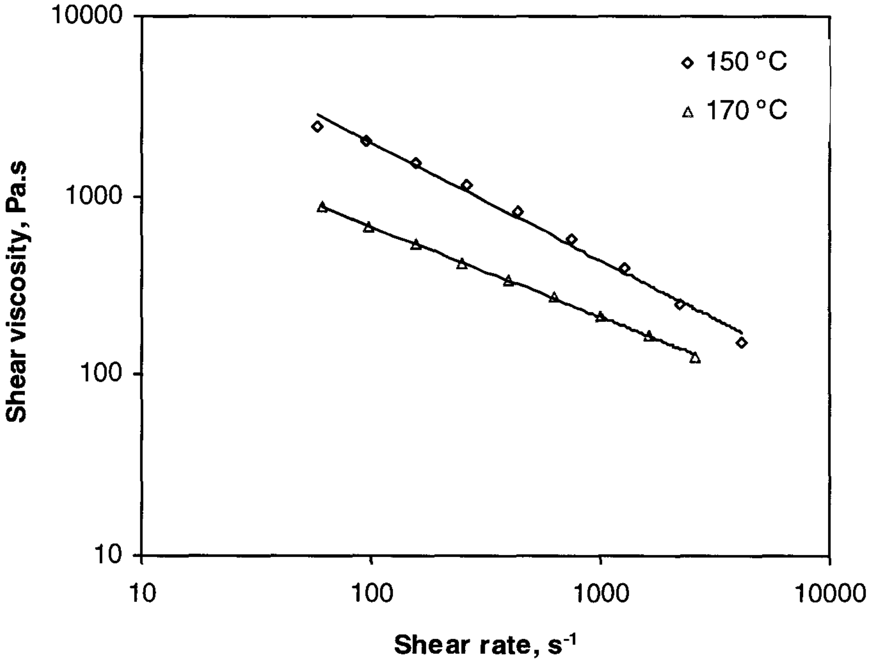

Figure 4-54. Rheological properties of thermoplastic normal starch/PLA (50/50) blend (starch/plasticizer ratio: 2/1wt/wt%; water/glycerol: 15/35wt/wt%).

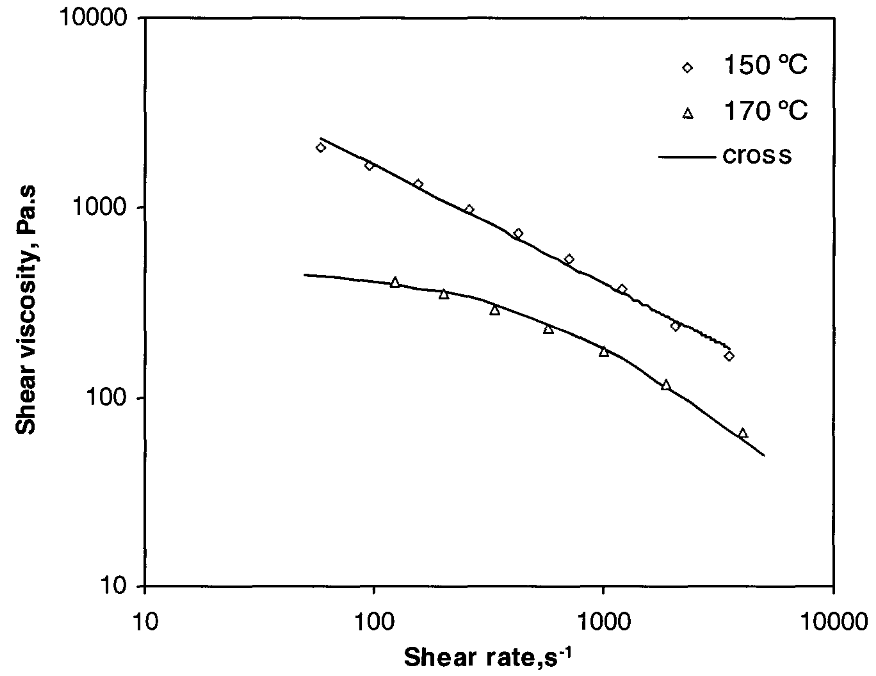

Figure 4-55. Rheological properties of thermoplastic normal starch/PLA (30/70) blend (starch/plasticizer ratio: 2/1wt/wt%; water/glycerol: 15/35wt/wt%).

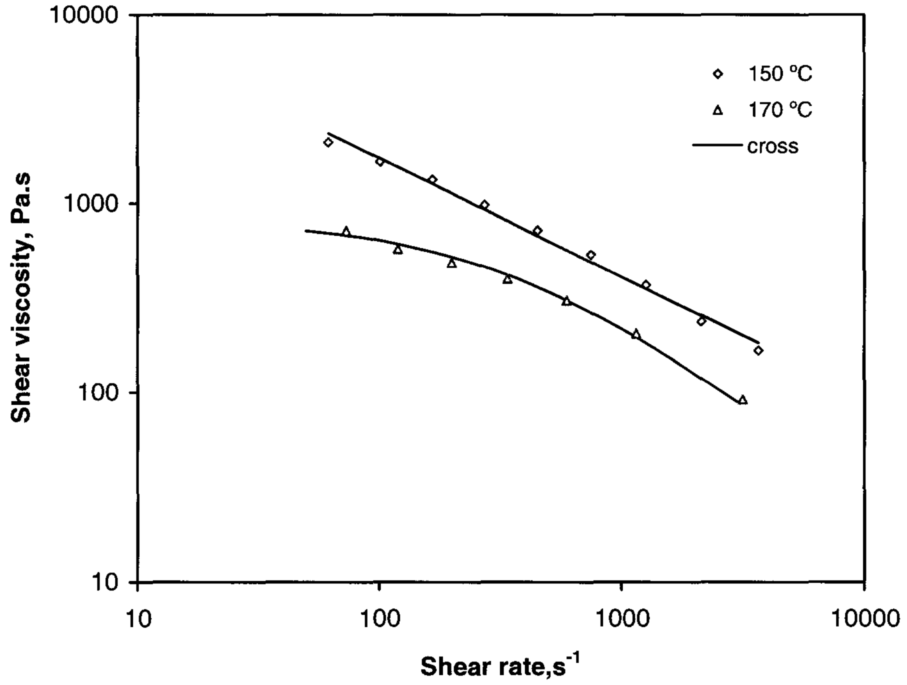

Figure 4-56. Rheological properties of the thermoplastic high amylose starch/PLA (50/50) blend (starch/plasticizers ratio: 2/1wt/wt%; water/glycerol: 15/35wt/wt%).

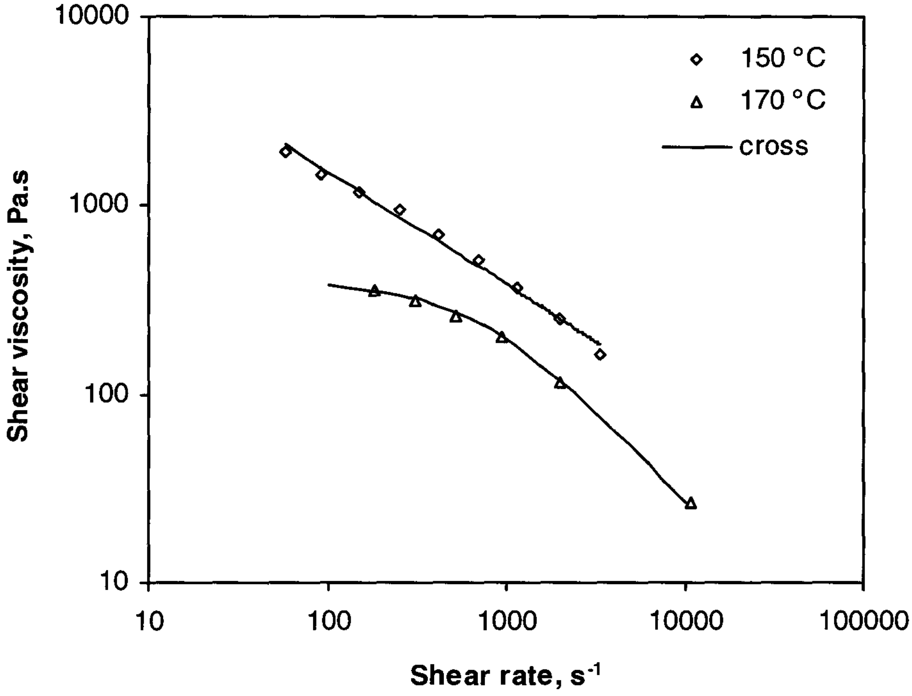

Figure 4-57. Rheological properties of thermoplastic waxy starch/PLA (50/50) blend (starch/plasticizers ratio: 2/1wt/wt%; water/glycerol: 15/35wt/wt%).

The parameters of the Cross model are presented in Table 4-20. Pure PLA exhibited the highest zero shear viscosity (1425 Pa.s) due to its strong interaction between molecular chains. The zero shear viscosity of thermoplastic high amylose starch/PLA blends decreases as PLA content in the blends increases. By comparing thermoplastic starch/PLA blends with same compositions (starch/PLA ratio is 50/50 wt/wt%, starch/plasticizer ratio is 2/1 wt/wt%) prepared with different starches, the blend prepared with high amylose starch showed the highest zero shear viscosity while the blend prepared with thermoplastic waxy starch showed the lowest zero shear viscosity. The difference in zero shear viscosity may be attributed to the difference in amylose content and structure in the starches. The linear amylose molecules have more molecular entanglement and hydrogen bonds, which increases the viscosity of the materials.

Table 4-19. Consistency, power-law index of thermoplastic starch/PLA blends

No.	Blends	Starch type	Starch/PLA (wt/wt)	Starch/ plasticizers ratio (wt/wt)	Measurement temperature, °C	m (Pa.s ^{n})	n	R^2
1	HAS/PLA	HAS	100/0	1/1	110	20343	0.31	0.99
					130	12410	0.34	0.99
					150	26777	0.32	0.99
					170	6163.0	0.26	0.99
2	HAS/PLA	HAS	70/30	1/1	150	11966	0.43	0.99
					160	8973.4	0.43	0.99
					170	5368.6	0.46	0.99
3	HAS/PLA	HAS	50/50	1/1	150	12498	0.42	0.99
4	HAS/PLA	HAS	30/70	1/1	150	34311	0.32	0.99
					160	7043.8	0.43	0.99
5	NS/PLA	NS	100/0	2/1	110	52883	0.38	0.99
					130	35459	0.35	0.99
					150	29445	0.3	0.99
					170	12134	0.33	0.99
6	NS/PLA	NS	70/30	2/1	150	38733	0.40	0.99
					170	12054	0.46	0.99
7	NS/PLA	NS	50/50	2/1	150	40881	0.34	0.99
					170	7094.3	0.49	0.99
8	NS/PLA	NS	30/70	2/1	150	29555	0.38	0.99
9	HAS/PLA	HAS	50/50	2/1	150	30959	0.37	0.99
10	WS/PLA	WS	50/50	2/1	150	23372	0.40	0.99

Table 4-20. Cross model parameters of thermoplastic starch/PLA blends

No.	Blends	Ratio of starch to PLA, wt/wt	Ratio of starch to plasticizers, wt/wt	F-108 content, wt%	η_0, Pa.s	m	λ, s^{-1}
1	HAS/PLA	70/30	1/1	5	648	1.091	0.0042
2	HAS/PLA	50/50	1/1	0	268	1.266	0.0019
3	HAS/PLA	50/50	1/1	5	611	1.269	0.0027
4	HAS/PLA	30/70	1/1	0	195	1.332	0.0011
5	HAS/PLA	30/70	1/1	5	312	1.231	0.0015
6	HAS/PLA	50/50	2/1	0	828	0.989	0.0028
7	NS/PLA	50/50	2/1	0	474	1.026	0.0016
8	WS/PLA	50/50	2/1	0	403	1.133	0.0010
9	PLA	/	/	/	1425	1.232	0.0024

Temperature: 170°C

An Arrhenius equation can be applied to describe the temperature dependence of the shear viscosities of the thermoplastic starch/PLA blends. The relationship between shear viscosity (η), shear rate ($\dot{\gamma}$) and temperature can be described by (Vlachopoulos, 2003):

$$\eta = m \exp\left(\frac{E}{RT}\right) \dot{\gamma}^{n-1} \qquad (4\text{-}11)$$

Where E = activation energy, J/g

R = gas constant, 8.314 J/mol-K

m = consistency index, $Pa.s^n$

The experimental data were regressed to obtain the model parameters, as presented in Table 4-21. Power-law index n is between 0.30 and 0.52. Activation energy E is between 41.0 KJ/mol-K and 118.7 KJ/mol-K. Activation energy increases with increasing PLA content in the blends. The increase of activation energy with PLA content may be attributed to stronger intermolecular forces in PLA. The blends prepared with high amylose starch had a higher activation energy than those with same starch/PLA ratio but prepared with normal starch. It is probably related to stronger intermolecular forces in high amylose starch. The consistency index, m, shows the opposite trend, as it decreases with increasing PLA content in the blends, and the m values of the blends prepared with high amylose starch were lower than those of the blends with same composition but prepared with normal starch.

Table 4-21. Arrhenius equation parameter of thermoplastic starch/PLA blends

No.	Blends	Starch type	Starch/PLA ratio (wt/wt)	Starch/ plasticizers ratio (wt/wt)	m_0, Pa.s^n	n	Activation energy E, KJ	R^2
1	HAS/PLA 100/0	HAS	100/0	1/1	0.23±0.11	0.30±0.02	37.06±1.53	0.98
2	HAS/PLA 70/30	HAS	70/30	1/1	0.011±0.003	0.44±0.01	48.89±1.09	0.99
3	HAS/PLA 50/50	HAS	50/50	1/1	$5.8\times10^{-7}\pm5.7\times10^{-7}$	0.47±0.04	88.37±8.73	0.93
4	HAS/PLA 30/70	HAS	30/70	1/1	$2.0\times10^{-10}\pm2.0\times10^{-10}$	0.41±0.05	118.7±8.02	0.96
5	NS/PLA 100/0	NS	100/0	2/1	0.19±0.06	0.34±0.01	41.01±1.05	0.99
6	NS/PLA 70/30	NS	70/30	2/1	$7.4\times10^{-4}\pm5.1\times10^{-4}$	0.44±0.02	62.70±2.95	0.99
7	NS/PLA 50/50	NS	50/50	2/1	$2.8\times10^{-4}\pm2.4\times10^{-4}$	0.41±0.02	67.08±4.59	0.98
8	NS/PLA 30/70	NS	30/70	2/1	$4.4\times10^{-7}\pm4.4\times10^{-7}$	0.52±0.05	92.67±10.84	0.91
9	HAS/PLA 50/50	HAS	50/50	2/1	$2.8\times10^{-6}\pm2.6\times10^{-6}$	0.39±0.03	85.16±5.49	0.98

Blending conditions of thermoplastic starch: 120°C/4mins/45rpm; blending conditions of TPS/PLA blends: 170°C/4mins/45rpm.

The effect of blend composition on the rheological behavior of thermoplastic high amylose starch/PLA blends was investigated. An addition of a small amount of PLA causes a decrease in shear viscosity of the blends (starch/PLA ratio is 70/30 and 50/50 wt/wt%), as shown in Figure 4-58. When PLA content in the blend increases (for example, starch/PLA ratio is 30/70), the blend showed a higher viscosity than pure thermoplastic starch and the blends with other composition. PLA is a polar polymer and has a higher shear viscosity than pure thermoplastic starch component used in this work. Garlotta (2001) reported that the relationship between shear viscosity and shear rate of semi-crystalline PLA at 150°C can be expressed by power law: $\eta = 609{,}159\,\dot{\gamma}^{-0.8134}$. The

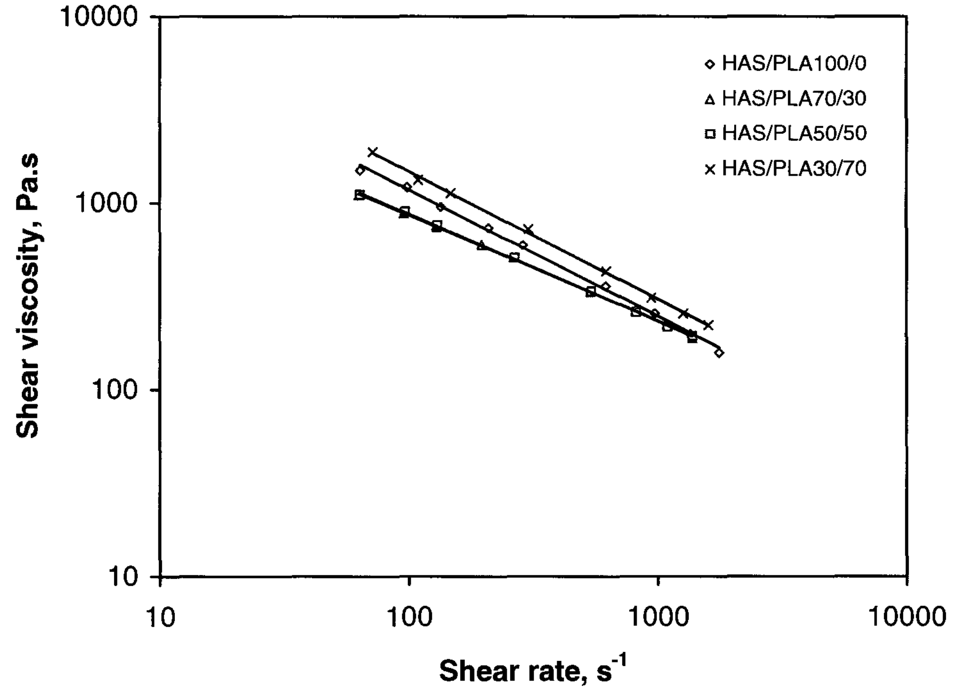

Figure 4-58. Composition dependence of the rheological properties of thermoplastic high amylose starch/PLA blends (temperature: 150 °C; starch/plasticizer ratio: 1/1wt/wt%; water/glycerol ratio: 15/35wt/wt%).

rheological properties of thermoplastic high amylose starch used in this work at 150 °C can be described as $\eta = 26{,}777\dot{\gamma}^{-0.679}$. The PLA component with higher viscosity causes an increase in viscosity of the blend with higher PLA content.

The shear viscosities of thermoplastic normal starch/PLA blends are higher than that of thermoplastic normal starch, as shown in Figure 4-59. The thermoplastic normal starch had lower shear viscosity ($\eta = 29{,}445\dot{\gamma}^{-0.7}$ at 150°C) than PLA. The addition of PLA component causes an increase in viscosity of the blends. However, by comparing the shear viscosity of thermoplastic normal starch/PLA blends with different normal starch/PLA ratios, it is found that the shear viscosity decreases when starch/PLA ratio in the blends decreases.

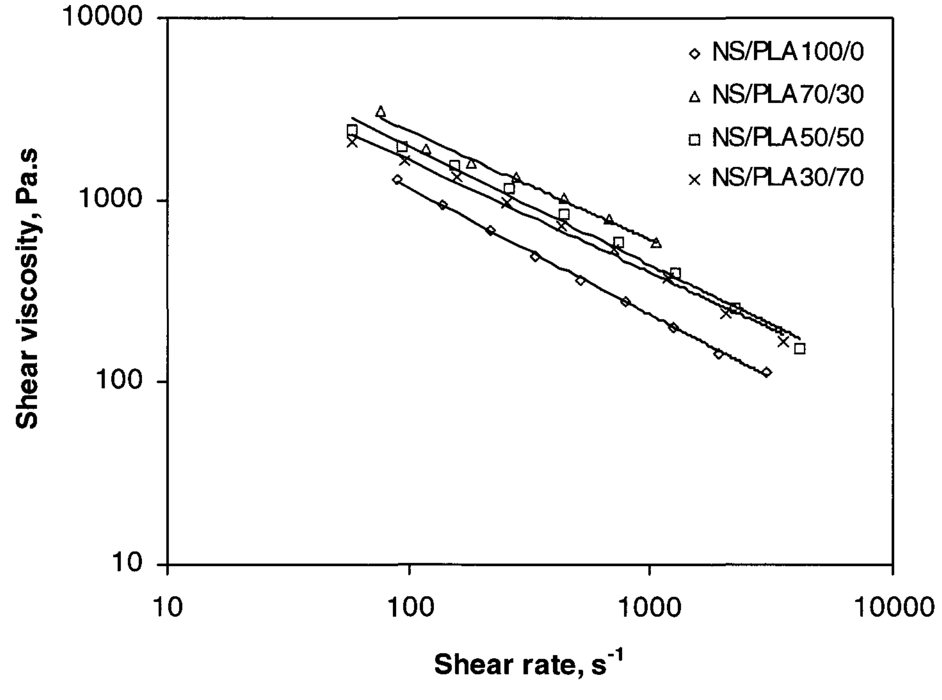

Figure 4-59. Composition dependence of the rheological properties of thermoplastic normal starch/PLA blends (temperature: 150 °C; starch/plasticizer ratio: 2/1wt/wt%; water/glycerol ratio: 15/35wt/wt%).

Figure 4-60 presents the rheological properties of thermoplastic starch/PLA blends prepared by using different type of starches. The blend prepared with thermoplastic high amylose starch shows the highest shear viscosity while the blend with waxy starch has the lowest shear viscosity. The different viscosity is probably related to difference in the amylose content and structure in the starches. The linear amylose molecules have more potential for formation of hydrogen bond and molecular entanglement, and therefore cause an increase in the shear viscosity.

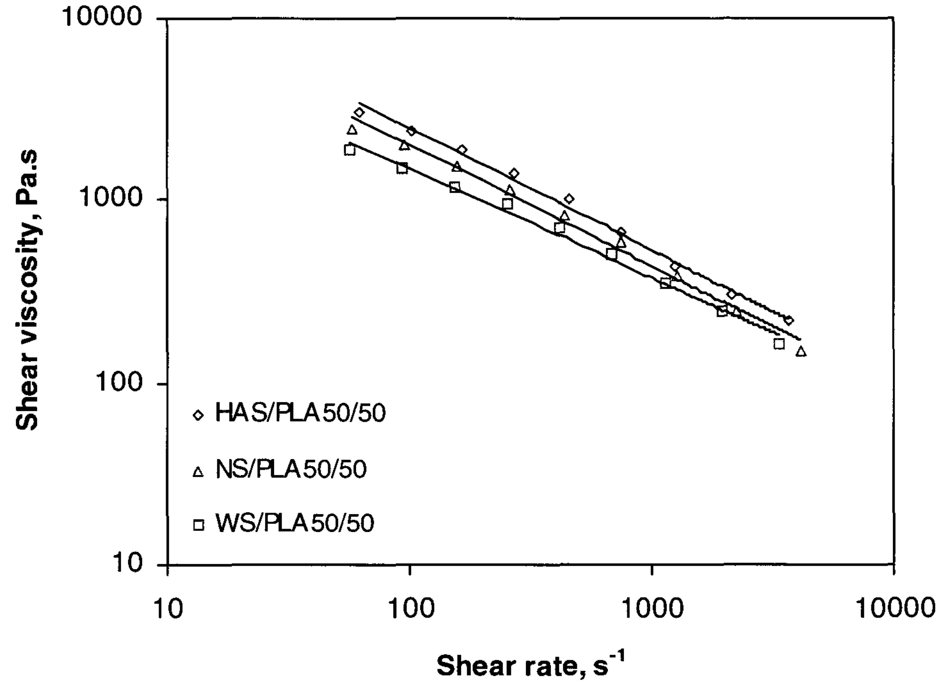

Figure 4-60. Comparison of rheological properties of thermoplastic starch/PLA blends prepared by different type of starch (measurement temperature: 150°C; starch/plasticizer ratio: 2/1wt/wt%; water/glycerol ratio: 15/35wt/wt%).

The effect of starch/plasticizer ratio on the rheological properties of high amylose starch/PLA blends (starch/PLA ratio is 50/50 wt/wt%) was investigated, as shown in

Figure 4-61. The shear viscosity decreases as the plasticizer content increases. Plasticizers (water and glycerol) can reduce the intermolecular forces in the blends and therefore causes a decrease in shear viscosity.

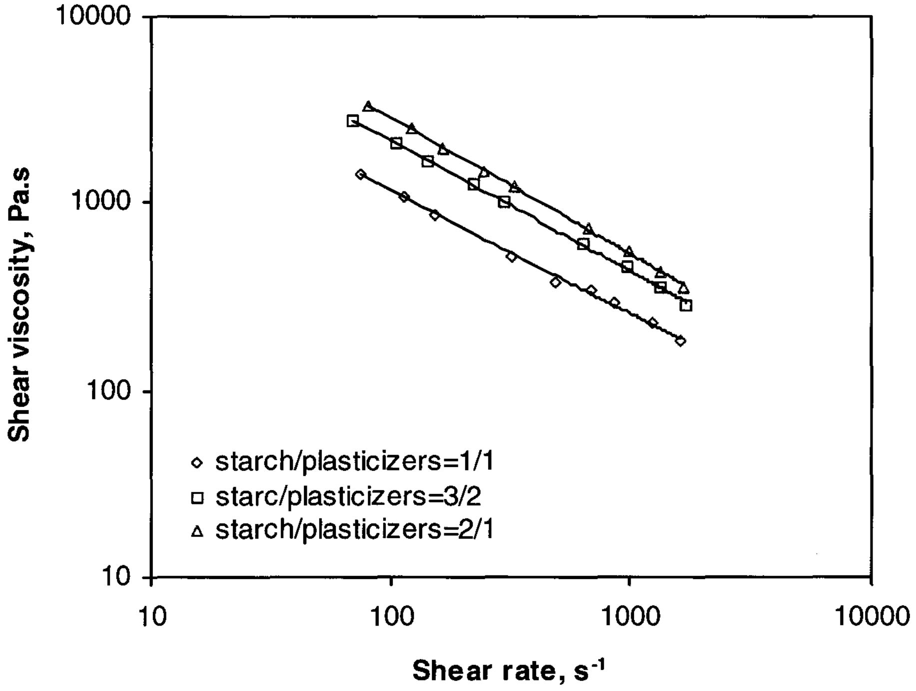

Figure 4-61. Effects of plasticizer content on the rheological properties of thermoplastic high amylose starch/PLA (50/50) blend containing 5% F-108 (temperature: 150 °C; starch/plasticizer ratio (wt/wt%): 1/1, 3/2and 2/1; water/glycerol: 15/35wt/wt%).

The effect of F-108 (polyethylene-polypropylene glycol copolymer) on the rheological properties of the thermoplastic high amylose starch/PLA blends was investigated. Addition of F-108 causes an increase in shear viscosity of the blends with high starch/PLA ratio (for example 70/30 and 50/50) (see Figures 4-62 and 4-63), but a decrease in viscosity of the blends with low starch/PLA ratio (for example 30/70 wt/wt%) (as shown in Figure 4-64). F-108 is reported to be a good plasticizer for PLA material. In the analysis of effects of F-108 on the mechanical properties of the blends, it is found that the F-108 plays as a plasticizer for PLA only when PLA content in the blends is high.

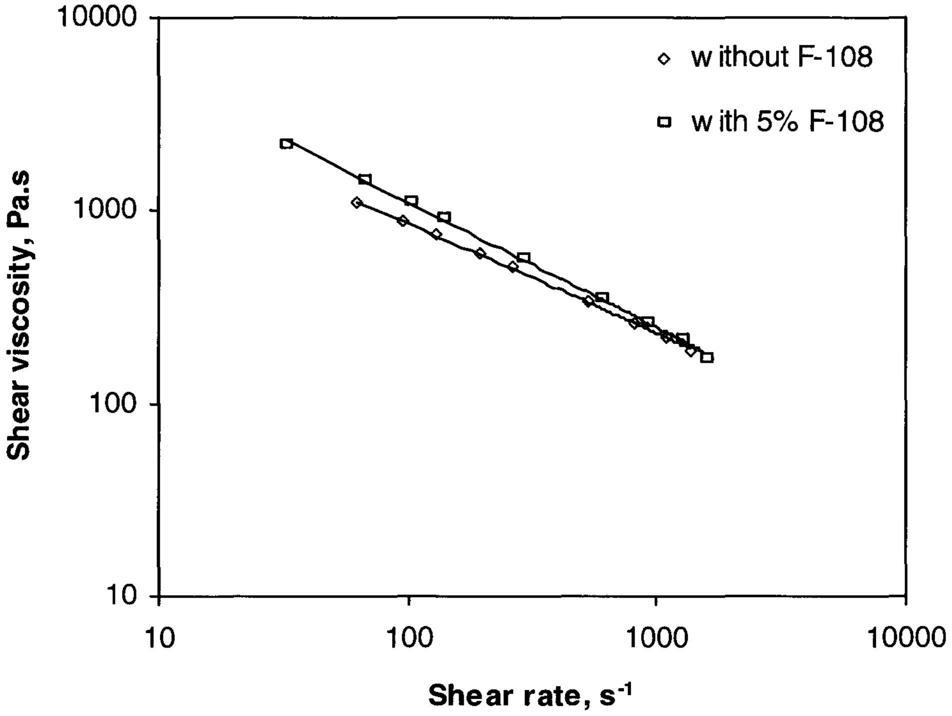

Figure 4-62. Effects of F-108 on rheological properties of thermoplastic high amylose starch/PLA (70/30) blend (measurement temperature: 150°C; starch/plasticizer ratio: 1/1 wt/wt%; water/glycerol ratio: 15/35 wt/wt%).

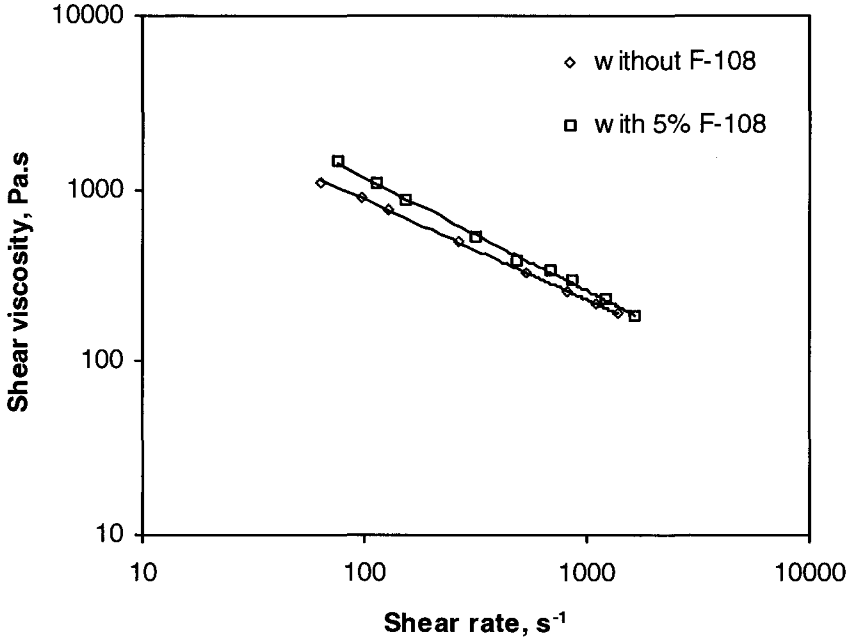

Figure 4-63. Effects of F-108 on rheological properties of thermoplastic high amylose starch/PLA (50/50) blend (measurement temperature: 150°C; starch/plasticizer ratio: 1/1wt/wt%; water/glycerol ratio: 15/35wt/wt%).

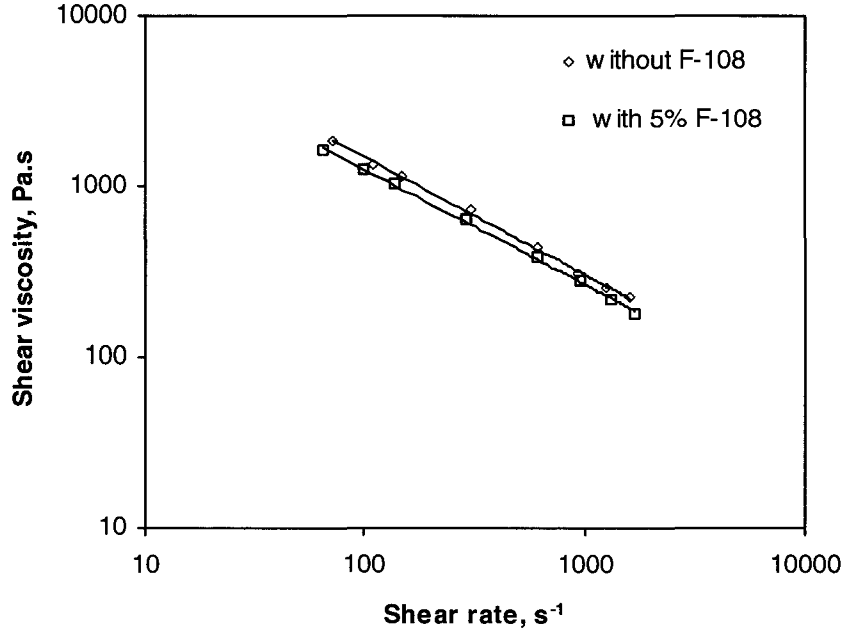

Figure 4-64. Effects of F-108 on rheological properties of thermoplastic high amylose starch/PLA (30/70) blend (measurement temperature: 150°C; starch/plasticizer ratio: 1/1wt/wt%; water/glycerol ratio: 15/35wt/wt%).

Chapter 5

Conclusions

In this research, cornstarches with various amylose contents were made thermoplastic using water and glycerol as plasticizers. The thermoplastic cornstarches were then blended with poly(lactic acid). The morphology, thermal properties, average molecular weights and molecular weight distribution of the thermoplastic starches and thermoplastic starch/PLA blends were analyzed using SEM, DSC and HPSEC. The rheological and mechanical of the materials were also measured. From the experimental results and discussions in Chapter 4, following conclusions can be obtained:

(1). Ratio of water to glycerol has the most significant effect on the mechanical properties of thermoplastic high amylose starch. An increase in water/glycerol ratio causes improved mechanical properties. Two-factor interaction of processing temperature and time has the most significant negative effect on the mechanical properties.

(2). Compression molded thermoplastic starch/PLA blends exhibit a two-phase structure. The separated PLA phase is dispersed in the continuous thermoplastic starch phase. The size of PLA phase in the blends increases with increasing PLA content. A partial compatibility exists between thermoplastic starch and PLA components.

(3). Starch phases and PLA phases in post-extrusion molded thermoplastic high amylose starch and thermoplastic high amylose starch/PLA blends were extended, resulting in higher degree of PLA crystallinity and improved mechanical properties.

(7). The crystalline structure in native starch granules is temperature resistant; DSC cannot detect the thermal transition of the crystalline structure in thermoplastic starch.

(9). The existence of thermoplastic starch and post-extrusion molding promote the crystallization of PLA component in thermoplastic starch/PLA blends. Thermoplastic normal starch has the strongest ability to promote the crystallization of PLA while thermoplastic high amylose starch is the weakest in promoting the crystallization of PLA.

(10). The MWD of native starches show a bimodal pattern; degradation of TPS during processing mainly occurred on amylose fraction.

(12). High amylose starch is more difficult to plasticize than normal starch and waxy starch. Thermoplastic waxy starch exhibits similar tensile strength, higher modulus and lower elongation at break, compared to thermoplastic normal starch with the same composition.

(13). The mechanical properties of thermoplastic starch and thermoplastic starch/PLA blends depend on starch molecular weight, amylose content, plasticizer content, ratio of water to glycerol, processing conditions, molding methods and PLA content. The addition of PLA greatly improves the tensile strength and modulus of the thermoplastic starch (tensile strength and modulus are increased by 10 to 70 times depending on starch/PLA ratio). The increase in the elongation at break of PLA is limited by addition of thermoplastic starch.

(14). The thermoplastic high amylose starch show improved tensile strength and modulus but poorer elongation at break after a storage of half year while thermoplastic starch/PLA blends with dominant PLA content exhibit poorer mechanical properties after the storage.

(15). The shear viscosities of thermoplastic normal starch and waxy starch decrease with increasing the temperature. The shear viscosity of thermoplastic high amylose starch does not always decrease with increasing the measurement temperature.

(16). The thermoplastic waxy starch exhibits higher viscosity, higher power-law index and activation energy but lower consistency index than thermoplastic normal starch with same composition.

(17). An addition of small amount of PLA component causes a decrease in shear viscosity of thermoplastic high amylose starch/PLA blends while the blend with a starch/PLA ratio of 30/70 wt% shows higher shear viscosity than those of pure PLA and TPS components.

(18). The shear viscosities of thermoplastic normal starch/PLA blends are higher than that of pure TPS, but decrease with increasing PLA content in the blends.

Chapter 6

Recommendations for future work

(1). Study of crystalline structure and thermal properties of thermoplastic starch and thermoplastic starch/PLA blends using, for example, X-ray diffraction and dynamic mechanical thermal analysis (DMTA).

(2). Investigation in processing of thermoplastic starch/PLA blends in a continuous mixer, for example, a single screw extruder.

(3). Reactive extrusion research of thermoplastic starch/PLA blends containing reactive agents such as methylenediphenyl diisocyanate (MDI), amine or maleic anhydride.

(4). Development of extruded or injection molded starch-based products for the application as packaging materials.

Appendix A

Mechanical properties of post-extrusion molded thermoplastic high amylose starch

Table A. Mechanical properties of post-extrusion molded thermoplastic high amylose starch

No.	Code	Starch/ plasticizer, wt/wt	Water/ glycerol, wt/wt	Blending conditions	Post-extrusion temperature, °C	Tensile strength, MPa	Modulus, MPa	Elongation at break (%)
1	HAS-120-4-45-1-15-35	1/1	15/35	120°C/ 4mins/ 45rpm	110	0.961±0.261	17.34±0.94	8.10±3.87
2	HAS-120-4-45-1-15-35	1/1	15/35	120°C/ 4mins/ 45rpm	130	0.866±0.147	17.17±0.65	9.69±2.31
3	HAS-120-4-45-1-15-35	1/1	15/35	120°C/ 4mins/ 45rpm	150	1.03±0.18	21.22±9.51	9.15±0.92
4	HAS-150-4-45-1-15/35	1/1	15/35	150°C/ 4mins/ 45rpm	110	1.07±0.27	19.50±2.90	13.0±5.5
5	HAS-150-4-45-1-15/35	1/1	15/35	150°C/ 4mins/ 45rpm	130	1.12±0.14	16.58±0.57	12.4±2.6
6	HAS-150-4-45-1-15/35	1/1	15/35	150°C/ 4mins/ 45rpm	150	1.27±0.09	19.44±3.21	14.3±4.3
7	HAS-120-4-45-1-35/15	1/1	35/15	120°C/ 4mins/ 45rpm	110	3.14±1.08	82.16±34.85	17.4±9.3
8	HAS-120-4-45-1-35/15	1/1	35/15	120°C/ 4mins/ 45rpm	130	3.73±1.22	88.03±30.13	21.8±10.3
9	HAS-120-4-45-1-35/15	1/1	35/15	120°C/ 4mins/ 45rpm	150	/	/	/
10	HAS-150-4-45-1-35/15	1/1	35/15	150°C/ 4mins/ 45rpm	130	7.60	108.33	36.2
11	HAS-120-4-65-1-15/35	1/1	15/35	120°C/ 4mins/ 65rpm	110	0.861±0.149	17.61±3.61	8.28±2.15
12	HAS-120-4-65-1-15/35	1/1	15/35	120°C/ 4mins/ 65rpm	130	1.12±0.29	18.24±2.29	12.4±3.7
13	HAS-120-4-65-1-15/35	1/1	15/35	120°C/ 4mins/ 65rpm	150	0.89±0.34	16.79±3.88	9.05±2.02
14	HAS-150-4-65-1-15-35	1/1	15/35	150°C/ 4mins/ 65rpm	110	1.54±0.01	20.14±5.52	18.4±3.3
15	HAS-150-4-	1/1	15/35	150°C/	130	1.26±0.07	19.05±2.9	12.5±1.1

	65-1-15-35			4mins/65rpm			1	
16	HAS-150-4-65-1-15-35	1/1	15/35	150°C/4mins/65rpm	150	1.28±0.10	19.69±3.16	18.5±4.5
17	HAS-120-4-65-1-35-15	1/1	35/15	120°C/4mins/65rpm	110	4.49±0.74	85.77±17.60	25.5±5.2
18	HAS-120-4-65-1-35-15	1/1	35/15	120°C/4mins/65rpm	130	5.82±0.84	131.38±40.02	27.4±10.7
19	HAS-120-4-65-1-35-15	1/1	35/15	120°C/4mins/65rpm	150	6.05±0.70	127.1±28.1	30.9±6.5
20	HAS-150-4-65-1-35/15	1/1	35/15	150°C/4mins/65rpm	110	/	/	/
21	HAS-150-4-65-1-35/15	1/1	35/15	150°C/4mins/65rpm	130	7.35±0.89	160.8±103.1	34.6±3.7
22	HAS-150-4-65-1-35/15	1/1	35/15	150°C/4mins/65rpm	150	/	/	/
23	HAS-120-10-65-1-15-35	1/1	15/35	120°C/10mins/65rpm	110	1.14±0.13	16.50±0.55	12.3±4.7
24	HAS-120-10-65-1-15-35	1/1	15/35	120°C/10mins/65rpm	130	1.05±0.57	17.75±4.76	10.5±0.1
25	HAS-120-10-65-1-15-35	1/1	15/35	120°C/10mins/65rpm	150	1.02±0.10	15.42±1.92	10.6±2.1
26	HAS-120-10-45-1-35-15	1/1	35/15	120°C/10mins/45rpm	110	/	/	/
27	HAS-120-10-45-1-35-15	1/1	35/15	120°C/10mins/45rpm	130	8.94±1.54	292.7±99.4	35.7±4.6
28	HAS-120-10-45-1-35-15	1/1	35/15	120°C/10mins/45rpm	150	7.00±0.38	157.5±15.2	38.5±2.4
29	HAS-120-10-45-1-15/35	1/1	15/35	120°C/10mins/45rpm	110	0.990±0.187	16.69±1.47	12.7±3.8
30	HAS-120-10-45-1-15/35	1/1	15/35	120°C/10mins/45rpm	130	1.02±1.35	18.10±1.29	11.8±3.5
31	HAS-120-10-45-1-15/35	1/1	15/35	120°C/10mins/45rpm	150	1.12±0.28	19.96±4.19	11.0±1.3

Post-extrusion temperature: the temperature at which the samples were post-extruded in a Rosand capillary rheometer.

Appendix B

The Calculation of the effect significance of processing conditions on the mechanical properties of thermoplastic high amylose starch

The effect significance of processing conditions on the mechanical properties of thermoplastic high amylose starch at 95% C.I. was estimated according to the following statistical model:

$$y=\beta_0+\beta_1x_1+\beta_2x_2+\beta_3x_3+\beta_{12}x_1x_2+\beta_{13}x_1x_3+\beta_{23}x_2x_3+\beta_{123}x_1x_2x_3$$

$$\beta_i=\frac{\sum x_i y}{\sum x_i^2}$$

y: responses (tensile strength, tensile modulus and elongation at break) ;
β_i: effects;
β x_i: variables.

Table B1. Sign for calculating effects for a 2^3 factorial experimental design, effects of processing conditions on the mechanical properties of thermoplastic high amylose starch

	I	1	2	3	12	13	23	123	Mechanical properties, y		
									Strength, MPa	Modulus, MPa	Elongation, %
	+	-	-	-	+	+	+	_	0.866	17.17	9.69
	+	+	-	-	-	-	+	+	1.12	16.58	12.3
	+	-	+	-	-	+	-	+	3.73	88.03	21.8
	+	+	+	-	+	-	-	-	7.60	108.30	36.2
	+	-	-	+	+	-	-	+	1.12	18.24	12.4
	+	+	-	+	-	+	-	-	1.26	19.05	12.5
	+	-	+	+	-	-	+	-	5.82	131.4	27.4
	+	+	+	+	+	+	+	+	7.35	160.8	34.6
divisor	8	4	4	4	4	4	4	4			

Effects on tensile strength,

$$\beta_0=(y_1+y_2+y_3+y_4+y_5+y_6+y_7+y_8)/8$$
$$=(0.866+1.12+3.73+7.60+1.12+1.26+5.82+7.35)/8$$
$$=3.608$$

$$\beta_1=(-y_1+y_2-y_3+y_4-y_5+y_6-y_7+y_8)/4$$
$$=(-0.866+1.12-3.73+7.60-1.12+1.26-5.82+7.35)/4$$
$$=1.449$$

$\beta_2 = (-y_1-y_2+y_3+y_4-y_5-y_6+y_7+y_8)/4$
$= (-0.866-1.12+3.73+7.60-1.12-1.26+5.82+7.35)/4$
$= 5.034$

$\beta_3 = (-y_1-y_2-y_3-y_4+y_5+y_6+y_7+y_8)/4$
$= (-0.866-1.12-3.73-7.60+1.12+1.26+5.82+7.35)/4$
$= 0.559$

$\beta_{12} = (y_1-y_2-y_3+y_4+y_5-y_6-y_7+y_8)/4$
$= (0.866-1.12-3.73+7.60+1.12-1.26-5.82+7.35)/4$
$= 1.252$

$\beta_{13} = (y_1-y_2+y_3-y_4-y_5+y_6-y_7+y_8)/4$
$= (0.866-1.12+3.73-7.60-1.12+1.26-5.82+7.35)/4$
$= -0.6135$

$\beta_{23} = (y_1+y_2-y_3-y_4-y_5-y_6+y_7+y_8)/4$
$= (0.866+1.12-3.73-7.60-1.12-1.26+5.82+7.35)/4$
$= 0.3615$

$\beta_{123} = (-y_1+y_2+y_3-y_4+y_5-y_6-y_7+y_8)/4$
$= (-0.866+1.12+3.73-7.60+1.12-1.26-5.82+7.35)/4$
$= -0.5565$

Effects on modulus,

$\beta_0 = (y_1+y_2+y_3+y_4+y_5+y_6+y_7+y_8)/8$
$=(17.17+16.58+88.03+108.3+18.24+19.05+131.4+160.8)/8$
$= 69.95$

$\beta_1 = (-y_1+y_2-y_3+y_4-y_5+y_6-y_7+y_8)/4$
$=(-17.17+16.58-88.03+108.3-18.24+19.05-131.4+160.8)/4$
$= 12.47$

$\beta_2 = (-y_1-y_2+y_3+y_4-y_5-y_6+y_7+y_8)/4$
$=(-17.17-16.58+88.03+108.3-18.24-19.05+131.4+160.8)/4$
$=104.4$

$\beta_3 = (-y_1-y_2-y_3-y_4+y_5+y_6+y_7+y_8)/4$
$=(-17.17-16.58-88.03-108.3+18.24+19.05+131.4+160.8)/4$
$=24.85$

$\beta_{12} = (y_1-y_2-y_3+y_4+y_5-y_6-y_7+y_8)/4$
$=(17.17-16.58-88.03+108.3+18.24-19.05-131.4+160.8)/4$
$=12.37$

$\beta_{13} = (y_1-y_2+y_3-y_4-y_5+y_6-y_7+y_8)/4$
$=(17.17-16.58+88.03-108.3-18.24+19.05-131.4+160.8)/4$
$=2.639$

$\beta_{23} = (y_1+y_2-y_3-y_4-y_5-y_6+y_7+y_8)/4$
$=(17.17+16.58-88.03-108.3-18.24-19.05+131.4+160.8)/4$
$=23.08$

$\beta_{123} = (-y_1+y_2+y_3-y_4+y_5-y_6-y_7+y_8)/4$
$=(17.17+16.58+88.03-108.3+18.24-19.05-131.4+160.8)/4$
$=1.938$

Effects on elongation at break,

$\beta_0 = (y_1+y_2+y_3+y_4+y_5+y_6+y_7+y_8)/8$
$=(9.69+12.3+21.8+36.2+12.4+12.5+27.4+34.6)/8$
$= 20.89$

$\beta_1 = (-y_1+y_2-y_3+y_4-y_5+y_6-y_7+y_8)/4$
$=(-9.69+12.3-21.8+36.2-12.4+12.5-27.4+34.6)/4$
$= 6.098$

$\beta_2 = (-y_1-y_2+y_3+y_4-y_5-y_6+y_7+y_8)/4$
$=(-9.69-12.3+21.8+36.2-12.4-12.5+27.4+34.6)/4$
$=18.30$

$\beta_3 = (-y_1-y_2-y_3-y_4+y_5+y_6+y_7+y_8)/4$
$=(-9.69-12.3-21.8-36.2+12.4+12.5+27.4+34.6)/4$
$=1.718$

$\beta_{12} = (y_1-y_2-y_3+y_4+y_5-y_6-y_7+y_8)/4$
$=(9.69-12.3-21.8+36.2+12.4-12.5-27.4+34.6)/4$
$=4.732$

$\beta_{13} = (y_1-y_2+y_3-y_4-y_5+y_6-y_7+y_8)/4$
$=(9.69-12.3+21.8-36.2-12.4+12.5-27.4+34.6)/4$
$=-2.408$

$$\begin{aligned}\beta_{23} &= (y_1+y_2-y_3-y_4-y_5-y_6+y_7+y_8)/4\\ &=(9.69+12.3-21.8-36.2-12.4-12.5+27.4+34.6)/4\\ &=0.3320\end{aligned}$$

$$\begin{aligned}\beta_{123} &= (-y_1+y_2+y_3-y_4+y_5-y_6-y_7+y_8)/4\\ &=(-9.69+12.3+21.8-36.2+12.4-12.5-27.4+34.6)/4\\ &=-2.452\end{aligned}$$

Table B2. Sign for calculating effects for a $\frac{1}{4}2^4$ factorial experiment design: effects of processing conditions on the mechanical properties of thermoplastic high amylose starch

	I	1+234	2	3+124	12+34	13+24	14+23	1234	Mechanical properties, y		
									Strength, MPa	Modulus, MPa	Elongation, %
	+	-	-	+	+	-	-	+	1.047	17.751	10.5
	+	-	+	-	-	+	-	+	8.942	292.72	35.7
	+	+	-	+	-	+	-	+	1.262	19.050	12.5
	+	+	+	-	+	-	-	+	7.596	108.30	36.2
divisor	4	2	2	2	2	2	2	2			

Effects on tensile strength,

$$\begin{aligned}\beta_0 &= (y_1+y_2+y_3+y_4)/4\\ &= (1.047+8.942+1.262+7.596)/4\\ &= 4.712\end{aligned}$$

$$\begin{aligned}\beta_{1+234} &= (-y_1-y_2+y_3+y_4)/2\\ &= (-1.047-8.942+1.262+7.596)/2\\ &= -0.5655\end{aligned}$$

$$\begin{aligned}\beta_2 &= (-y_1+y_2-y_3+y_4)/2\\ &= (-1.047+8.942-1.262+7.596)/2\\ &= 7.115\end{aligned}$$

$$\begin{aligned}\beta_{3+124} &= (y_1-y_2+y_3-y_4)/2\\ &= (1.047-8.942+1.262-7.596)/2\\ &= -7.115\end{aligned}$$

$$\begin{aligned}\beta_{4+123} &= (y_1+y_2-y_3-y_4)/2\\ &= (1.047+8.942-1.262-7.596)/2\\ &= 0.5655\end{aligned}$$

$$\beta_{12+34} = (y_1-y_2-y_3+y_4)/2$$

$= (1.047-8.942-1.262+7.596)/2$
$= -0.7810$

$\beta_{13+24} = (-y_1+y_2+y_3-y_4)/2$
$= (-1.047+8.942+1.262-7.596)/2$
$= 0.7810$

$\beta_{14+23} = (-y_1-y_2-y_3-y_4)/2$
$= (-1.047-8.942-1.262-7.596)/2$
$= -9.424$

$\beta_{1234} = (y_1+y_2+y_3+y_4)/2$
$= (1.047+8.942+1.262+7.596)/4$
$= 9.424$

Effects on modulus,

$\beta_0 = (y_1+y_2+y_3+y_4)/4$
$= (17.751+292.72+19.050+108.30)/4$
$= 109.46$

$\beta_{1+234} = (-y_1-y_2+y_3+y_4)/2$
$= (-17.751-292.72+19.050+108.30)/2$
$= -91.56$

$\beta_2 = (-y_1+y_2-y_3+y_4)/2$
$= (-17.751+292.72-19.050+108.30)/2$
$= 182.1$

$\beta_{3+124} = (y_1-y_2+y_3-y_4)/2$
$= (17.751-292.72+19.050-108.30)/2$
$= -182.1$

$\beta_{4+123} = (y_1+y_2-y_3-y_4)/2$
$= (17.751+292.72-19.050-108.30)/2$
$= 91.56$

$\beta_{12+34} = (y_1-y_2-y_3+y_4)/2$
$= (17.751-292.72-19.050+108.30)/2$
$= -92.86$

$\beta_{13+24} = (-y_1+y_2+y_3-y_4)/2$
$= (-17.751+292.72+19.050-108.30)/2$

$= 92.86$

$\beta_{14+23} = (-y_1-y_2-y_3-y_4)/2$
$= (-17.751-292.72-19.050-108.30)/2$
$= -218.9$

$\beta_{1234} = (y_1+y_2+y_3+y_4)/2$
$= (1.047+8.942+1.262+7.596)/2$
$= 218.9$

Effects on elongation at break,

$\beta_0 = (y_1+y_2+y_3+y_4)/4$
$= (10.5+35.7+12.5+36.2)/4$
$= 23.73$

$\beta_{1+234} = (-y_1-y_2+y_3+y_4)/2$
$= (-10.5-35.7+12.5+36.2)/2$
$= 1.258$

$\beta_2 = (-y_1+y_2-y_3+y_4)/2$
$= (-10.5+35.7-12.5+36.2)/2$
$= 24.47$

$\beta_{3+124} = (y_1-y_2+y_3-y_4)/2$
$= (10.5-35.7+12.5-36.2)/2$
$= -24.47$

$\beta_{4+123} = (y_1+y_2-y_3-y_4)/2$
$= (10.5+35.7-12.5-36.2)/2$
$= -1.258$

$\beta_{12+34} = (y_1-y_2-y_3+y_4)/2$
$= (10.5+35.7+12.5+36.2)/2$
$= -1.253$

$\beta_{13+24} = (-y_1+y_2+y_3-y_4)/2$
$= (-10.5+35.7+12.5-36.2)/2$
$= 1.253$

$\beta_{14+23} = (-y_1-y_2-y_3-y_4)/2$
$= (-10.5-35.7-12.5-36.2)/2$
$= -47.38$

β_{1234} $= (y_1+y_2+y_3+y_4)/2$

$= = (10.5+35.7+12.5+36.2)/2$

$= 47.38$

Appendix C

Rheological properties of the thermoplastic high amylase starch prepared under different processing conditions

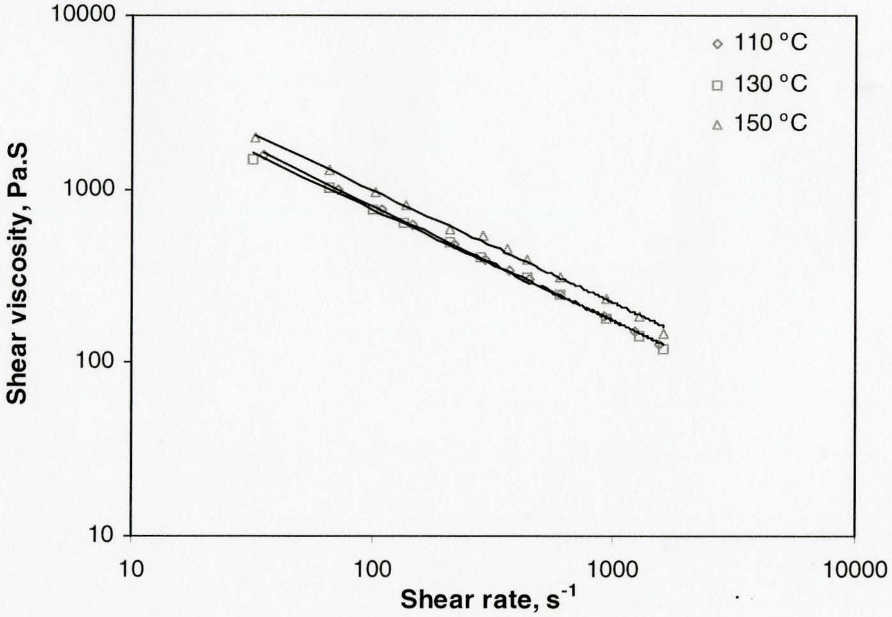

Figure C1. Shear viscosity of thermoplastic high amylose starch (sample 1, HAS-120-4-45-1-15/35) at different temperature (starch/plasticizers ratio: 1/1 wt/wt%; water/glycerol ratio: 15/35 wt/wt%; blending conditions: 120ºC / 4mins / 45rpm).

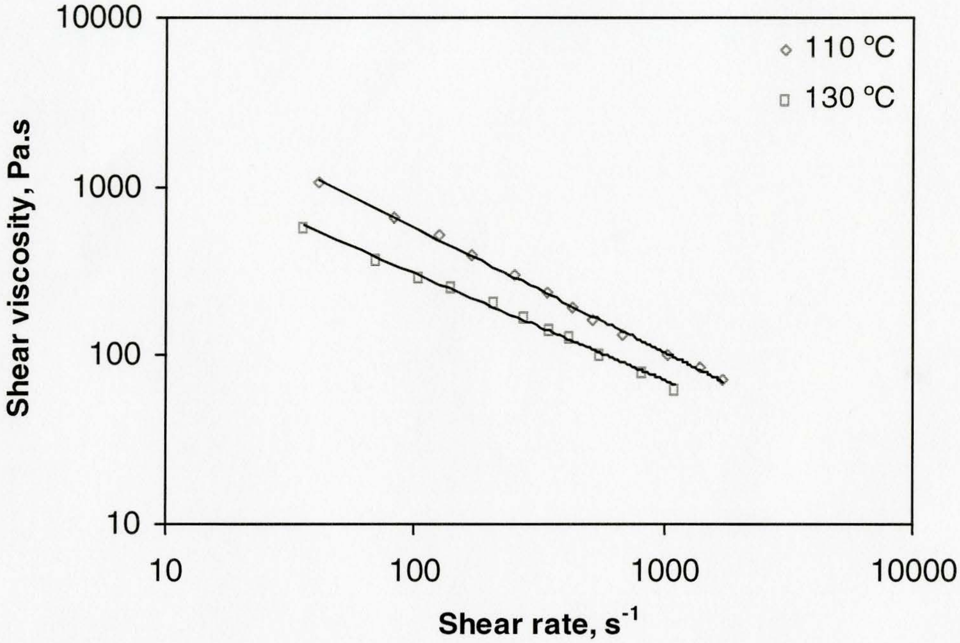

Figure C2. Shear viscosity of thermoplastic high amylose starch (sample 3, HAS-120-4-45-1-35/15) at different temperature (starch/plasticizers ratio: 1/1 wt/wt%; water/glycerol ratio: 35/15 wt/wt%; blending conditions: 120°C/4mins/45rpm).

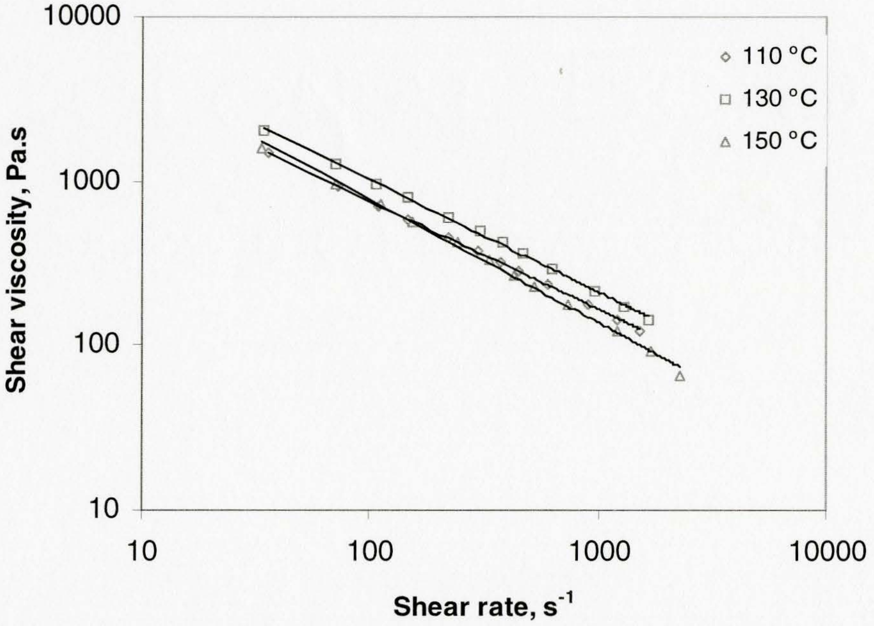

Figure C3. Shear viscosity of thermoplastic high amylose starch (sample 5, HAS-120-4-65-1-15/35) at different temperature (starch/plasticizers ratio: 1/1 wt/wt%; water/glycerol ratio: 15/35 wt/wt%; blending conditions: 120°C/4mins/65rpm).

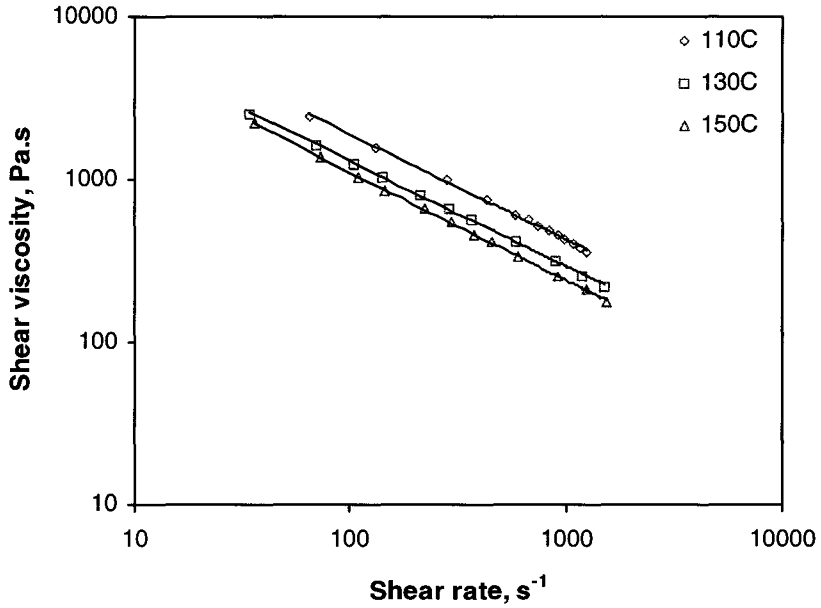

Figure C4. Shear viscosity of thermoplastic high amylose starch (sample 6, HAS-150-4-65-1-15/35) at different temperature (starch/plasticizers ratio: 1/1 wt/wt%; water/glycerol ratio: 15/35 wt/wt%; blending conditions: 150°C/4mins/65rpm).

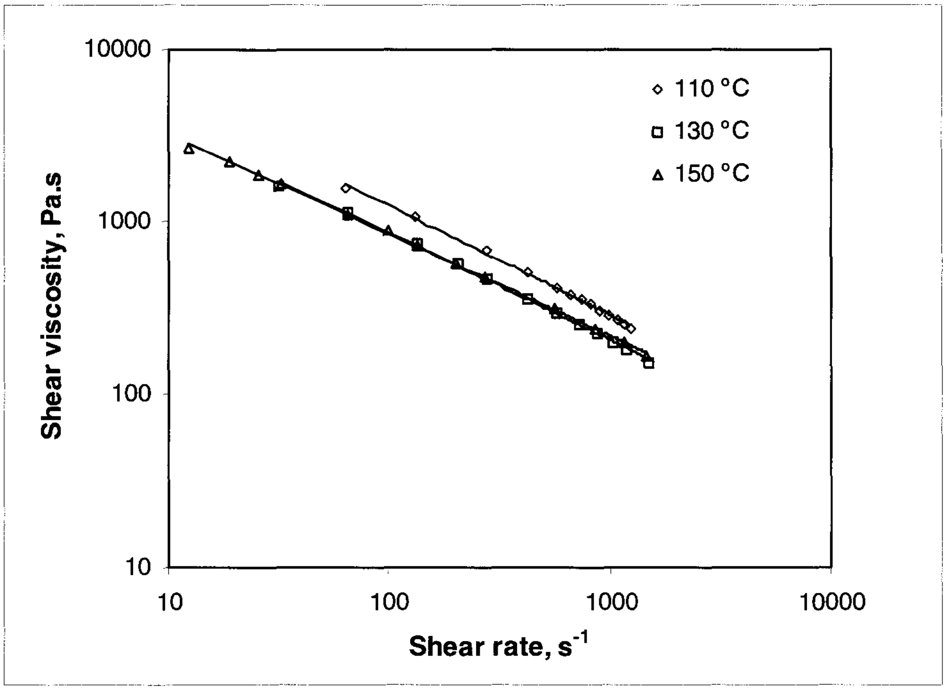

Figure C5. Shear viscosity of thermoplastic high amylose starch (sample 9, HAS-120-10-65-1-15/35) at different temperature (starch/plasticizers ratio: 1/1 wt/wt%; water/glycerol ratio: 15/35 wt/wt%; blending conditions: 120°C/10mins/65rpm).

Table C-1. Rheological properties of thermoplastic starch

Sample code	Temperature, ^C	Shear viscosity, Pa.s	Shear rate, s-1	Temperature, ^C	Shear viscosity, Pa.s	Shear rate, s-1	Temperature, ^C	Shear viscosity, Pa.s	Shear rate, s-1
Has-120-4-45-1-15/35	110	1540.3	128.8	130	1616.6	120.3	150	1618	148.7
		1224.8	151.0		1266.3	144.9		1269.3	185
		912.0	184.9		925.8	182.3		930.1	233.5
		601.7	245.6		597.2	247.0		601.3	313.7
		448.2	302.2		438.4	309.0		442.1	391.2
		371.9	337.7		284.1	404.7		364.0	449.4
		295.9	393.3		209.2	488.4		287.0	535.5
		220.5	480.0		136.1	634.6		211.6	593
		145.6	630.9		100.5	770.4		137.8	799.2
		108.5	765.3		65.6	1016.3		101.8	970.1
		71.7	992.9		31.7	1487.1		66.5	1275.6
		35.3	1568.9					32.2	1968.7
HAS-150-4-45-1-15/35	110	1486.1	288.6	130	1549.5	190.9	150	1601.2	160.1
		1188.5	340.3		1231.9	225.7		1266.7	190
		891.6	415.6		917.2	279.5		937.4	239.1
		594.2	540.1		605	373.0		613.5	322.6
		445.8	646.5		450.6	451.0		454.5	393.3
		371.5	727.1		373.8	512.6		375.9	449.3
		297.1	847.1		297.4	593.8		298.0	521.3
		222.9	1013.6		221.6	721.7		221.0	637.9
		148.6	1335.9		146.3	945.4		145.0	834.9
		111.4	1627.1		109.1	1144.7		107.7	1015.5
		74.3	2112.7		72.1	1511.0		70.8	1339.8
		37.1	3345.9		35.5	2391.8		34.6	2118.6
HAS-120-4-45-1-35/15	110	1728.6	70.9	130	1093.2	62.2			
		1378.5	85.8		822.4	80.95			
		1030.3	101.1		550.2	101.49			
		683.2	133.4		413.9	130.38			
		510.7	164.7		345.5	143.09			
		424.6	191.7		277.0	171.21			
		338.7	234.2		208.4	206.89			
		253.1	303.2		139.5	250.6			
		167.9	393.8		104.9	291.08			
		125.5	511		70.2	368.42			
		83.3	665.7		35.4	572.51			
		41.3	1052.8						
HAS-120-4-65-1-15/35	110	1523.0	121.9	130	1655.5	142.5	150	2260.9	64.7
		1212.5	144.7		1304.2	174.4		1704.8	91.3
		904.3	177.5		960.3	216.3		1196.6	122.1
		597.8	234.6		624.4	293.2		736.4	178.6

		445.9	286.5		460.7	360.5		526.2	231.2
		370.3	325.4		380.1	420.9		426.4	269.1
		295.0	372.8		300.4	492.0		330.4	331.4
		220.0	452.1		222.0	602.2		238.7	420.4
		145.6	586.4		145.1	796.4		151.9	569.9
		108.6	709.8		107.4	956.1		110.6	716.8
		71.9	927.7		70.3	1255.8		71.0	971.2
		35.5	1490.6		34.2	2019.0		33.6	1596.2
HAS-150-4-65-1-25/35	110	1249.8	359.6	130	1516.8	218.3	150	1550.7	174.5
		1164.3	384.0		1203.5	257.4		1232.8	207.5
		1079.4	409.8		894.0	319.2		917.8	256.7
		995.4	434.6		587.9	423.3		605.4	339.2
		912.1	460.1		362.0	574.3		450.9	415.3
		829.5	492		287.6	666.8		374.0	466.3
		747.8	528.6		213.8	807		297.6	550.0
		667.0	576.0		140.9	1042.4		221.7	662.6
		586.9	620.3		104.8	1269.4		146.4	867.5
		430.4	759.8		69.1	1640		109.1	1052.8
		278.6	1012.9		33.9	2540.9		72.1	1373.9
		133.2	1584.0					35.5	2203.1
		64.1	2444.6						
HAS-120-10-65-1-15/35	110	1237.8	241.5	130	1512.7	153.2	150	1455.6	165.4
		1153.0	255.0		1193	181.8		1152.9	197
		1068.9	271.4		1035.1	200.0		854.0	237.3
		985.4	288.5		879.2	222.4		559.9	309.8
		903.2	306.7		724.9	252.2		272.6	479.5
		821.3	326.6		572.5	293.9		202.3	573
		740.2	349.5		422.9	356		133.0	726.2
		660.4	374.6		276.2	466.3		98.8	874.5
		581.1	408.5		204.3	567.7		65.0	1107.9
		426.1	499.9		133.7	732		31.9	1648.6
		275.8	668.8		64.9	1120.3		25.3	1872.3
		131.9	1053.9		31.6	1626.7		18.8	2216.6
		63.5	1570.8					12.4	2711.5
HAS-120-45-1-15/35	110	64.4	1055.0	130	80.4	704.3	150	1770.2	157.1
		105.1	816.8		125.3	520.3		1362.9	196.9
		172.8	596.5		195.3	384.6		977.7	253.9
		283.6	434.0		304.7	282.6		617.1	356.6
		466.9	306.7		476.7	210.6		285.7	595.8
		780.3	215.4		743.5	157.9		208.5	734.9
		1303.1	147.7		1163.8	118.2		134.3	953.9
		2203.0	99.3		1823.2	89.9		98.5	1212.9
		3773.1	64.5		2848.9	66.9		63.8	1488.9
NS-120-45-2/1-15/35	110	88.1	3582.1	130	72.9	2226.2	150	90.4	1289.5

		130.5	2466.8		115.6	1654.8		139.3	931.9
		195.3	1969.5		183.8	1222.8		215.6	683.8
		294.7	1566.9		290.9	902.7		332.9	493.4
		447.3	1234.2		460.9	669.4		515.2	365.6
		684.8	953.5		731.9	498.2		797.3	273.9
		1051.7	726.7		1155.9	379.5		1239.2	200.7
					1835.6	279.2		1927.5	145.0
					2909.1	202.9		2993.5	112.5
WS-120-45-2/1-15/35	110	60.2	4097.7	130	67.8	2437.0	150	65.2	1509.7
		95.4	3435.5		107.5	1946.1		103.4	1032.9
		151.8	2820.1		170.3	1571.1		163.9	575.5
		239.8	2370.7		269.9	1294.2		259.9	414.2
		380.9	1887.6		428.9	1024.5		411.6	287.8
		602.8	1428.3		678.7	707.9		653.3	248.5
					1078.6	529.9		1036.9	189.8
					1709.4	387.9		1645.3	239.3
					2707.3	282.4		2609.4	200.5

Table C-2. Rheological properties of thermoplastic starch/PLA blends

Samples	Temperature, ^C	Shear viscosity, Pa.s	Shear rate, s-1	Temperature, ^C	Shear viscosity, Pa.s	Shear rate, s-1	Temperature, ^C	Shear viscosity, Pa.s	Shear rate, s-1
TP-HAS/PLA (70/30), starch/plasticizer:1/1	150	1380	187.6	160	1367.9	142.93	170	1074.9	119.67
		1095.4	220.4		1088	165.4		796.6	146.58
		813.5	262.3		809.9	196.57		522.5	186.59
		535.1	332.7		534.5	250.03		254.7	267.59
		261.9	509		262.9	377.43		189.2	317.69
		194.8	598.2		195.9	444.88		124.4	407.88
		128.4	748.5		129.4	565.53		92.5	467.54
		95.5	876.5		96.5	651.64		60.9	563.68
		63	1104.4		63.8	825.19			
TP-HAS/PLA(70/30) containg 5%F-108, starch/plasticizer:1/1	150	1616.3	170.4	160	2590.2	75.1	170	1514.8	93.77
		1269.3	211.7		1708.4	107.8		1159.3	113.27
		931.2	263.4		1081.2	150.8		828.1	132.23
		603	348.7		614	228.1		521.1	181.37
		288.3	571.2		259.5	414.5		241.4	279.68
		138.6	917.7		117	698.1		113.9	423.33
		102.5	1123.9		85	831.8		83.8	461.24
		67	1465.1		54.6	1020		54.5	491.91
		32.5	2181.6		25.9	1026.2		26.3	622.09
TP-HAS/PLA(50/50), starch/plasticizer:1/1	150	1383.4	192	160	51.6	311.8	170	1360.4	74.9
		1099.3	215.5		84.7	450.7		1046	87.2
		817.6	257.2		138.5	344.2		750.8	103.4
		538.8	333		230.8	253.8		475.6	133.2
		264.4	507.3		386.4	182.4		222.4	183.8
		129.9	760.4		657. 6	126.1		163.1	204.5
		96.8	898.5		1144.8	90.6		105.8	243.6
		63.9	1101.3		2087.8	61.8		78	248.9
					4112.5	38.7		50.9	256.7
TP-HAS/PLA(50/50) containing 5% F-108, starch/plasticizer:1/1	150	1633.2	185.0	160	1238.9	145.5	170	1761	107.4
		1226.3	232.9		877.8	185.8		1264.6	137.5
		859.7	297.5		547.6	252.3		855.3	181.3
		690.8	347.3		395	310.3		677	211.9
		484.11	385.7		251.2	409.1		513.8	253.1
		317.01	529.6		117.8	604.6		364.7	309.2
		154.04	874.5		86.4	690.7		228.8	399.9
		114.26	1080.6		56	804.0		165.8	460.7
		75	1435.7					106.2	535.8
								77.8	559.4
								50.4	574.8
TP-HAS/PLA(30/70), starch/plasticizer:1/1	150	1609.4	219.4	160	1413.3	108.42	170	942.52	102.8
		1274.7	252.8		1038.4	135.9		684.54	117.3
		944	308.4		718.5	167.87		439.27	136.1
		618.7	429.2		442.3	212.1		208.69	174.7

		301.1	723.7					153.82	178.3
		146.8	1131.3					100.35	185.8
		109	1319.9						
		71.7	1860.5						
TP-HAS/PLA(30/70)containing 5% F-108, starch/plasticizer:1/1	150	1701.8	177.2	160	/	/	170	2876.4	47.5
		1322.2	215.4					1461.6	84.25
		957.8	278.1					844.9	125.72
		611.1	382.9					470.1	177.07
		286.7	631.3					203	254.71
		135.9	1024.4					146.9	275.84
		100	1245.2					94.2	285.49
		65	1597.2					69.2	292.59
TP-HAS/PLA(50/50)containing 5% F-108, starch/plasticizer:2/1	150	1675.9	364.2	160	/	/	170	1138.6	217.9
		1337.7	433.8					905.5	245.3
		1000.3	548.7					674.1	280.0
		664.1	739.2					444.9	330.6
		329.8	1208.7					218.9	421.7
		246.6	1481					163.1	451.1
		163.8	1943.2					107.8	466.8
		122.5	2488.9					80.4	480.5
		81.3	3357					53.2	498.3
								26.3	715.4
TP-HAS/PLA(50/50) containing 5% F-108, starch/plasticizer:3/2	150	1705.4	286.2	160	/	/	170	1244.9	163.3
		1336.3	356.3					974.7	189.4
		977.3	455.8					712.8	223.7
		630.5	620.9					460.6	272.9
		299.9	1022.8					220.3	360.3
		220.8	1265					162.6	391.7
		143.6	1681.3					106.2	435.5
		105.9	2055.7					78.6	438.3
		69.1	2742.6					51.6	498.7
								25.1	545.1
TP-NS/PLA(70/30), starch/plasticizer:2/1	150	76.1	3149.3	160			170	57.0	1254.5
		117.5	1957.5					92.3	1013.4
		180.9	1615.1					149.7	843.9
		280.5	1340.1					243.4	658.9
		436.9	1033.4					396.7	505.9
		678.9	775.9					650.0	386.9
		1057.8	575.3					1071.6	289.4
								1769.3	210.1
								2941.8	149.1
TP-NS/PLA(50/50), starch/plasticizer:2/1	150	58.0	2454.9	160	/	/	170	60.6	880.8
		95.0	2004.5					96.8	678.1
		156.5	1547.9					154.0	539.6
		259.7	1144.8					247.6	428.7
		436.1	830.6					395.7	343.9

		738.0	585.2					632.5	274.8
		1275.9	394.1					1012.0	215.5
		2261.1	250.4					1618.3	165.9
		4172.5	149.8					2590.4	124.3
TP-NS/PLA(30/70), starch/plasticizer:2/1	150	58.6	2098.2	160	/	/	170	123.5	412.2
		95.5	1656.7					202.5	351.6
		156.9	1331.9					337.4	290.2
		257.7	979.4					573.2	234.8
		424.9	728.1					1001.9	176.6
		710.5	540.3					1855.5	117.1
		1196.8	374.3					3993.4	66.6
		2040.4	238.1						
		3547.7	166.6						
TP-WS/PLA(50/50), starch/plasticizer:2/1	150	57.4	1907.6	160	/	/	170	185.9	355.2
		93.5	1466.4					307.5	314.2
		152.8	1182.9					524.6	260.7
		250.7	941.7					939.3	201.3
		414.8	697.1					1956.1	115.5
		688.1	511.6					10883.7	26.5
		1156.0	358.7						
		1964.9	248.6						
		3394.8	162.5						
Pure PLA	150	/	/	160	/	/	170	4334	79.7
								1397	230.7
								627	461.6
								240	932.3
								169	1131.5
								106	1399.8
								77	1490.9
								49	1396

Appendix D

Mechanical properties of thermoplastic starch/PLA blends post-extruded at different temperature

Table D. Mechanical properties comparison of thermoplastic starch/PLA blends post-extruded at different temperature

No.	Blends	Starch/ PLA ratio, wt/wt	Starch/ plasticizer ratio, wt/wt	Temperature extruded, °C	Content Of F-108, wt%	Tensile properties		
						Strength (MPa)	Modulus (MPa)	Elongation at break (%)
1	HAS/PLA	100/0	1/1	150	0	0.888±0.120	18.59±1.09	10.1±2.0
2	HAS/PLA	100/0	1/1	170	0	/[a]	/[a]	/[a]
3	HAS/PLA	70/30	1/1	150	0	3.72±0.72	162.3±23.7	10.1±3.7
4	HAS/PLA	70/30	1/1	170	0	3.25±0.84	166.1±57.0	7.6±2.1
5	HAS/PLA	50/50	1/1	150	0	9.70±1.60	629.1±158.2	6.59±3.42
6	HAS/PLA	50/50	1/1	170	0	7.55±2.47	489.1±83.5	4.02±1.16
7	HAS/PLA	30/70	1/1	150	0	22.8±2.5	1522±76	7.59±2.07
8	HAS/PLA	30/70	1/1	170	0	20.0±4.4	1430±139	4.21±2.70
9	HAS/PLA	50/50/	3/2	150	5	14.8±0.8	1067±43	3.46±0.86
10	HAS/PLA	50/50/	3/2	170	5	11.5±0.4	692.3±13.3	4.15±1.01
11	HAS/PLA	50/50	2/1	150	5	16.8±2.3	1740±384	2.17±1.19
12	HAS/PLA	50/50	2/1	170	5	16.8±2.0	1386±96	1.61±0.27
13	NS/PLA	70/30	2/1	150	0	5.08±1.19	250.6±57.2	13.0±2.9
14	NS/PLA	70/30	2/1	170	0	5.09±0.15	198.9±63.9	15.5±5.1
15	NS/PLA	50/50	2/1	150	0	15.1±2.3	926.2±220.3	6.22±2.59
16	NS/PLA	50/50	2/1	170	0	10.4±3.5	721.7±162.5	3.02±3.94
17	NS/PLA	30/70	2/1	150	0	24.5±1.1	1557±49	5.30±2.90
18	NS/PLA	30/70	2/1	170	0	19.2±7.9	1496±31	1.99±0.80
19	HAS/PLA	50/50	2/1	150	0	13.85±1.33	937.5±171.1	3.32±1.97
20	HAS/PLA	50/50	2/1	170	0	11.84±2.27	854.8±134.1	2.06±0.36
21	WS/PLA	50/50	2/1	150	0	13.79±1.22	784.8±68.4	7.03±0.62
22	WS/PLA	50/50	2/1	170	0	14.45±4.19	968±276	3.17±2.26
23	PLA	0/100	/	150	0	/[b]	/[b]	/[b]
24	PLA	0/100	/	170	0	68.2±5.8	3119±125	4.80±2.20

a, The specimen was degraded at 170°C in the Rosand Rheometer.

b, The specimen was not melted at 150°C in the Rosand Rheometer.

Appendix E

Rheological properties of thermoplastic high amylase starch containing 5% F-108 blends with PLA

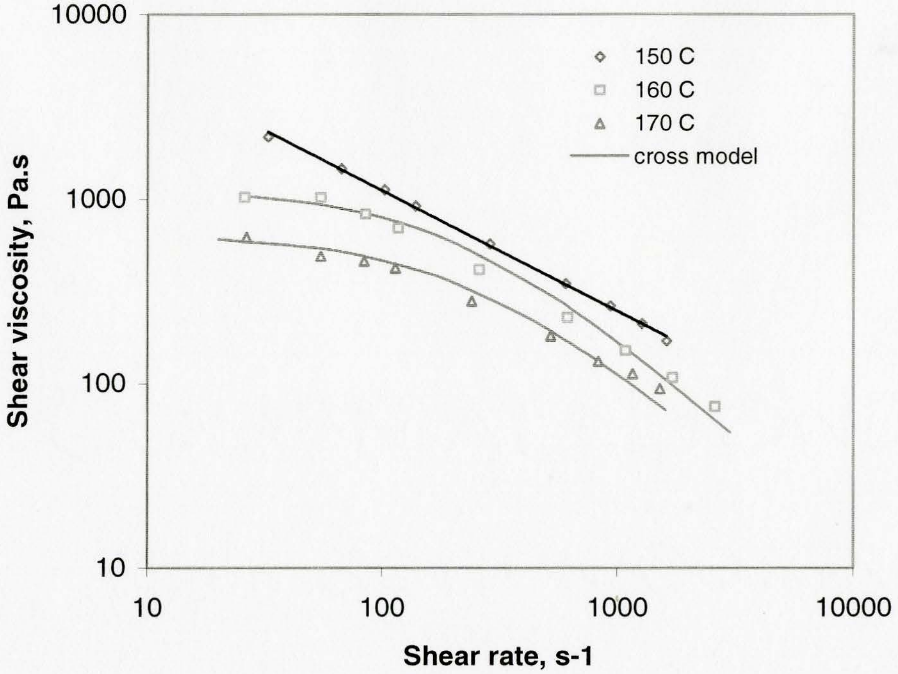

Figure E1. Temperature dependence of the rheological properties of the thermoplastic high amylose starch/PLA (70/30) blend containing 5% F-108 (starch/plasticizers ratio: 1/1wt/wt%; water/glycerol: 15/35wt/wt%).

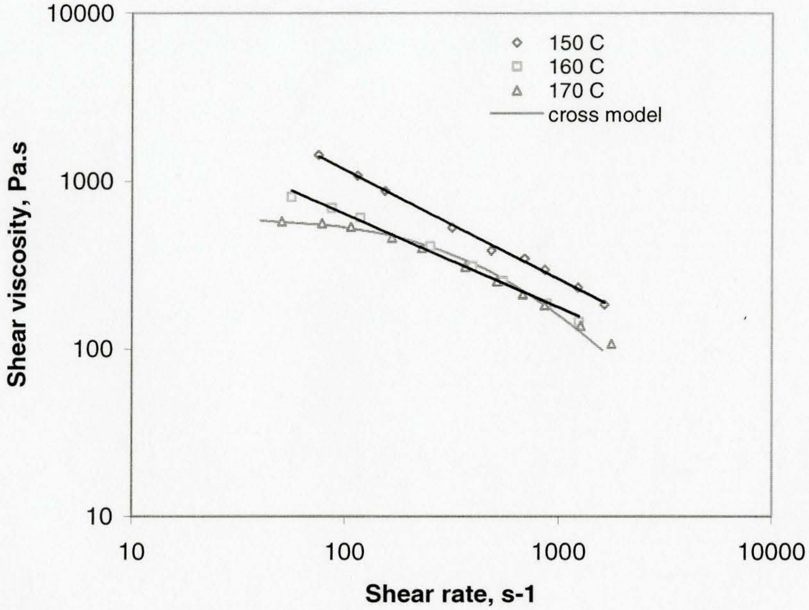

Figure E2. Temperature dependence of the rheological properties of the thermoplastic high amylose starch/PLA (50/50) blend containing 5% F-108 (starch/plasticizers ratio: 1/1wt/wt%; water/glycerol: 15/35wt/wt%).

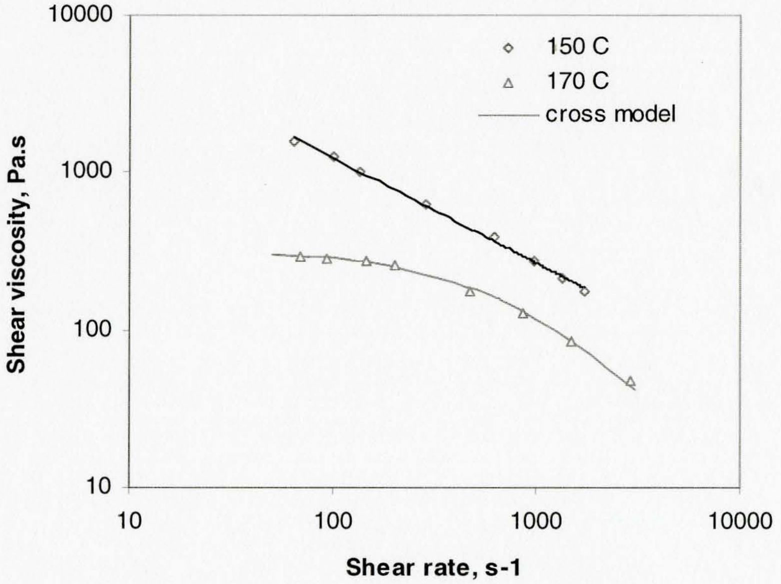

Figure E3. Temperature dependence of the rheological properties of thermoplastic high amylose starch/PLA (30/70) blend containing 5% F-108 (starch/plasticizers ratio: 1/1wt/wt%; water/glycerol: 15/35wt/wt%).

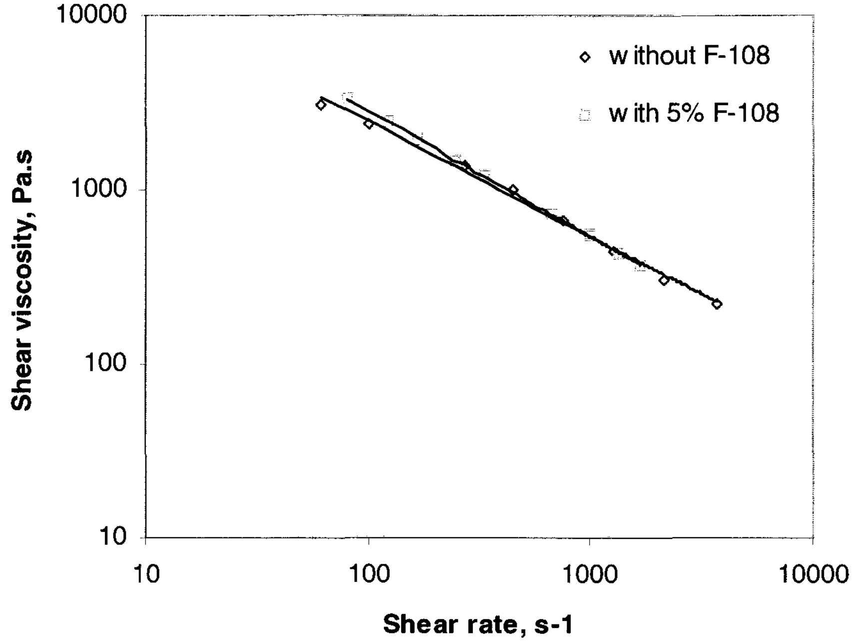

Figure E4. The effect of F-108 on rheological properties of thermoplastic high amylose starch/PLA (50/50) blend (measurement temperature: 150°C; starch/plasticizer ratio: 2/1; water/glycerol ratio: 15/35).

References

Avella, M., Errico, M. E., Rimedio, R., Sadocco, P., "Preparation of Biodegradable polyester/high-amylose starch composites by reactive blending and their characterization," *Journal of Applied Polymer Science*, **83**, 1432-1442 (2002).

Avella, M., Errico, M. E., "Preparation of PHBV/starch blends by reactive blending and their characterization," *Journal of Applied Polymer Science*, **77**, 232-236 (2000).

Avella, M., Martuscelli, E. and Raimo, M., "Review properties of blends and composites based on poly(3-hydroxybutyrate) and poly(3-hydroxybutyrate-hydroxyvalerate) copolymers," *Journal of Materials Science*, **35** (3), 523–545(2000).

Averous, L., Boquillon, N., "Biocomposites based on plasticized starch: thermal and mechanical behaviours," *Carbohydrate Polymers*, **56**, 111-122 (2004).

Averous, L., Fringant, C., Moro, L., "Plasticized starch-cellulose interaction in polysaccharide composites," *Polymer* **42**, 6565-6572 (2001a).

Averous, L. and Fringant, C., "Association between plasticized starch and polyesters: processing and performances of injected biodegradable systems," *Polymer Engineering and Science*, **41**, No. 5, 727-734 (2001b).

Averous, L., Fauconnier, N., Moro, L., Fringant, C., "Blends of thermoplastic starch and polyesteramide: processing and properties," *Journal of Applied Polymer Science*, **76**, 1117-1128 (2000a)

Averous, L. Moro, L., Dole, P., Fringant, C., "Properties of thermoplastic blends: starch-polycaprolactone," *Polymer*, **41**, 4157-4167 (2000b).

Bastioli, C., “Global status of the production of biobased packaging materials”, *Starch/Starke*, **53**, 351-355 (2001).

Bastioli C., “Properties and applications of Mater-Bi starch-based materials,” *Polymer degradation and stability* **59**, 263-272 (1998).

Bastioli, C., Cerutti, A., Guanella, I., Romano, G. C., Tosin, M., “Physical state and biodegradation behavior of starch-polycaprolactone systems,” *J. Enviro. Polym. Degrad.*, **3** (2), 81-95 (1995).

Carvalho, A. J. F., Zambon, M. D., Curvelo, A. A. S., Gandini, A., “Size exclusion chromatography characterization of thermoplastic starch composites: 1. influence of plasticizer and fibre content”, *Polymer degradation and Stability*, **79,** 133-138 (2003).

Colonna, P., and Mercier, C., “gelatinization and melting of maize and pea starches with normal and high-amylose genotypes”, *Phytochemistry*, **24**, 1667-1674 (1985).

Dell, P. A., Kohlman, W. G., “Effects of water content on the properties of starch/poly(ethylene-vinyl alcohol) blends,” *Journal of Applied Polymer Science*, **52,** 353-363 (1994).

Desai, S., Thakore, I. M., Sarawade, B. D., Devi, S., “Structure-property relationship in polyurethane elasomers containg crosslinker,” *Polymer Engineering and Science*, **5** (2000).

Drumright, R. E., Gruber P. R. and Henton, D. E. “Polylactic acid technology,” *Advanced materials*, **12**, No. 23, 1841-1846 (2000)

Evans, I. D., and Haisman, D. R., “The effect of solutes on the gelatinization temperature range of potato starch”, *starch*, **34**, 224-231 (1982).

Forssell, P., Mikkila, J., Suortti, T., "Plasticization of barley starch with glycerol and water"; *Pure Appl. Chem.*, A**33** (5), 703-715 (1996).

Fringant, C., Desbrières J. and Rinaudo, M., "Physical properties of acetylated starch-based materials: relation with their molecular characteristics," *Polymer*, **37**, 2663–2673. (1996).

Funk, U., Bergthaller, W., Lindhauer, M. G., "Processing and characterization of biodegradable products based on starch," *Polymer Degradation and Stability*, **59**, 293-296 (1998).

Garlotta, D., "A literature review of poly(lactic acid)," *Journal of Polymers and the Environment*, **9**, No. 2, 63-84 (2002).

George, E. R., Sullivan, T. M., Park, E. H., "Thermoplastic starch blends with a poly(ethylene-co-vinyl alcohol): processability and physical properties," *Polymer Engineering and Science*, **34**, 17-23 (1994).

Graaf, R. A. D., and Janssen, L. P. B. M., "Properties and manufacturing of a new starch plastics," *Polymer Engineering and Science*, **3** (2001).

Halley, P., Rutgers, R., Coombs, S., Kettels, J., Gralton, J., et al., "Developing biodegradable mulch films from starch-based polymers," *Starch/Starke* ***53***, 362-367 (2001).

Hoover, R., " Composition, molecular structure, and physico-chemical properties of tuber and root starches: a review," *Carbohydrate Polymers*, **45**, 253–267 (2001).

Huda, M. S., Mohanty, A. K., Misra, M., Drzal, L. T., Schut, E., "Effect of processing conditions of the physico-mechanical properties of cellulose fiber reinforced poly(lactic acid)", *ANTEC*, 1614 (2004)

Ishigaki, T., Kawagoshi, Y., Ike M. and Fujita, M., "Biodegradation of a polyvinyl alcohol-starch blend plastic film," *World Jounal of Microbiology & Biotechnology* **15**, 321-327 (1999).

Jane, J., Chen, Y., Lee, L. F., McPherson, A. E., Wong, K. S., Radosavljevic, M., Kasemsuwan T., "Effects of amylopectin branch chain length and amylose content on the gelatinization and pasting properties of starch"; *Cereal Chemistry*, **76**, 629-637 (1999).

Jun, C. L., "Reactive blending of biodegradable polymers: PLA and starch," *Journal of Polymers and the Environment*, **8**, No. 1, 33-37 (2000).

Ke, T., Sun, S. X., Seib, P., "Blending of poly(lactic acid) and starches containing varying amylose content," *Journal of Applied Polymer Science*, **89**, 3639-3646 (2003).

Koller, I. and Owen, A. J., "Starch-filled PHB and PHB/HV copolymer," *Polymer International*, **39,** 175-181 (1996)

Koenig, M. F. and Huang, S. J., "Biodegradable blends and composites of polycaprolactone and starch derivatives," *Polymer*, **36**, 1877-1882 (1995).

Lai, L. S. and Kokini, J. L., "The effect of extrusion operating conditions on the on-line apparent viscosity of 98% amylopectin (Amioca) and 70% Amylose(Hylon 7) cornstarches during extrusion," *J. Rheol.*, **34** (8), 1245-1266 (1990).

Li, J.H., Vasanthan, T., Rossnagel B. and Hoover, R., "Starch from hull-less barley: I. Granule morphology, composition and amylopectin structure," *Food Chemistry* **74**, 395–405 (2001).

Liu, Z., Yi, F., Xiaosu, Y., “Thermoplastic starch/PVAI compounds: Preparation, processing, and properties”, *J. Appli. Polym. Sci.*, **74**, 2667-2673(1999).

Lorcks, J., “Properties and applications of compostable starch-based plastic materials”, *Polymer Degradation and Stability* **59**, 245-249 (1998)

Lunt J., “Large-scale production, properties and commercial applications of polylactic acid polymers,” *Polymer Degradation and Stability* **59**, 145-152 (1998).

Martin, O., Averous, L., Valle, G. D., “In-line determination of plasticized wheat starch viscoelastic behavior: impact of processing”, *Carbohydrate Polymer* **53** 169-182 (2003).

Martin, O., and Averous, L., “Poly(lactic acid): plasticization and properties of biodegradable multiphase systems,” *Polymer* **42**, 6209-6219 (2001a).

Martin, O., Schwach, E., Averous, L., Couturier, Y., “Propertiesof biodegradable multiplayer films based on plasticized wheat starch”, *Starch/Starke* **53**, 372-380 (2001b).

Mercier, C., Charbonniere, R., Grebaut, J. and Gueriviere, J. F. L., ‘‘Formation of amylose–lipid complexes by twin screw extrusion cooking of manioc starch,’’ *Cereal Chemistry*, **57**, 4–9 (1980).

Mohanty, A. K., Misra, M., Hinrichsen, G., “Biofibres, biodegradable polymers and biocomposites: an overview,” *Macromol. Mater. Eng.*, **276/277**, 1-24 (2000).

Morrison, W.R., Milligan, T. P. and Azudin, M. N., “A relationship between the amylose and lipids contents of starches from diploid cereals,” *Journal of Cereal Science*, **2**, 257–260 (1984).

Donovan, J. W., “Phase transitions of the starch-water system”, *Biopolymers*, **18**, 263-275, (1979).

Petersen, K., Nielsen, P. V., Olsen, M. B., "Physical and mechanical properties of bio-based materias – starch, polylactate and polyhydroxybutyrate," *Starch/Starke* **53**, 356-361 (2001)

Riggle D., "Moving towards consensus on degradable plastics," *BioCycle, Emmaus*, **3** (1998).

Poutanen, K., Forssell, P., "Modification of starch properties with plasticizers," *TRIP* **4**, 128-132 (1996).

Rodriguez-Gonzalez, Ramsay, F. J., Favis B. A., "Rheological and thermal properties of thermoplastic starch with high glycerol content", *Carbohydrate Polymers* **58** 139-147 (2004).

Singh N., Singh, J., Kaur, L., Sodhi, N. S., Gill, B. S., "Morphological, thermal and rheological properties of starches from different botanical sources," *Food Chemistry* **81**, 219-231 (2003).

Slade, L., and Levine, H., "Recent advances in starch retrogradation", in: industrial Polysaccharide, Eds.: Stilva, S. S., Crescenzi, V., and Dea, I., C., M., Gordon and Breach Sci., New York, 387-430 (1987).

Soest, J. J. G. and Borger, D. B., "Structure and properties of compression-molded thermoplastic starch materials from normal and high-amylose maize starches," *Journal of Applied Polymer*, Vol. **64**, 631-644 (1997).

Stepto, R. F. T., "The properties of starch as a thermoplastic," *Macromol. Symp.* 201, 203-212 (2003).

Stirna, U. K., Tupureina, V. V., Sevastyanova, I. V., Dzene, A. V. and Misane, M. M., "Synthesis and characterization of biodegradable segmented poly(ester urethanes) derived from poly(caprolactone diols) and Poly(L-lactic diols)," *Polymer Science*, A**44**, 1227-1234 (2002).

Sun, X. and Ke, T., *Cereal Chemistry,* **77**(6), 761-768 (2000).

Tu, J., Gao, J., Lin, T., "Biodegradable thermoplastic starch", *Journal of Applied. Polymer Science*, **62**, 1491-1494 (1996).

Valle, G. D., Buleon, A., "Relationship between structure and viscoelastic behavior of plasticized starch", *J. Rheol.* **42**(3), 507-525 (1998).

Valle, G. D., Colonna, P., and Patria, A., "Influence of amylose content on the viscous behavior of low hydrated molten starches", *J. Rheol.*, **40**(3), May/June (1996).

Vikman, M., Hulleman, S. H., Van Der Zee, M., Myllarinen, P., Feil, H., "Morphology and enzymatic degradation of thermoplastic starch-polycaolactone blends," *Journal of Applied Polymer Science*, **74**, 2594-2604 (1999).

Vlachopoulos, J., "Introduction to plastics processing," McMASTER UNIVERSITY, Hamilton, Canada (2003).

Waigh, T.A., Perry, P., Riekel, C., Gidley, M.J., and Donald, A.M., "Communications to the editor: chiral side-chain liquid-crystalline polymeric properties of starch", *Macromolecules,* **31**, 7980-7984 (1998).

Wang, H., Sun, X., Seib, P., "Mechanical properties of poly(lactic acid) and wheat starch blends with methylenediphenyl diisocyanate," *Journal of Applied Polymer Science*, **84**, 1257-1262 (2002).

Willemse, R. C., Langeraar, A. E., Posthuma, A., "Tensile moduli of co-continuous polymer blends", *Polymer* **40**, 6645-6650 (1999).

Willett, J. L., Jasberg, B. K. and Swanson, C. L., "Rheology of thermoplastic starch: effects of temperature, moisture content, and additions on melt viscosity", *Polymer Engineering and Science*, **35**, No 2., 202-210 (1995).

You, X., Li, L., Gao, J., Yu, J., Zhao, Z., "Biodegradable extruded starch blends," *Journal of Applied polymer Science*, **88**, 627-635 (2003).

Yu, J., Gao, J., Lin, T., "Biodegradable thermoplastic starch," *Journal of Applied Polymer Science*, **62**, 1491-1494 (1996).

Zobel, H.F., "Starch crystal transformations and their industrial importance", *Starch*, **40**, 1-7(1988a).

Zobel, H. F., "Molecules to granules – a comprehensive starch review", *Starch*, **40**, 44-50 (1988b).